ÉCOLE DE TECHNOLOGIE SUPÉRIEURE
UNIVERSITÉ DU QUÉBEC

MANUSCRIPT BASED THESIS PRESENTED TO
ÉCOLE DE TECHNOLOGIE SUPÉRIEURE

IN PARTIAL FULFILLEMENT OF THE REQUIREMENTS FOR
THE DEGREE OF DOCTOR OF PHILOSOPHY
Ph. D.

BY
Hoang Quan TRAN

ASYMMETRICAL ROLL BENDING PROCESS STUDY: DYNAMIC FINITE ELEMENT MODELING AND EXPERIMENTS

MONTREAL, OCTOBER 27, 2014

© Copyright 2014 reserved by Hoang Quan Tran

© Copyright

Reproduction, saving or sharing of the content of this document, in whole or in part, is prohibited. A reader who wishes to print this document or save it on any medium must first obtain the author's permission.

BOARD OF EXAMINERS

THIS THESIS HAS BEEN EVALUATED

BY THE FOLLOWING BOARD OF EXAMINERS

Mr. Henri Champliaud, Thesis supervisor
Department of Mechanical Engineering at École de technologie supérieure

Mr. Thien My Dao, Thesis co-supervisor
Department of Mechanical Engineering at École de technologie supérieure

Ms. Botez Ruxandra, President of the board of examiners
Department of Automated Manufacturing Engineering at École de technologie supérieure

Mr. Victor Songmene, Member of the jury
Department of Mechanical Engineering at École de technologie supérieure

Mr. Zhaoheng Liu, Member of the jury
Department of Mechanical Engineering at École de technologie supérieure

Mr. Lyès Hacini, External evaluator
Raufoss Automative Components Canada

THIS THESIS WAS PRENSENTED AND DEFENDED

IN THE PRESENCE OF A BOARD OF EXAMINERS AND THE PUBLIC

OCTOBER 17, 2014

AT ÉCOLE DE TECHNOLOGIE SUPÉRIEURE

“If we knew what it was we were doing, it would not be called research, would it?”

Albert Einstein (1879-1955)

ACKNOWLEDGMENTS

I would like to express my sincere appreciation to all who helped me for this thesis.

First and foremost, I am extremely grateful to my Ph.D. advisor, Prof. Henri Champliaud, for his excellent advice, encouragement and support. He was the most influential person that impacted me on both an academic and a personal level. His supervision was critical to the successful completion of this thesis.

I would also like to thank very much Prof. Thien My Dao, my Ph.D. co-advisor, Prof. Van Ngan Le, and Dr. Zhengkun Feng, researcher, for their valuable advices over these years.

I would like also to thank Prof. Botez Ruxandra (Department of Automated Manufacturing Engineering at École de technologie supérieure), Prof. Victor Songmene, Prof. Zhaoheng Liu (Department of Mechanical Engineering at École de technologie supérieure) and Dr. Lyès Hacini (Raufoss Automative Components Canada) for being on my committee members. Their valuable and useful advices are gratefully acknowledged here.

I am thankful to Mr. Michel Drouin and Mr. Serge Plamondon for technical support during experiments.

I express my thanks to the Natural Sciences and Engineering Research Council (NSERC) of Canada for its financial support during this research.

Great appreciation is extended to the help given by my teachers and my colleagues in Department of Mechanical engineering - Cantho University (Vietnam), Department of Mechanical engineering - National Kaohsiung University of Applied Sciences (Taiwan).

Finally, I wish to thank my family, my wife and my friends for their kindness and continuous encouragement that was essential for the completion of my Ph.D. thesis.

ANALYSE DU PROCÉDÉ ASYMÉTRIQUE DE ROULAGE: SIMULATION DYNAMIQUE PAR ÉLÉMENTS FINIS ET EXPÉRIMENTATIONS

Hoang Quan TRAN

RÉSUMÉ

Le procédé de roulage est une technique efficace pour former des tôles à la courbure désirée en utilisant des rouleaux de formage. Ce type de procédé de formage de métal en feuille est l'une des techniques les plus utilisées pour la fabrication de formes creuses axisymétriques. En outre, ce processus commence à être sérieusement pris en considération par les industries pour produire de grandes pièces épaisses, comme la forme conique d'une couronne d'une roue de turbine Francis ou de celle de la tour d'une éolienne.

A cause des nombreux paramètres du procédé, réduire la force de flexion et améliorer la précision de la forme finale sont des défis importants pour le cintrage. Par conséquent, l'objectif principal de cette recherche est de trouver des stratégies pour réduire les forces de formage et d'améliorer la qualité finale de la pièce en utilisant des méthodes numériques et expérimentales. Dans cette thèse, un modèle 3D dynamique par éléments finis (FE) d'un processus de formage par roulage asymétrique est développé en utilisant le logiciel Ansys/LS-Dyna. Les résultats des simulations sont ensuite comparés aux expériences réalisées avec des tôles instrumentées et une machine de roulage. Les paramètres qui influencent la précision de la forme finale, c'est-à-dire les forces de flexion et les contraintes résiduelles laissées dans la plaque formée, ont été étudiés. L'application de ce modèle EF dynamique en 3D dans un contexte industriel permet de prédire l'intensité des forces de formage ou la précision du rayon de la forme finale et donc diminue le temps de mise au point avant la fabrication.

Les forces de formage peuvent être réduites en chauffant la plaque. Dans cette recherche, les relations entre la température de la plaque chauffée et les paramètres de sortie du procédé de cintrage tels que les forces appliquées et la qualité de la forme finale ont été étudiées en effectuant une simulation par EF et des calculs analytiques. Ces résultats amènent à une meilleure compréhension du mécanisme de formage avec ce procédé et permettent de fournir une opportunité pour la conception d'un système de chauffage efficace pour contrôler l'énergie thermique entrant dans la plaque pendant le processus de cintrage.

Cette recherche propose également une nouvelle approche simple pour réduire l'étendue des zones non-cintrées et l'intensité des forces de formage. Cette approche consiste à déplacer légèrement le rouleau inférieur le long de la direction d'alimentation et à ajuster l'emplacement du rouleau inférieur. Les résultats par EF indiquent que cette nouvelle approche minimise efficacement l'étendue des zones planes et réduit également les forces de formage.

Mots clés: procédé de roulage, analyse dynamique par éléments finis, force de formage, formage à chaud, étendue de plaque non-cintrée, Ansys/LS-Dyna

ASYMMETRICAL ROLL BENDING PROCESS STUDY: DYNAMIC FINITE ELEMENT MODELING AND EXPERIMENTS

Hoang Quan TRAN

ABSTRACT

Roll bending is an efficient metal forming technique, where plates are bent to a desired curvature using forming rolls. This type of sheet forming process is one of the most widely used techniques for manufacturing axisymmetric hollow shapes. Moreover, this process is beginning to be taken into serious consideration by industries for producing large, thick parts such as the conically shaped crown of a Francis turbine runner or of a wind turbine tower.

Because of the numerous processing parameters, reducing the bending force and improving the accuracy of the final shape are significant challenges in the roll bending process. Therefore, the primary aim of this research is to find the strategies for reducing forming forces and improving final part quality by employing numerical and experimental methods. In this thesis, a 3D dynamic Finite Element (FE) model of an asymmetrical roll bending process is developed using the Ansys/LS-Dyna software. The simulation results are then compared with experiments performed with instrumented parts and roll bending machine. The parameters that affect the accuracy of the final shape, the bending forces and the residual strain left in the formed plate have been investigated. Applying this 3D dynamic FE model in an industrial context may predict the forming forces or the accuracy of the final shape's radius and thus will decrease the setup time before manufacturing.

The forming forces can be reduced by heating the plate. In this research, the relationships between the heating plate temperature and the output parameters of roll bending process such as applied forces and final shape quality have been studied by performing FE simulation and analytical computations. These results yield to a better understanding of the mechanism of the process and provide an opportunity for the design of an efficient heating system to control the heat energy to be input in the plate during the roll bending process.

This research also proposes a new, simple approach for reducing flat areas and forming forces. This approach includes moving the bottom roll slightly along the feeding direction and adjusting the bottom roll location. The FE results indicate that this new approach effectively minimizes the flat area extents and reduces also the forming forces.

Key words: roll bending process, dynamic FEM, forming force, hot forming, flat end areas, Ansys/Ls-dyna

TABLE OF CONTENTS

Page

INTRODUCTION 1

CHAPTER 1 GENERAL INFORMATION AND THESIS ORGANIZATION 3
1.1 Overview of the roll bending process 3
1.2 Scope of research 7
    1.2.1 Study the effects of the roll bending process parameters 8
    1.2.2 Develop 3D dynamic FE model of the roll bending process 8
    1.2.3 Perform roll bending process experiments 9
    1.2.4 Analysis theory of roll bending process.. 9
    1.2.5 Live strain gauge measurements 9
1.3 Outline of thesis 10

CHAPTER 2 LITERATURE REVIEW 13
2.1 The roll bending process - state of the art...13
2.2 Investigation techniques for studying the roll bending process..........................20
    2.2.1 Analytical approach 20
        2.2.1.1 Relationship between the curvature and displacement of the forming roll 20
        2.2.1.2 Forming process principle... 21
        2.2.1.3 Reaction force 22
        2.2.1.4 Accuracy of the final shape... 23
    2.2.2 Finite element analysis approach 24
    2.2.3 Experimental approach 25
2.3 Heat assisted metal forming..27
2.4 Summary 31

CHAPTER 3 ARTICLE #1: ANALYSIS OF THE ASYMMETRICAL ROLL BENDING PROCESS THROUGH DYNAMIC FE SIMULATIONS AND EXPERIMENTAL STUDY 35
3.1 Abstract 35
3.2 Introduction...37
3.3 Geometric setup of roll bending machine..40
3.4 Finite element model..41
    3.4.1 Elements and mesh 42
    3.4.2 Contact surface and friction 44
    3.4.3 Loading 44
3.5 Experimental validation and measuring methodologies 44
    3.5.1 Verifying the final shape.. 45
    3.5.2 Recording and computing the bending force acting on the lateral roll..... 45
    3.5.3 Computing the bending force acting on the top roll 50
    3.5.4 Strain variation and deformed behavior of the plate................................. 53

3.5.5 Examining the rotational speed and supplied power of the roll bending machine 53
3.6 Results and discussion 54
3.6.1 Geometric verification model 54
3.6.2 Influence of plate thickness (t) and center location of lateral roll (i.e., a) on final shape radius (R) 57
3.6.3 Deformation characteristics of the forming plate 58
3.6.4 Influence of plate thickness “t” and center location “a” of lateral roll on bending forces F 63
3.6.5 Influence of the plate widths (H) on the bending force 66
3.6.6 Influence of the plate thickness (t) on supplied power (W) and rotational speed (RPM) of the rolls 67
3.7 Conclusions 68
3.8 Acknowledgements 69
3.9 References 69

CHAPTER 4 ARTICLE #2: HEAT ASSISTED ROLL BENDING PROCESS DYNAMIC SIMULATION 73
4.1 Abstract 73
4.2 Introduction 75
4.3 Analytical model 76
4.3.1 Elastic deformation P_1P_e 79
4.3.2 Elastic-perfectly plastic deformation P_eP_2 80
4.3.3 Elasto-plastic deformation P_2P_3 82
4.4 Computational modeling of heat forming technique 84
4.5 Finite element model 86
4.5.1 Element and mesh 86
4.5.2 Contact surface and friction model 89
4.5.3 Loading 89
4.6 Simulations and numerical results 90
4.7 Conclusion 99
4.8 Acknowledgements 99
4.9 References 99
4.10 Biographies 102

CHAPTER 5 ARTICLE #3: FE STUDY FOR REDUCING FORMING FORCES AND FLAT END AREAS OF CYLINDRICAL SHAPES OBTAINED BY ROLL BENDING PROCESS 105
5.1 Abstract 105
5.2 Introduction 106
5.3 Asymmetrical roll bending machine and flat areas definition 110
5.4 Finite element model of the asymmetrical roll bending process 112
5.5 Experimental study to validate the FE model 115
5.6 Results and discussion 120
5.6.1 Moving the bottom roll in the horizontal plane 121

    5.6.2 Moving the bottom roll in the vertical plane 124
5.7 Conclusions...127
5.8 Acknowledgement 128
5.9 References...128

CONCLUSION..131

RECOMMENDATIONS..135

APPENDIX I: EXPERIMENTS OF HEATING PLATE BY INDUCTION.......................137

LIST OF BIBLIOGRAPHICAL REFERENCES...140

LIST OF PUBLICATIONS 147

LIST OF TABLES

Page

Table 2.1 The features of the three-roll asymmetric and pyramidal model 19

Table 3.1 FE model and material properties parameters 43

LIST OF FIGURES

Page

Figure 1.1 The roll bending process in the manufacturing process classification 3

Figure 1.2 The roll bending process capability (Semiatin, 2006) 4

Figure 1.3 Examples of roll bending process's products (Iseltek Co., 2010) 5

Figure 1.4 Products made by roll bending process (Haeusler, 2010)...........................6

Figure 1.5 Example of Francis turbine runners (Alstom, 2014) 7

Figure 1.6 Scope of research diagram 8

Figure 2.1 The steam-powered roll bending machine (Allen, 1985) 14

Figure 2.2 Example of patent relating to roll bending machine (Patented-US807352A, 1905)...15

Figure 2.3 Three-roll asymmetric configuration 16

Figure 2.4 Three-roll pyramidal configuration...17

Figure 2.5 Four-roll configuration..18

Figure 2.6 Location of load-cells of four-roll model bending machine (Hua *et al.*, 1999) 26

Figure 2.7 Location of load-cells of three-roll model (Chudasama and Raval, 2012) 27

Figure 2.8 Effect of temperature on forming force (Juneja, 2013) 28

Figure 2.9 Temperature for different metal forming conditions (Mukherjee, 2013)..29

Figure 2.10 Example of conventional line heating work (Yoshihiko *et al.*, 2011).......30

Figure 2.11 Induction heating system (Larsson, 2005) 31

Figure 3.1 Asymmetrical three-roll bending machine..40

Figure 3.2 FE simulation model of asymmetrical three-roll bending machine...........42

Figure 3.3 Tensile testing curves and dog-bone specimen...43

Figure 3.4 Final shape radius verification 45

Figure 3.5 Recording deflection of the lateral roll with laser sensors........................46

Figure 3.6 Diagram of deflection checking by laser system 47

Figure 3.7 Measuring the bending force of the lateral roll..50

Figure 3.8 Measurement of the top roll deflection..51

Figure 3.9 Free body diagram of deflection..52

Figure 3.10 Strain gauges fixed onto workpieces 53

Figure 3.11 FE simulations of roll bending process at beginning of the process..........54

Figure 3.12 FE simulations of roll bending process at a) midpoint of the process and b) completion of the process 55

Figure 3.13 Geometric verification model 56

Figure 3.14 Final radius depending on the plate thickness and the lateral roll center location 57

Figure 3.15 Strain gauges setup for rolling 59

Figure 3.16 Strain variation at locations of strain gauges J_1, J_2 and J_3 a) experiments; b) typical location of A, B and C 60

Figure 3.17 Strain variations depending on center location “a” of the lateral roll........61

Figure 3.18 Strain variations depending on the plate thickness...................................62

Figure 3.19 Top roll bending force based on the plate thickness and center location of the lateral roll..64

Figure 3.20 Lateral roll bending force depending on the plate thickness and center location of the lateral roll..65

Figure 3.21 Top roll bending force depending on the plate width...............................66

Figure 3.22 Lateral roll bending force depending on the plate width 67

Figure 3.23 Supplied power depending on plate thickness..68

Figure 4.1 Asymmetrical three-roll bending machine geometry setup 77

Figure 4.2 Free body diagram of system...78

Figure 4.3 Equilibrium of forces of deformation 79

Figure 4.4 Heating approach a) at the early stage of heating up; b) during the forming process 85

Figure 4.5 FE simulation model of heating assisted roll bending process 86

Figure 4.6 Material properties: thermal expansion coefficient [24] 87

Figure 4.7 Material properties: a) Young's modulus and b) Yield stress [24] 88

Figure 4.8 Temperature distributions at 1 sec 90

Figure 4.9 Temperature distributions at: a) 30 sec and b) the process is completed 91

Figure 4.10 Temperature distributions at various heat flux values and plate thickness 92

Figure 4.11 Applied force as a function of heat input: t = 0.001 m and 0.002 m 93

Figure 4.12 Applied force as a function of heat input: t = 0.004 m and 0.008 m 94

Figure 4.13 Applied force for plate thicknesses at room temperature 95

Figure 4.14 Stress distribution at 1 sec 95

Figure 4.15 Stress distribution at: b) 30 sec and c) the process is completed 96

Figure 4.16 Geometric verification procedure 97

Figure 4.17 Radius of final shape on the different of heating temperature 98

Figure 5.1 Flat areas left by a roll bending process 107

Figure 5.2 Varying the location of the bottom roll a) offset d_i, and b) the “gap” value g_i 109

Figure 5.3 Parameter of three-roll asymmetric roll bending machine 110

Figure 5.4 Flat-end definition 112

Figure 5.5 FE model of the asymmetrical roll bending process 113

Figure 5.6 Stress-strain curve of plate material 114

Figure 5.7 Instrumented roll bending machine 115

Figure 5.8 Final shape obtained by the FEM 116

Figure 5.9 Flat end and radius computational procedure 117

Figure 5.10 Flat end length computational procedure..119

Figure 5.11 Final radius versus plate thickness and location of the lateral roll 120

Figure 5.12 Forming force on the rolls versus the values of d_i 121

Figure 5.13 Free body diagram of the roll bending process.......................................122

Figure 5.14 Flat-end length at the leading-end versus the value of d_i.........................123

Figure 5.15 Plate configuration when the bottom moves horizontally 124

Figure 5.16 Forming force of the rolls versus the value of g_i 125

Figure 5.17 Flat end versus the value of g_i...126

Figure 5.18 Varying plate contact lines with rolls when moving the bottom roll downward...127

LIST OF ABREVIATIONS

a	Center location of lateral roll along action line
E	Young's modulus of plate material
I	Moment of inertia of plate
k_1, k_2, k_3	Curvature of plate at region P_1P_e, P_eP_2 and P_2P_3
k_e	The maximum elastic curvature
K_p	The stiffness coefficient of system at P_1
M_1, M_2, M_3	Bending moment of plate at P_1, P_2 and P_3
M_e	The maximum elastic moment
P_t, P_b	Coordinates of the top and the bottom laser dots on the deformed lateral roll
P_{t0}, P_{b0}	Initial coordinates of the top and the bottom laser dots on the lateral roll
q_1, q_2, q_3	Contact forces at their respective angle θ_1, θ_2 and θ_3
Q_1, Q_2, Q_3	The applied forces by the respective top, bottom and lateral roll
R	Radius of the rolled cylinder
r	Radius of the rolls
s_1, s_2, s_3	Arc length coordinate of P_1P_e, P_eP_2 and P_2P_3
s	Initial arc length made by two laser beams dotting in lateral roll
t	Plate thickness
x_{os}, y_{os}	Initial location of the lateral roll center
x_{od}, y_{od}	Location of the lateral roll center under force
Y	the yield stress of plate
λ	Angle between the two laser beams
θ_1, θ_2, θ_3	Inclined angle of plate at P_1, P_2 and P_3
θ	Operating action line angle of offset cylinder
δ	The deflection of the roll at contact point P_1
ν	Poisson's ratio of the material
υ	Deflection of the top roll
υ_{lr}	Deflection of the lateral
μ	Friction coefficient

INTRODUCTION

The high strength steel axisymmetric hollow shapes are widely used in many fields of industry dealing with heavy cyclic loads and corrosive environments. But processing this type of steel is not easy, and it becomes a hard-to-solve problem when the part to produce is large and quasi-unique. Examples of high strength steel axisymmetric hollow parts are the crown of a Francis turbine runner or the tower of a wind turbine. Several processes can be envisaged for the manufacturing processes of such large parts (welding or casting…), but few processes can deliver one within a reasonable time and at competitive cost. Among them the roll bending is considered as an interesting alternative method.

Roll bending process is the plastic deformation of a metal that uses a set of rolls to bend a flat plate into various shapes such as cylinders, cones or ovals. It is a continuous three-point bending process with negligible change in plate thickness. Many different types of roll bending machines have been developed over the past few decades to adapt to various forming production specifications. However, the three-roll asymmetric model produces more accurate final shape, capable of forming a wider range of plate thicknesses, and especially, this kind of machine can be loaded and unloaded much faster than a three-roll pyramidal model. According to a literature review, most theoretical models, FE simulations and experimental verifications focused on four-roll model or three-roll pyramidal model but rarely on three-roll asymmetrical configuration.

After Chapter 1, general information about the roll bending process, and Chapter 2, which presents literature review, the thesis continues with Chapter 3 where a 3D dynamic finite element to simulate the forming process of the asymmetrical roll bending machine is compared to experiments. Parameters that affect the accuracy of the final shape, the bending forces and the residual strain left in the formed plate are investigated. In Chapter 4, the second step of this research is to find the strategies for reducing forming forces and improving final part quality. Two techniques are proposed to reduce forming forces: heating plate and optimize the setup for the rolls position. Heat assisted metal forming will be unavoidable if the forming forces necessary to bend the plate in cold working conditions exceed the capacity of the machine. The relationships between the heating plate temperature and the output parameters of roll bending process such as applied forces and final shape quality have been studied by performing FE simulation and analytical computations. These results yield to a better understanding of the mechanism of the process and provide an opportunity for the design of an efficient heating system to control the heat energy to be input in the plate during the roll bending process. Chapter 5 proposes one more method to reduce forming forces and to improve the accuracy of the cylindrical shapes obtained by the roll bending process. This approach includes moving the bottom roll slightly along the feeding direction and adjusting the bottom roll location. Sensitivity analyses were performed using a developed 3-D dynamic finite element model of an asymmetrical roll bending process in the Ansys/LS-Dyna software package. Simulations were validated by experiments run on an instrumented roll bending machine. The FE results indicate that this new approach not only minimizes the flat end areas but also reduces the forming forces.

Since large-casting possibilities have disappeared from Canada's industry, this research is a real opportunity for finding interesting alternatives to manufacture large and hollow axisymmetric parts.

CHAPTER 1

GENERAL INFORMATION AND THESIS ORGANIZATION

This chapter gives first an overview of the roll bending process and secondly scope and structure of the thesis.

1.1 Overview of the roll bending process

Roll bending is a continuous forming process that uses a set of rolls to bend a flat plate into various shapes such as cylinders, cones or ovals. As categorized by German standard DIN-8580 in Figure 1.1, this is a subgroup of forming process which is the plastic deformation of a metal around a linear axis with little or no change in surface area and thickness (Schuler, 1998).

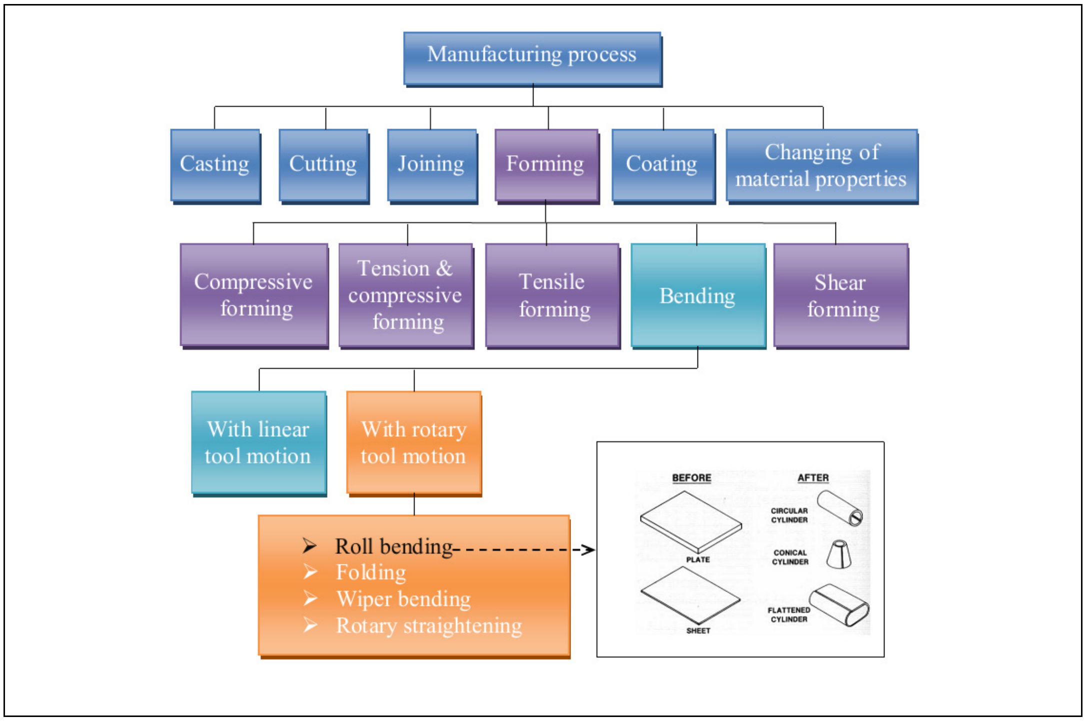

Manufacturing process
Casting
Cutting
Joining
Forming
Coating
Changing of material properties
Compressive forming
Tension & compressive forming
Tensile forming
Bending
Shear forming
With linear tool motion
With rotary tool motion
Roll bending
Folding
Wiper bending
Rotary straightening
BEFORE
AFTER
PLATE
SHEET
CIRCULAR CYLINDER
CONICAL CYLINDER
FLATTENED CYLINDER

Figure 1.1 The roll bending process in the manufacturing process classification

Like other forming processes, roll bending can be used to form any plate or sheet having enough ductile properties to be cold formed. It includes mild steels, stainless steels and heat resistant alloys (Todd *et al.*, 1994). Furthermore, nonferrous light alloys such as aluminum and copper alloys can also be successfully formed by this forming process. In practice, the minimum radius of the parts produced by roll bending process are typically limited by diameter of the rolls and type of machines, while the size and power of machine are the principal factors limiting the plate thickness and the width of final shape. As shown in Figure 1.2, the process capable can range from 150 mm (6.0 inch) to 5000 mm (200 inch) in final shape diameter with the plate thickness of approximately from 0.5 mm (0.02 inch) to 254 mm (10 inch) (Todd *et al.*, 1994). Today, the products of the roll bending process can be larger, wider and very much thicker. In a few applications, final shape with 300 mm in plate thickness or 12000 mm in width can be successfully formed by roll bending process (Semiatin, 2006).

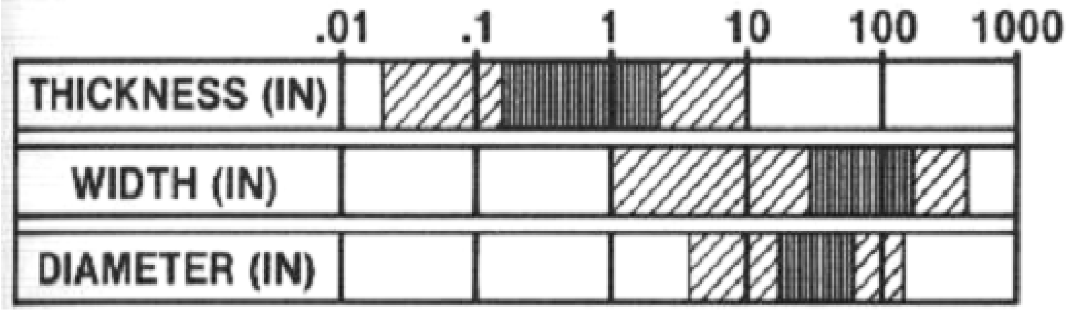

Figure 1.2 The roll bending process capability (Semiatin, 2006)

In comparison with other cold forming processes, such as deep drawing or contour roll forming, roll bending process has some unique advantages: wide range of final shape dimension, large plate thickness, numerous material applicability, process flexibility and good surface finish. Therefore, although it is an old process having a long history over of century, roll bending process is still the most practical method of producing large cylinders and axisymmetric hollow shapes. Figure 1.3 illustrates some example parts could be produced by roll bending process.

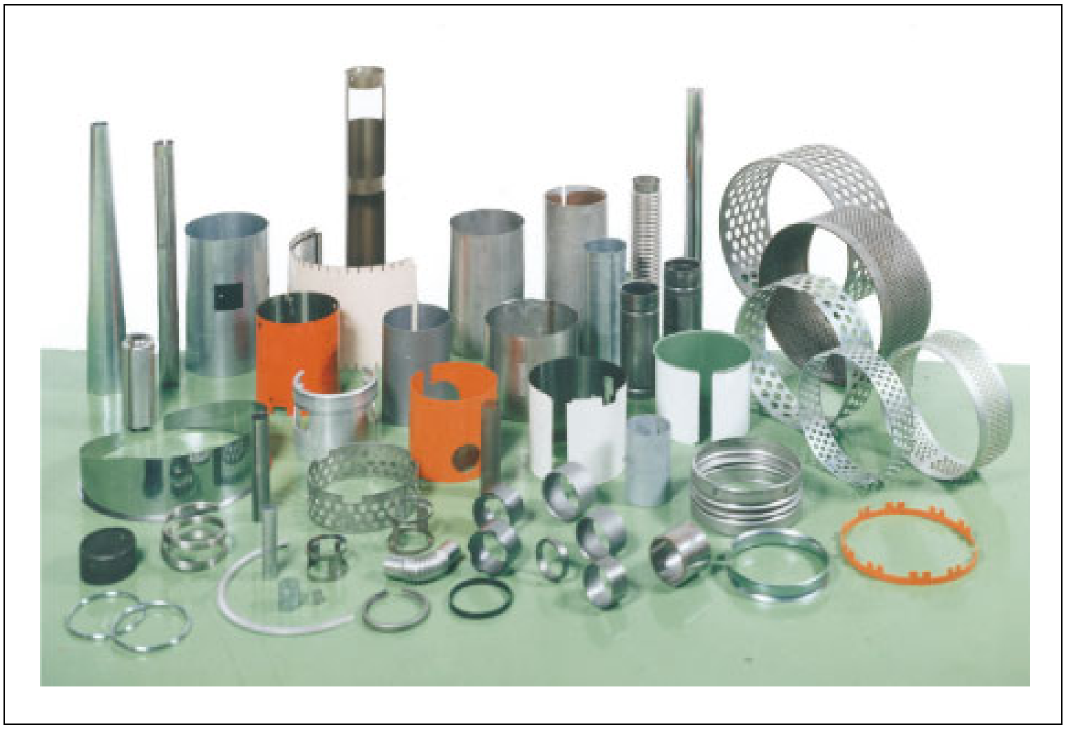

Figure 1.3 Examples of roll bending process's products (Iseltek Co., 2010)

This kind of forming process can be also used for manufacturing a wide range of products for various industries (see Figure 1.4) such as, asymmetrical cones (wind tower), silo construction or semi-finished products.

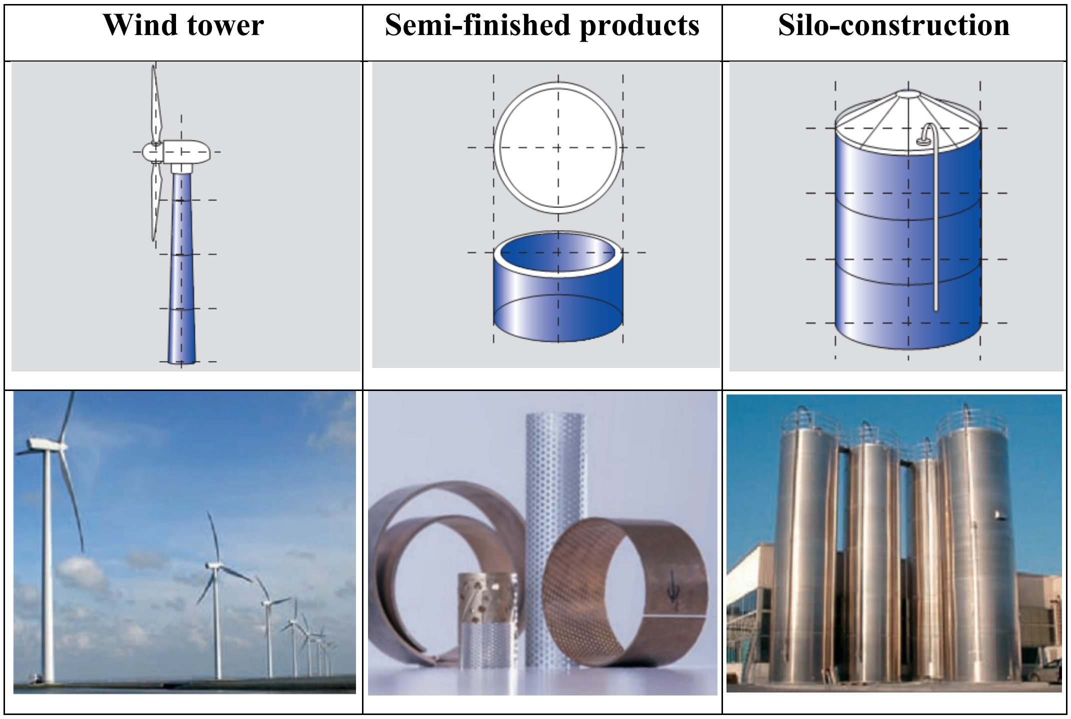

Figure 1.4 Products made by roll bending process (Haeusler, 2010)

Moreover, this process is beginning to be taken into serious consideration by industries for producing large, thick parts such as the thick, conically shaped of wind tower (Seravesi, 2006) or the crown (see Figure 1.5) of Francis turbine runner (Seravesi, 2006; Zeng, 2007). Some Francis turbine runners installed in the dam basement of a hydraulic power plant are 10 meters in diameter with more than 5 meters in height, while plate thickness can exceed 100 millimeters (Zeng, 2007). Several processes can be envisaged for the manufacturing processes of such large parts (welding or casting…), but few processes can deliver one within a reasonable time and at competitive cost. Among them the roll bending process, causing plastic deformation of a plate around a linear axis with little or no change in plate thickness, is considered as an interesting alternative.

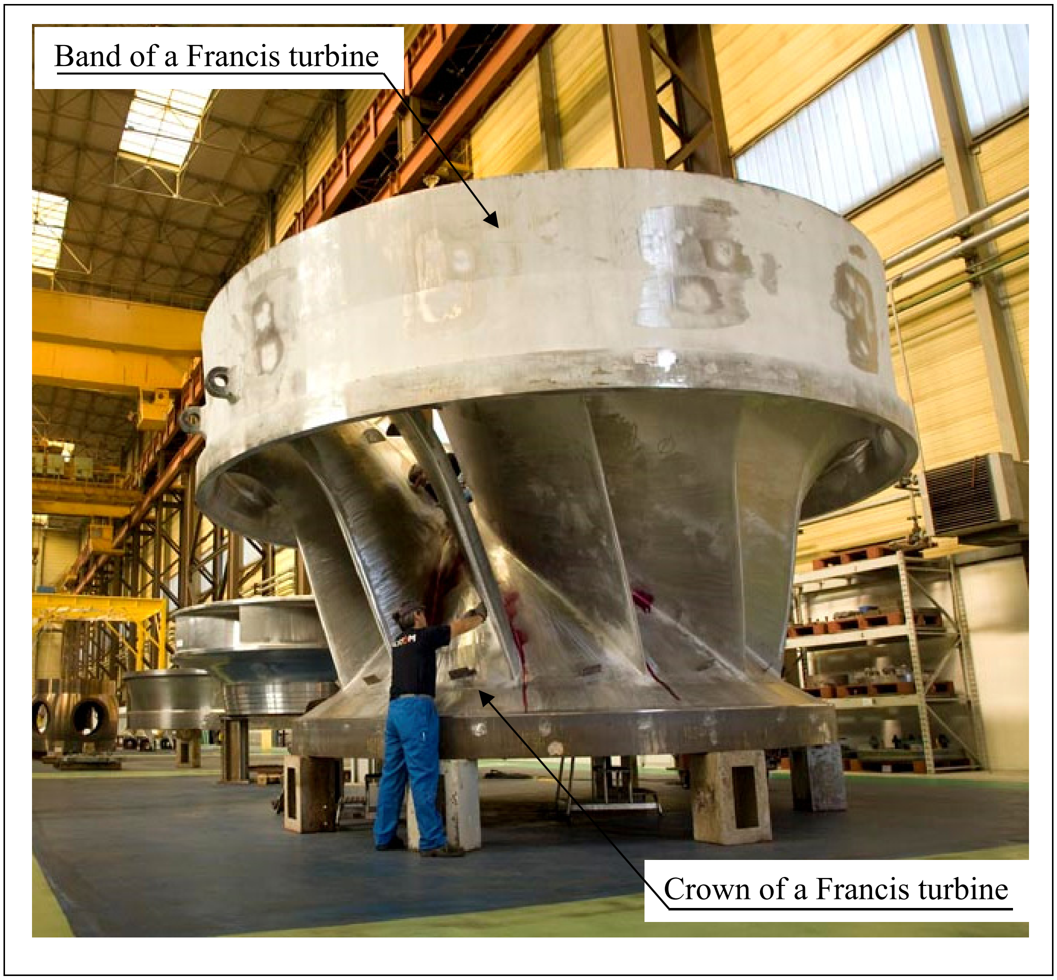

Figure 1.5 Example of Francis turbine runners (Alstom, 2014)

1.2 Scope of research

One goal of this research is to find the forces needed to shape axisymmetric hollow parts and thus to provide the methods for reducing the forming forces. Another goal is to predict the final shape geometry and quality. Currently, the finite element method is one of the most powerful numerical tools for achieving these goals. The diagram in Figure 1.6 indicates the relationship between input and output parameters of the roll bending process that have been investigated via this thesis.

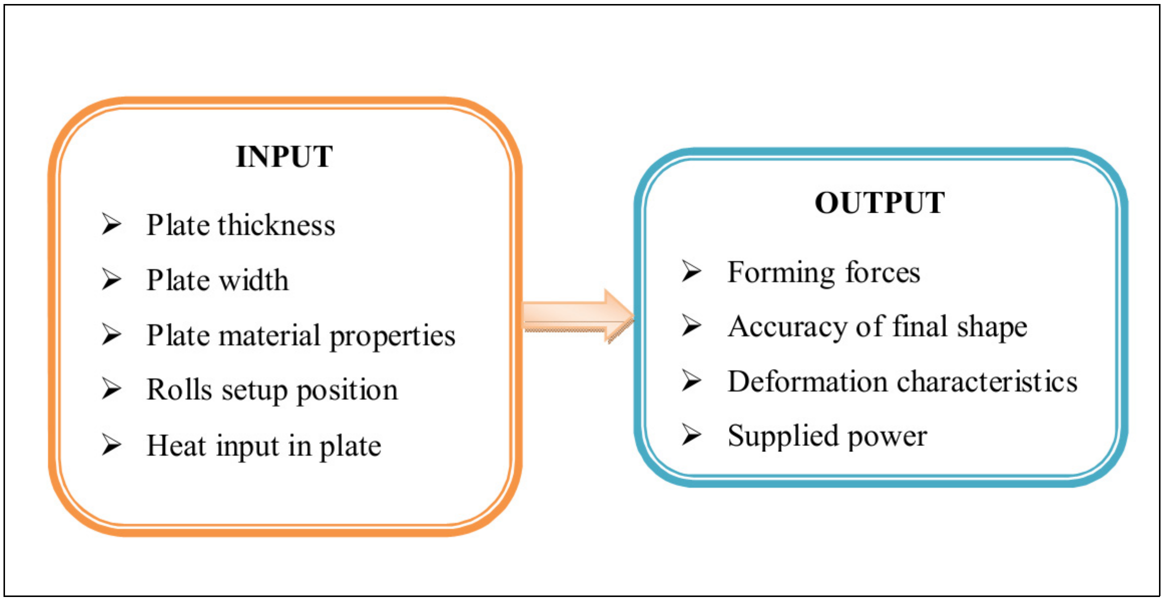
INPUT
Plate thickness
Plate width
Plate material properties
Rolls setup position
Heat input in plate
OUTPUT
Forming forces
Accuracy of final shape
Deformation characteristics
Supplied power

Figure 1.6 Scope of research diagram

Throughout this research, contributions have been made in five areas on the roll bending process.

1.2.1 Study the effects of the roll bending process parameters

This model investigates the parameters that affect the accuracy of the final shape, the forming forces and the residual strains left in the formed plate. The relationships between temperature, forming forces and plate thickness have also been investigated. A setup for the rolls was proposed in order to reduce forming forces and the flat areas at leading and trailing edges.

1.2.2 Develop 3D dynamic FE model of the roll bending process

A 3D dynamic FE model was developed in the Ansys/LS-Dyna environment and was validated satisfactorily through experiments. In an industrial context, the radius of the final shape in the roll bending process is generally determined based on “trial-and-error” or an empirical approach, which requires several attempts. Therefore, applying this FE model in manufacturing plants will be beneficial in providing the accuracy of the final shape's radius. This FE model also provides a better understanding of forming force for selecting or designing a machine capacity based on the plate thickness and the final shape sizes. Additionally, using this FE model will considerably reduce the setup time before manufacturing and increase the effectiveness of an existing asymmetrical roll bending machine.

1.2.3 Perform roll bending process experiments

A three-roll asymmetric bending machine was used to validate the FE models. To ensure qualitative experimental results, different measuring devices were used to verify the same output quantities of forming forces in this research such as indicators, load-cells and laser sensors. The final shape radii were evaluated by EXAscan laser scanner. The rotational speed of the rolls, supplied power, friction coefficient between the plate and rolls was checked by suitable equipments. In addition, a new experimental approach for measuring strains with strain gauges to obtain the strain variation left in the formed plate is also proposed in this research.

1.2.4 Analysis theory of roll bending process

By equilibrium of forces for each zone of bending plate, the theoretical study was developed in this research to study the forming forces depending on the various forming parameters.

1.2.5 Live strain gauge measurements

The analysis and measurement of the residual strain left in a roll bent plate are usually difficult to obtain, and no rigorous study on measuring strains during roll bending has been reported in literature to our knowledge. In this study, the strain gauges were mounted on the specimen surface and passed the rolls through grooves at the bottom and lateral rolls during the bending process to record the strain variations. FE results and experiments were compared and analysed for a better understanding of the deformation behavior of the workpiece before and after passing the bending roll. It also provides an accurate residual strain measurement procedure that relates the workpiece properties to the final shape dimensions and process parameters.

1.3 Outline of thesis

This thesis is divided in five chapters. It starts with chapter one about general information and chapter two on literature review. The three following chapters, presented as three journal articles, expose the main results of the research. Finally, conclusions, recommendations and suggestions for future work are also outlined. The detailed content is as follows:

Chapter 2, l**iterature review**, gives a comprehensive review related to roll bending process of the published literature to gain a better understanding the scope of thesis. It starts with a review of classification, advantage and disadvantage and the state of art of the roll bending process. In the second section, three main investigation techniques usually used in the research of the roll bending process are discussed. It includes analytical study, experimental investigation and finite element analysis. Detailed reviews on heat assisted and finite element theory on sheet metal forming are also presented in the final section of this chapter

Chapter 3, **journal article No. 01 - "Analysis of the asymmetrical roll bending process through dynamic FE simulations and experimental study"**, explains in details the techniques used to analyse the asymmetrical roll bending process through dynamic FE simulations and experimental study. This chapter then investigates the parameters that affect the accuracy of the final shape, the bending forces and the residual strains left in the formed plate. The FE simulation results are compared with experiments performed on an instrumented roll bending machine and are in good agreement.

Heat assisted roll bending process dynamic simulation is presented in Chapter 4, **journal article No. 02 – "Heat assisted roll bending process dynamic simulation"**. In this paper, a computer aided simulation program has been built in the Ansys/LS-Dyna environment to study the relationships between temperature, applied forces and plate thickness. The finite element modelling of the formed geometry is sequential with first a thermal simulation followed by a structural one. The numerical results are then compared to analytical ones. The analyses of the process with numerical simulations yield to a better understanding of the mechanism of the process and provide an opportunity for the design of an efficient heating system to control the heat energy to be input in the workpiece during the roll bending process.

Chapter 5, **journal article No. 03 – "FE study for reducing forming forces and flat end areas of cylindrical shapes obtained by roll bending process"**, proposes one more method to reduce forming forces and to improve the accuracy of the cylindrical shapes obtained by the roll bending process. This approach includes moving the bottom roll slightly along the feeding direction and adjusting the bottom roll location. Sensitivity analyses were performed using a developed 3-D dynamic finite element model of an asymmetrical roll bending process in the Ansys/LS-Dyna software package. Simulations were validated by experiments run on an instrumented roll bending machine. The FE results indicate that this new approach not only minimizes the flat areas but also reduces the forming forces.

The thesis will be concluded in final section. It summarises key conclusions of this research about the parameters that may affect the output of the roll bending process, the method to reduce the forming forces and improve the final shape quality. Recommendations and suggestions for future work are also proposed in this section.

CHAPTER 2

LITERATURE REVIEW

This chapter presents a literature review of published studies on the roll bending process to enhance understanding of the thesis objective. As mentioned, this research deals with finding the forming forces and predicting the final shape geometry via experiments and FE simulations. The literature review is divided in four sections, as follow:

1 The roll bending process - state of the art: history, classification, operation, advantage and disadvantage.
2 Investigation techniques for studying the roll bending process:
   - Analytical approach;
   - Experimental approach;
   - Finite element analysis approach.
3 Heat assisted sheet metal forming.
4 Summary.

2.1 The roll bending process - state of the art

It is not known when the first roll bending machine was introduced in the industry (Jenkins, 1936) but a similar machine was already operated in 1828. A few years later - in 1840, Sir William Fairbairn, a shipbuilder, built plate bending rolls to make boilers and other products made of iron and steel plates. During the Industrial revolution, steam engine was used to power the roll bending machine. Figure 2.1 shows a steam-powered plate bending rolls found at Sheepford Boiler Works, Scotland (Allen, 1985).

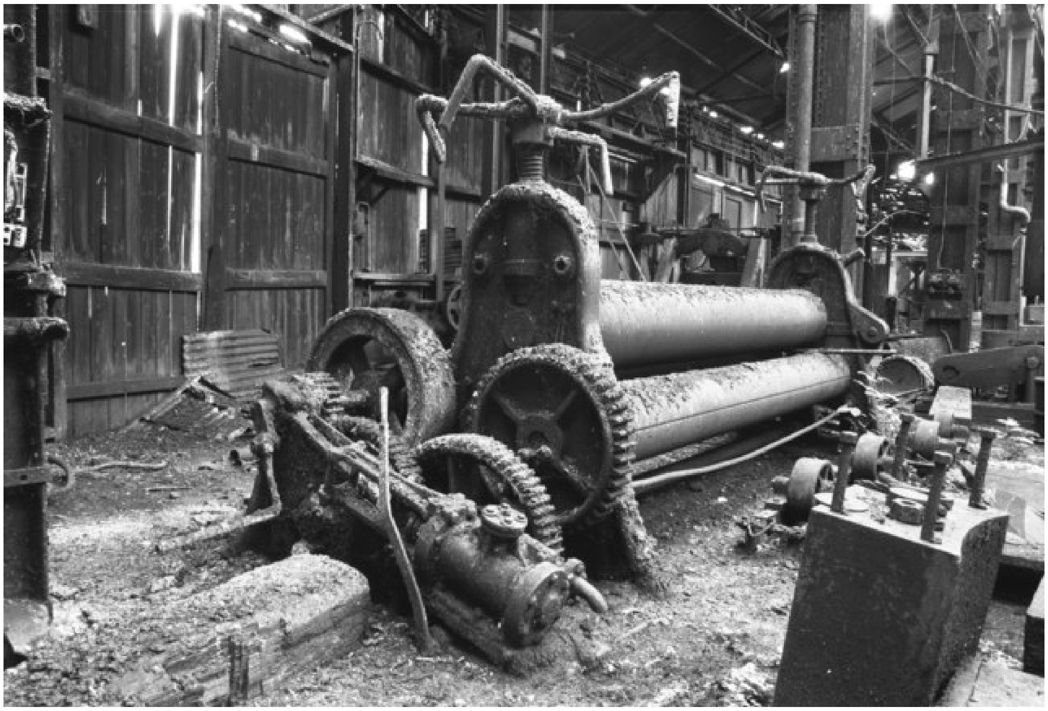

Figure 2.1 The steam-powered roll bending machine (Allen, 1985)

Between the late 19th and mid-20th centuries, the core technology of the roll bending machines was handheld. Various patents relating to such machines were found in these times with Figure 2.2 showing an example. Individual electric motors replaced progressively steam engine as power source.

Since the 1950's, servomechanisms and then hydraulic motors were applied to control the paths of the roll bending machine. The products of the roll bending machine are thus more accurate.

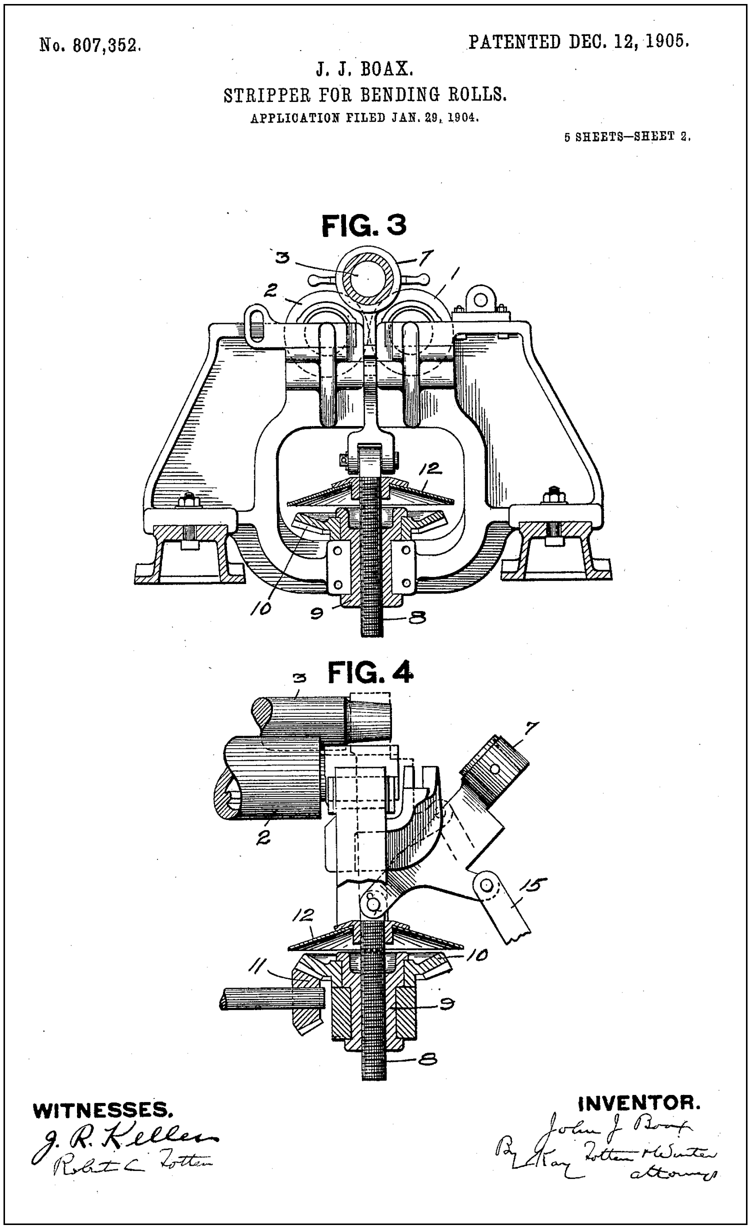

No. 807,352. PATENTED DEC. 12, 1905.

J. J. BOAX.

STRIPPER FOR BENDING ROLLS.

APPLICATION FILED JAN. 29, 1904.

5 SHEETS—SHEET 2.

FIG. 3

FIG. 4

WITNESSES.

J. R. Keller

Robert C. Totten

INVENTOR.

John J. Boax

By Kay Totten & Winter attorneys

Figure 2.2 Example of patent relating to roll bending machine (Patented-US807352A, 1905)

Nowadays, many different types of roll bending machines have been developed over the past few decades to adapt to various forming production specifications. However, these roll bending machines can be classified into two major types in the currently market: a three-roll model (including pyramidal and asymmetrical models) and a four-roll model (Hua and Lin, 1999). Roll bending process operations can be described as follows:

Three-roll asymmetric configuration (shown in Figure 2.3)

The manufacturing steps are described below (Semiatin, 2006) and (Faccin, 2014):

- Feed the plate into machine and move up the roll No.1 to "pinch" the plate.
- Rotate the roll No.1 and No.2 to pre-bent the plate.
- Reverse the roll No.1 and No.2 to remove the plate.
- Enter the plate into the machine from the other end and adjust the roll No.3 to final position.
- Complete cylinder and move down the roll No.1 to remove the final part.

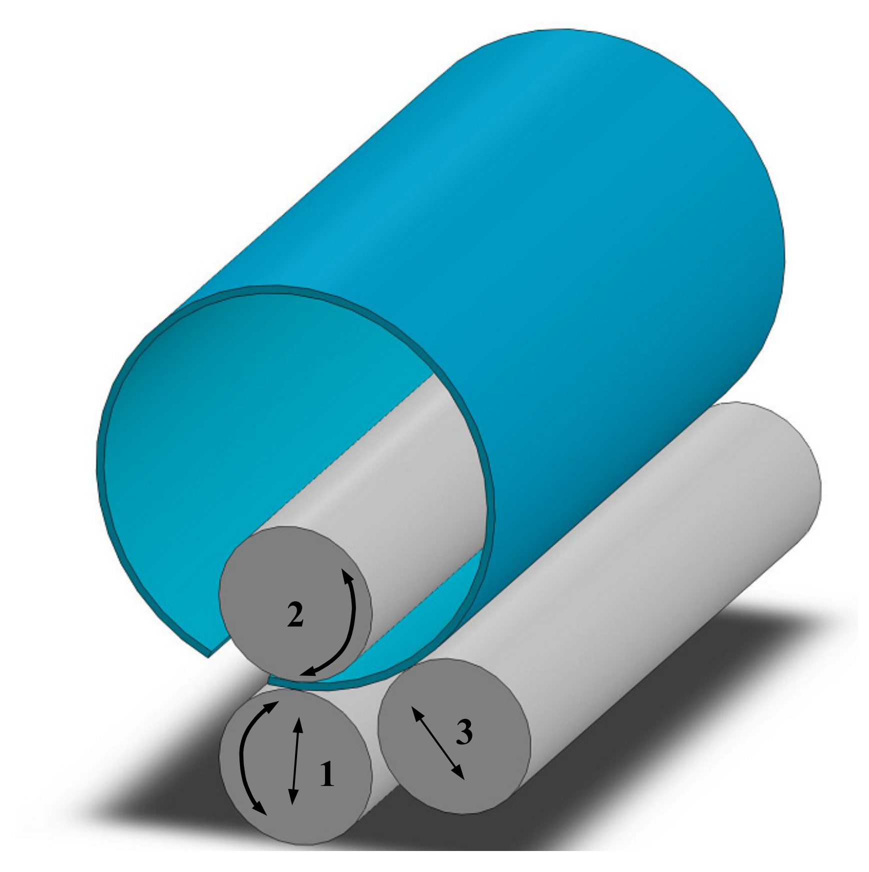

Figure 2.3 Three-roll asymmetric configuration

Three-roll pyramidal configuration (shown in Figure 2.4)

The manufacturing steps are described below (Semiatin, 2006), (Zeng, 2007) (Schleifstein, 2014) and (Faccin, 2014) :

- Feed the plate into machine and move down the roll No.2 to a defined position.
- Rotate the roll No.1 and No.3 to rough forming the plate.
- Edge bending 1 at the leading edge of the final part.
- Reverse the roll No.1 and No.3 to edge bending 2 at the trailing edge of final part.
- Complete cylinder and move up the roll No.2 to remove the final part.

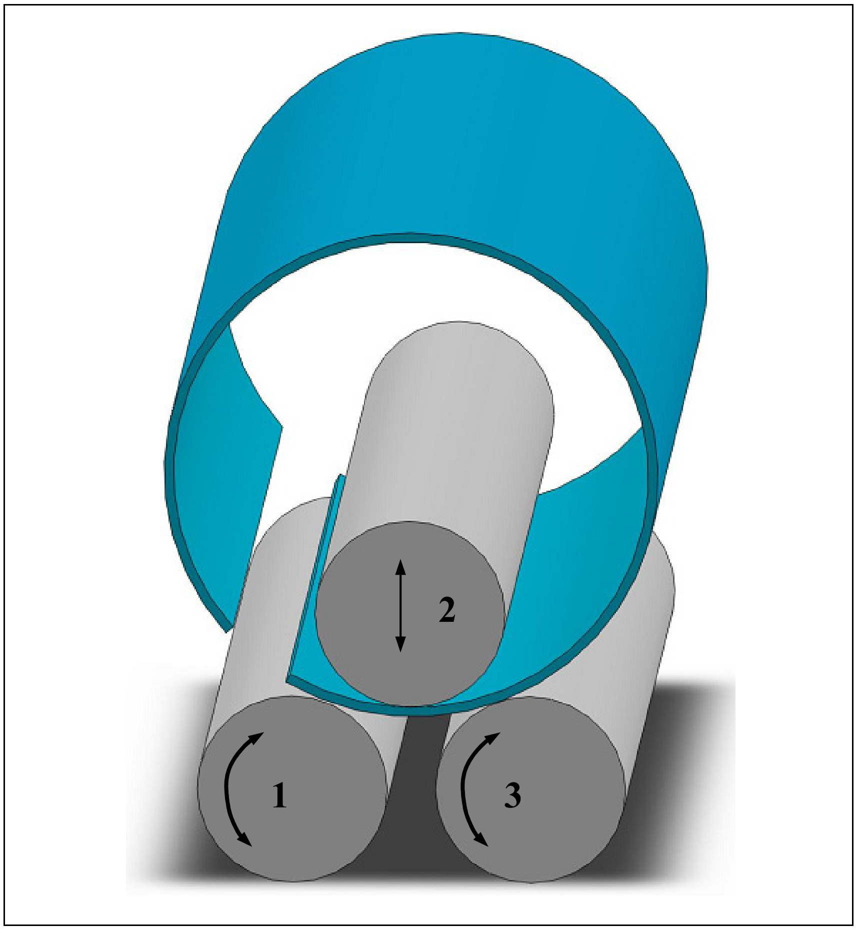

Figure 2.4 Three-roll pyramidal configuration

Four-roll configuration (shown in Figure 2.5)

The manufacturing steps are described below (Zeng, 2007), (Roundo, 2012; Schleifstein, 2014) and (Faccin, 2014):

- Place the plate to machine and move up the roll No.1 to "pinch" the plate.
- Move up the roll No 3-b and rotate the roll No.1 and No.2 to form the plate.
- Swap the roll No.3-a up and move down the roll No.3-b to continue form the plate.
- Complete cylinder and move down the roll No.1 and No.3-a to remove the final part.

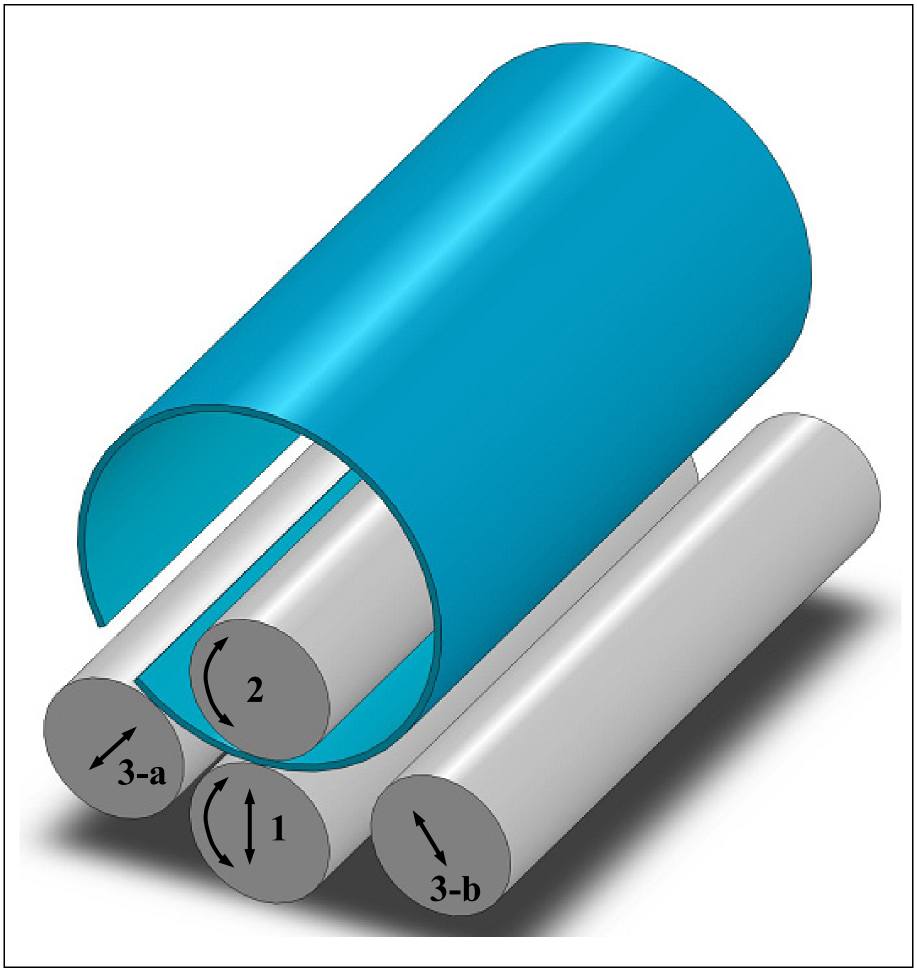

Figure 2.5 Four-roll configuration

Selection between a three-roll model and four-roll model machines depends mainly on the accuracy requirements, the dimension of products to achieve, the shape of the parts to be produced and the cost of machine (Marshall, 2010). The biggest advantage of four-roll model that have over the other three-roll machines is simplicity and easy cone bending (Hua and Lin, 1999) and (Zeng, 2007). But one advantage of three-roll model is its cost in current market. Three-roll model typically cost less than comparable four-roll model machines (Marshall, 2010). In this thesis, three-roll asymmetric model is selected to study forming forces and bending quality. Since there are two types of three-roll bending machines, let's briefly review the features of both. Table 2.1 compares main characteristics of three-roll bending machines.

Table 2.1 The features of the three-roll asymmetric and pyramidal model

Three-roll asymmetric configuration	**Three-roll pyramidal configuration**
Capable to pre-bend, leaves a smaller flat area at the leading and trailing ends in comparison to a three-roll pyramidal machine.	Unable to pre-bend, leave larger flat areas at both leading and trailing ends of the final shape.
Capable of forming a wider range of plate thickness than a three-roll pyramidal machine because of the method of feeding.	Definite limitations on the minimum thickness of the plate that can be rolled because the top roll is an idler
Unsuitable for forming the workpieces from angles, channels, and other structural shape.	Permissive for forming irregular shapes of the plate that is not adaptable to three-roll asymmetric model.
More accurate final shapes and it can be loaded and unloaded much faster than the three-roll pyramidal machine.	Less force demanded for a given deflection because forming forces are almost applied midway between the two bottom rolls.

The three-roll asymmetric model produces more accurate final shape, capable of forming a wider range of plate thicknesses, and especially, this kind of machine can be loaded and unloaded much faster than a three-roll pyramidal model.

The objective of this thesis is to study the feasibility of three-roll asymmetric model in forming axisymmetric hollow shapes for reducing forming forces and improving final part quality by employing numerical and experimental methods

2.2 Investigation techniques for studying the roll bending process

2.2.1 Analytical approach

2.2.1.1 Relationship between the curvature and displacement of the forming roll

Roll bending process seems to be a rather simple process, but the curvature of the bent plate is not that easy to handle by a theoretical analysis (Hansen and Jannerup, 1979). Since 1970s researchers focused on analysis of deformation of the plates in order to produce parts with better accuracy, (Hansen and Jannerup, 1979) proposed a function based on simple theory of plastic bending to find the position of top roller corresponding to a desired curvature for the final shape. (Hardt *et al.*, 1982) developed a shape control for a three-roll pyramidal model. This closed-loop control was designed to determine the relationship between bending moment and curvature and to compensate the springback of the workpiece in real time. In a research by (Seddeik and Kennedy, 1987), theoretical analyses lead to the minimization of total potential energy with a Rayleigh-Ritz technique. This analytical approach is used to calculate the relationship between the radius of curvature of bent plate and the resulting distortion in the cross section. (Yang and Shima, 1988) simulated deformation of the plate with a U-shaped cross section bent in a pyramid type three-roll bending machine. In this study, based on the properties of the plate, the authors calculated the bending moment and the curvature distribution of the plate in accordance with the displacement of the center roll and the rotation of the side rolls. Via elementary method, (Yang *et al.*, 1990) also analysed the relationship between the bending moment and the curvature distribution of the plate. These results were then used to build an automatic control system for producing a U-shaped cross section bent bar with a pyramid type three-roll bending machine. The analysis of the motion of rolls for forming a plate into a desired curvature in a pyramid type three-roll bending machine has been carried out by (Yang *et al.*, 1994). In this research, the authors used FEM simulation and fuzzy reasoning to determine the path of the forming roll. In each deformation step of FEM simulation, the movement of forming rolls is iteratively adjusted by a feedback control based on fuzzy reasoning. Others have concentrated on relationship between the curvature and displacement of the forming roll. By assuming the contact point to be shifting at the bottom roll plate interfaces and neglecting the changing of material properties during deformation and the effecting of initial strain, (Gandhi and Raval, 2008) proposed an analytical to estimate the position of the top roll as a function of final radius of curvature for a pyramid type three-roll plate bending machine.

2.2.1.2 Forming process principle

Most of the published literature along history focused on working principle and relevant deformation mechanisms see for example the work of Hua *et al*. However, all of these theory models were developed for four-roll model but not for three-roll asymmetric model.

By separating the bending process into 1) the edge preparation bending mode and 2) the continuous bending mode, (Hua *et al.*, 1994) discussed relevant mechanism and its influential parameters for the continuous four-roll model. (Hua *et al.*, 1995) developed a mathematical model to determine the internal bending resistance at the top rolls contact for multiple pass process on a four-roll bending model. In 1997, (Hua *et al.*, 1997) proposed a formulation by equilibrium of the internal and external bending moment about the top roll contact to determine the bending force on the rolls in the continuous single pass four-roll model. Some mathematical models have been also established by (Hua and Lin, 1999) to simulate the forming of elastic-perfectly plastic plates on a continuous four-roll model bending machine.

(Hua *et al.*, 1999) analyzed the working principles and some relevant bending mechanics of the rolls to exploit more fully the potential of the benders for manufacturing large and medium sized tubular sections on four-roll model.

(Hua and Lin, 1999) provided an analytic approach to study the effect of an arbitrary strain hardening plate in edge bending mode with the four-roll model. The mathematical model is developed by solving the governing differential equation for the large deflection of an elasto-plastic thin plate having general strain-hardening law. Influence of material strain hardening on the mechanics relevant to the whole process of four-roll bending machine was then investigated via this mathematical model. Based on the same analysis technique of (Hua and Lin, 1999), in a more recent study, (Lin and Hua, 2000) analyzed influence of material strain hardening on the mechanics relevant to the continuous mode on the four-roll model bending machine. Deformation of plate for edge bending mode on four-roll model bending machine was discussed via mathematical model by (Lin and Hua, 1999). The parameters relevant to this forming process were also defined in this research. (Hu and Wang, 2001) applied upper bound and lower bound methods to study the mechanism of the roll bending process. In their paper, a new roll bending model was proposed. This model resolves a few inadequacies of traditional roll bending processes and allows more flexibility in the formation of large bending parts.

2.2.1.3 Reaction force

The reaction forces during bending process are dependent on several parameters: plate thickness, plate width, material properties and diameter of final shape to be bent. With consuming most of the machine power, the maximum bending force is one of the most important information for designing bending equipment. Analytical models developed in the literature addressed the problem of bending force prediction for three-roll pyramidal model. (Gajjar *et al.*, 2007) developed analytical models for equivalent thickness and equivalent width, which are based on the power law material model for studying the bendability within the machine capacity. By equating the external bending moment to internal bending moment developed in the plate, (Chudasama and Raval, 2012) proposed an analytical model for the prediction of bending force during the multiple pass 3-roller conical bending. A similar approach has also been employed by (Chudasama and Raval, 2013) to present mathematical model for force prediction for 3-roller conical bending process. Effects of various material properties and geometrical parameters on the bending forces have been studied in detail. (Chudasama and Raval, 2014) developed the numerical model for the prediction of the bending force during dynamic stage of 3-roller conical bending process. In considering shear stresses developed in the plate along with the normal stresses during the roll bending, this analyis can be effectively used to get the roller bending force as well as the effects of various parameters like material parameters and geometrical parameters on it.

2.2.1.4 Accuracy of the final shape

Most of the analytical models developed in previous studies focus on forming process principle, reaction forces and relationship between the curvature and displacement of the forming roll. But few references are addressing the problem of the flat ends extents and the accuracy of the final shape.

The mechanics of the three-roll bending process for smoothly curved plates has been proposed by (Shin *et al.*, 2001). Both analytical and finite element approaches were applied to develop a logical and accurate procedure for determining the center roller displacement required for the fabrication of a plate with the desired curvature. The analytical approach has been obtained by modifying and extending an existing model based on the beam theory. The finite element models built for comparison purposes, one with beam elements and the other one with plane strain shell elements, show that the analytical approach yields to sufficiently accurate results for smoothly curved plates and may be used to determine the center roller displacement according to the desired curvature. In order to improve the quality and productivity of final shape that is produced by roll bending process, (Gandhi *et al.*, 2009) develop the formulation of springback and machine setting parameters for continuous multi-pass bending of conical shape on three-roll bending machines. In this paper, effect of change of flexural modulus during the deformation was incorporated to study the effect on spring-back prediction. (Cai and Lan, 2011) analyzed the straight end problem in a thin plate, pyramid-type machine through the development of an analytical method. However, the authors did not discuss the flat areas produced by a three-roll asymmetric machine and did not propose a method to reduce the straight end.

2.2.2 Finite element analysis approach

Through the last decades it has been discovered that it is expensive and time consuming to run experimental investigations that may only give a limited understanding of the roll bending process. Moreover, the interest in simulating and accurately predicting the deformations during the roll bending process and the geometrical characteristics on the final product has been increased. Therefore, the application of numerical simulation of the roll bending process was suggested.

According to (Logan, 2006), "The Finite Element Method (FEM) is a numerical method for solving problems of engineering and mathematical physics" The term FEM was coined by Ray W. Clough in his publish in 1960 (Logan, 2006). The first commercial finite element analysis code came of age in the early 1960's with the replacement of analogue with digital computers. At this early stage, the application was confined to static analysis to evaluate the performance of the machine structure. For studying about roll bending machine stands, (Ramamurti et al., 1992) performed FE simulation to study the static response of the frame of a three-roll pyramidal machine when it is in operation.

Roll bending process modeling is a high nonlinear problem and required intensive and costly computational operations. With the continuous development of computers, memory requirements and computer performance are extremely improved in recent years. The limited nonlinear solvers such as, nonlinear behaviors of material, nonlinearity due to contact or nonlinear loading, were developed and made available in commercial FEM software, such as ANYSY/LS-DYNA, ABAQUS, AUTOFORM, etc. Instead of using an implicit analysis, 3D explicit FE analysis method has been chosen by most researchers to analyse and simulate such kind of nonlinear behaviour exhibited by the roll bending process. (Zeng *et al.*, 2008) developed 3-D simulations based on the elastic-plastic explicit finite element method with Ansys/LS-Dyna to study the dynamic process of the three-roll pyramidal model. In this study, the kinematic relationship existing between rolls and workpieces, the geometrical setup and the finite element mode are discussed in detail for manufacturing a conical tube using the conical rolls of a three-roll pyramidal model. Feng *et al* conducted a considerable amount of FE modeling and simulation to investigate the three-roll bending process. In 2009, (Feng *et al.*, 2009) developed a finite element model for studying non-kinematical pyramidal three-roll bending. By using the attachments to reduce the velocity on the area close to the top edge of the plate, this FE model can be used to simulate the manufacturing of the conical parts with cylindrical rolls on a pyramidal three-roll bending machine. Based on the same approach, (Feng and Champliaud, 2012) developed a FE model of pyramidal three-roll bending process to produce the conical shapes with conical rolls. In 2011, (Feng and Champliaud, 2011) proposed a three-stage process to improve the geometrical quality of a bent cylinder obtained from FE simulations. The asymmetrical three-roll bending process was also developed by (Feng and Champliaud, 2011) in 2011. This FE models were capable of predicting the position of the lateral roll and helped to increase the productivity by improving the traditional trial and error technique. (Ktari *et al.*, 2012) and (Fu *et al.*, 2013) also used the commercial finite element package, ABAQUS/Explicit environment, to study the forming process of the pyramidal three-roll bending.

2.2.3 Experimental approach

FE simulations or theoretical analyses may have the potential to provide a better understanding of the phenomena in the roll bending process, and can therefore decrease the setup time before manufacturing and the amount of materials wasted by using the trial-and-error approach. However, before applying these techniques to the actual process, verification via experiments are used to validate the numerical model. Most of the experimental published works that addressed the relationship between the curvature and displacement of the forming roll were used to validate the theoretical approach. It includes the publications of (Hansen and Jannerup, 1979), (Hardt *et al.*, 1982), (Seddeik and Kennedy, 1987), (Yang and Shima, 1988), (Yang *et al.*, 1990), (Yang *et al.*, 1994) and (Gandhi and Raval, 2008). Different experiments have been conducted to study: a) the forming process principle (Hu and Wang, 2001) and (Ramamurti *et al.*, 1992); b) the FE simulations (Feng and Champliaud, 2011) and (Fu *et al.*, 2013). Experimental investigations of forming forces have been carried out by some researches. (Hua *et al.*, 1999) used the load-cells to measure the forming force acting on the rolls of four model roll bending machine as shown in Figure 2.6.

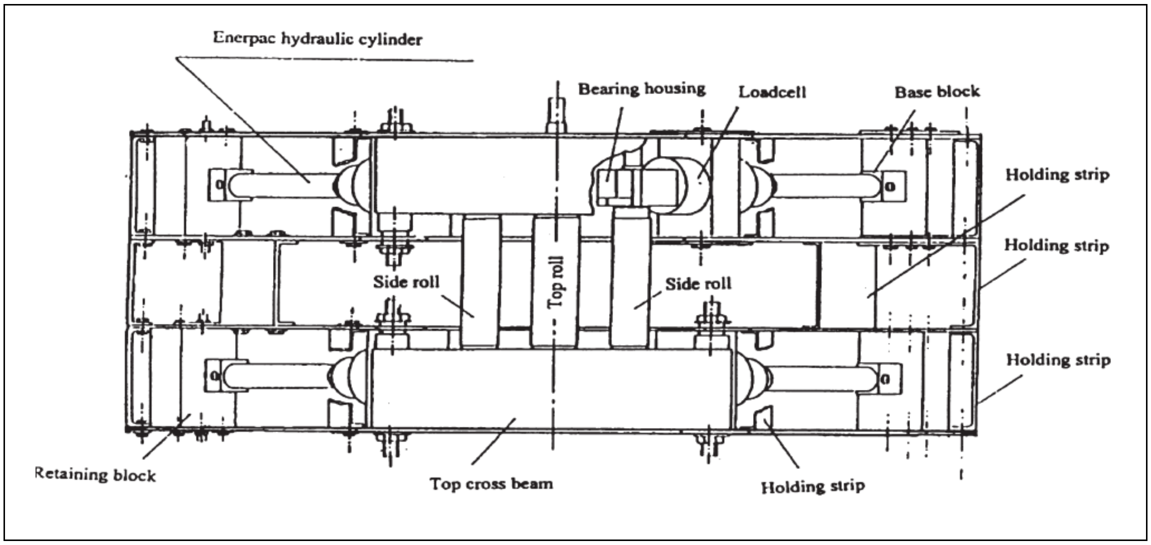
Enerpac hydraulic cylinder
Bearing housing
Loadcell
Base block
Holding strip
Holding strip
Side roll
Top roll
Side roll
Holding strip
Retaining block
Top cross beam
Holding strip

Figure 2.6 Location of load-cells of four-roll model bending machine (Hua *et al.*, 1999)

Each load-cell can measure the axial force and bending force and the recorded signal was converted to a resultant force. Using the same measurement approach, (Chudasama and Raval, 2012) attached the load-cells to the rolls of a three-roll pyramidal model to measure the reaction force at the top and at the bottom roll as shown in Figure 2.7

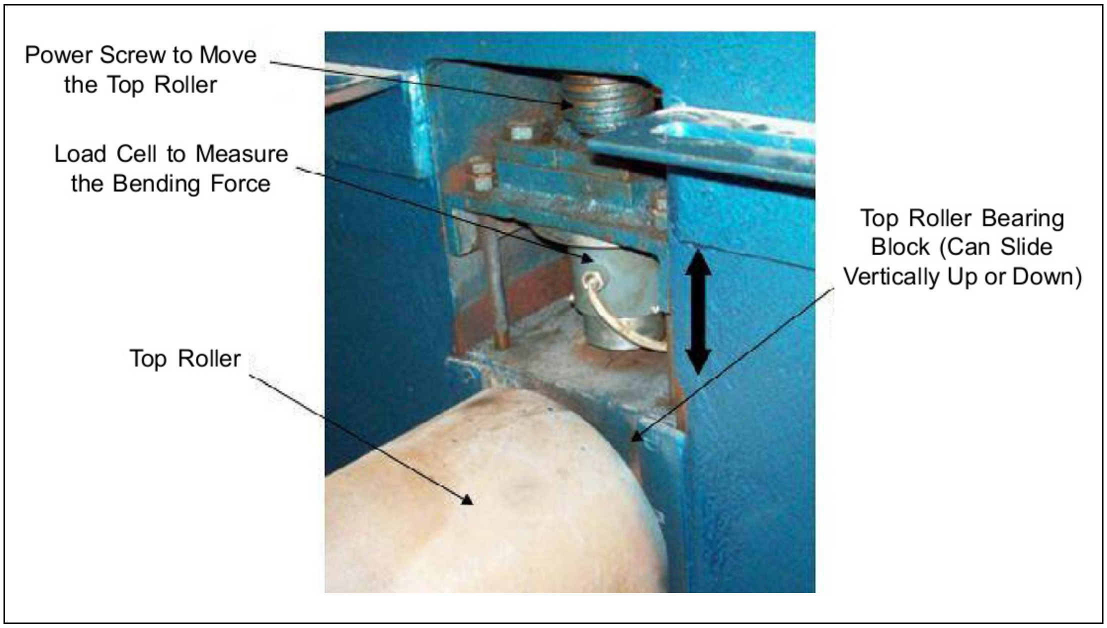
Power Screw to Move the Top Roller
Load Cell to Measure the Bending Force
Top Roller
Top Roller Bearing Block (Can Slide Vertically Up or Down)

Figure 2.7 Location of load-cells of three-roll model (Chudasama and Raval, 2012)

2.3 Heat assisted metal forming

In metal forming industries, processes may be carried out for three basic working temperature ranges: cold, warm and hot (Mukherjee, 2013). The review of manufacturers' practices indicated that most the metal forming process is generally performed at room temperature because it offers a number of distinct advantages at this working condition. However, heat assisted metal forming will be unavoidable if the forming forces necessary to bend the plate in cold working conditions exceeded the capacity of the machine.

As shown in Figure 2.8, most of the metallic materials become softer at high temperatures. Strategic use of heat input could help to lower forces required for forming.

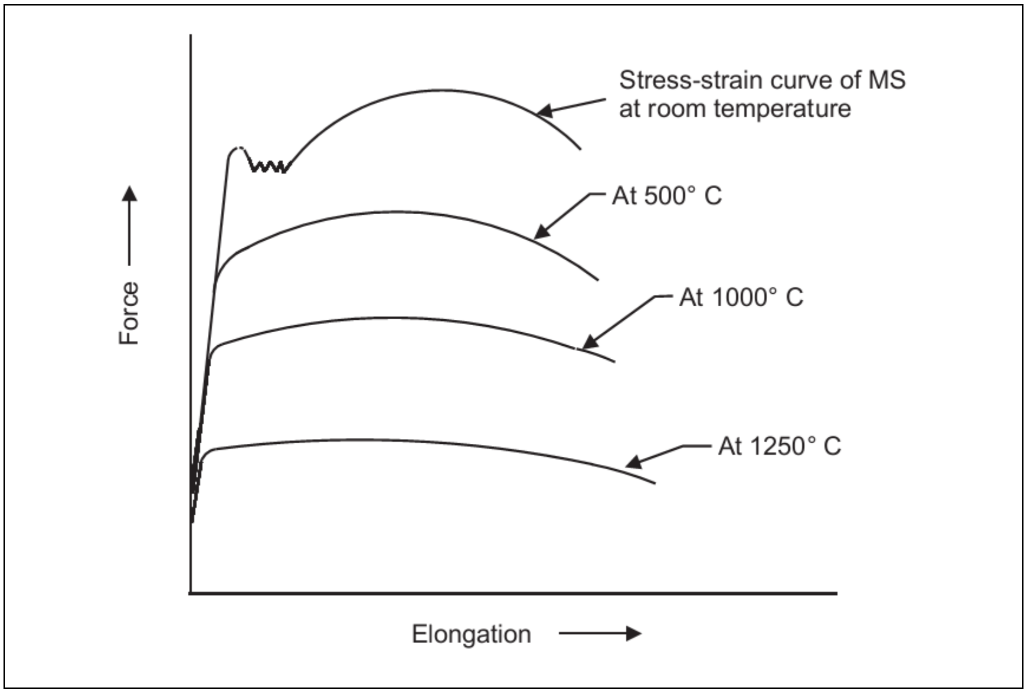

Figure 2.8 Effect of temperature on forming force (Juneja, 2013)

Lower accuracy and surface finish, higher production cost and shorter tool life are basically drawbacks of the hot forming. But in comparison with cold and warm forming, hot forming has some advantages such as, lowering forces and power required, increasing the amount of deformation and reducing strain hardening (Mukherjee, 2013) and (Juneja, 2013). Therefore, at higher temperature any deformation operation can be performed with lower forces and less power. It leads to reduce the cost of equipment needed for the process.

As shown in Figure 2.9, where T_A is the room temperature and T_m is the melting temperature of the material, the boundary between warm and hot conditions is defined by temperature of re-crystallization. Cold working is metal forming at room temperature, warm forming is performed at a temperature higher than room temperature but lower than the re-crystallization temperature while hot working is carried out at temperatures above the re-crystallization temperature (Mukherjee, 2013).

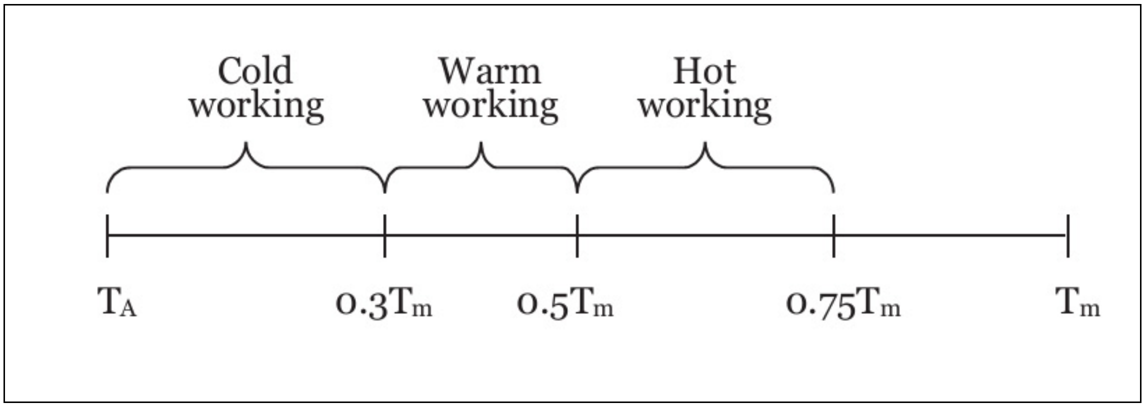

Figure 2.9 Temperature for different metal forming conditions (Mukherjee, 2013)

The metal forming process in hot condition is basically done using one of these two options: globally heated plate or locally heated plate (Larsson, 2005). Globally heated plate is heat assisted metal forming where the entire of the bent plate is heated uniformly to one target temperature in an oven. The heated plate is then fed into the machine for forming. Another method used for softening the material in hot forming is known as locally heating or line heating. This forming technique has been an active research topic in manufacturing, especially in ship-building (Yu *et al.*, 2001). A simple example of conventional line heating work can see in Figure 2.10.

Globally heated plate can be formed more easily than when it is locally heated, but the plate has to be removed from the oven to the machine itself with heat loss occurring during the transfer (Larsson, 2005). Maintaining the temperature at an acceptable working limit in the plate thus is a great challenge for this heat assisted forming process.

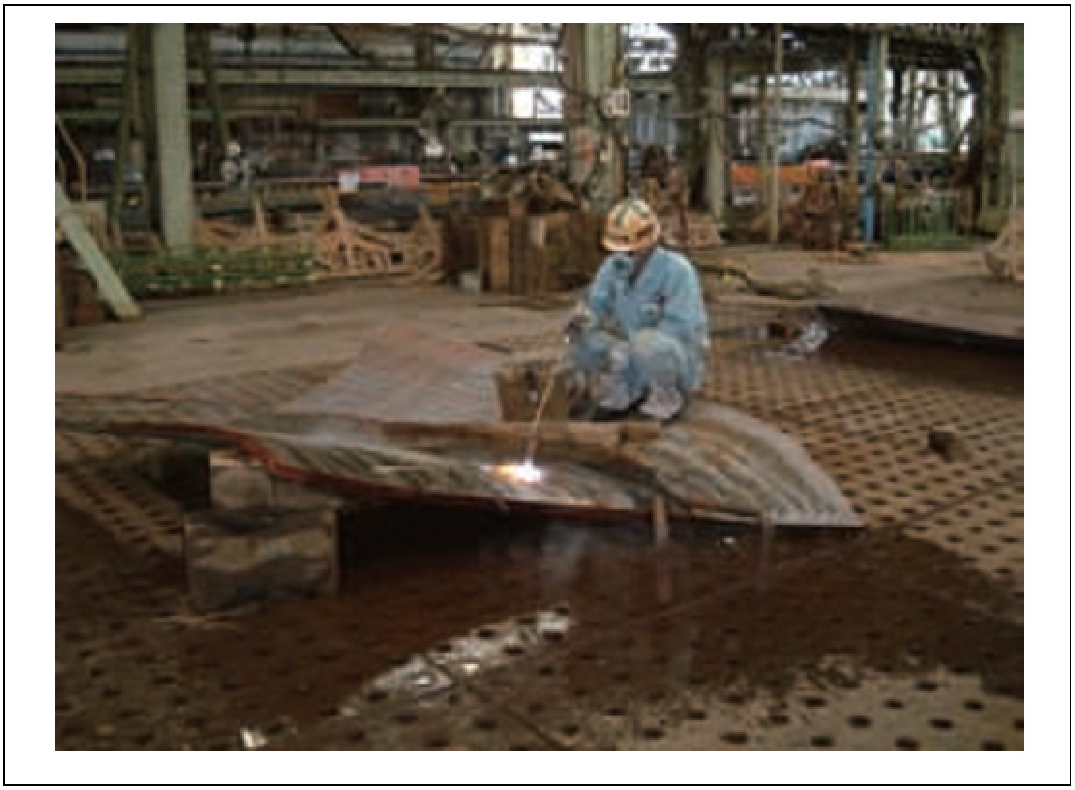

Figure 2.10 Example of conventional line heating work (Yoshihiko *et al.*, 2011)

The literature review illustrate that most of the researchers in previous studies focused on thermal forming, known as tool less or non contact material forming technology of sheet metals. There are limited studies available in heat assisted process in metal forming. For thermal forming, gas (oxy-fuel) flame, laser, plasma and inductor are mainly heat sources using for sheet metal bending (Tangirala, 2006), (Liu *et al.*, 2009). With the earliest work on laser forming beginning in the mid-1980s (Yu *et al.*, 2001), many of the process and material parameters were analyzed using laser heat sources both experimentally and analytically. In comparison with plasma, laser provides a highly controllable heat source. The plate surface therefore could be rapidly heated by this heat source (Tangirala, 2006). An alternative to lasers to provide a cheaper and safer means to bend plate (Tangirala, 2006), plasma jet forming used a non transferred plasma arc as a heat source to create the necessary thermal gradient in the plate. Compared to other heat sources, induction heating has good controllability, repeatability and a pollution-free working environment (Larsson, 2005). It is therefore a promising technology that will be used in a wide range of industries for metal forming application. This system mainly consists of an induction coil, an electrically conductive part and switched power electronics as shown in Figure 2.11 (Larsson, 2005). According to Faraday's Law, an electrically conductive part is located inside or in the nearness of the coil and eddy currents will be induced in the object when alternating voltage is applied. As a result of the Joule effect, eddy currents will produce heat.

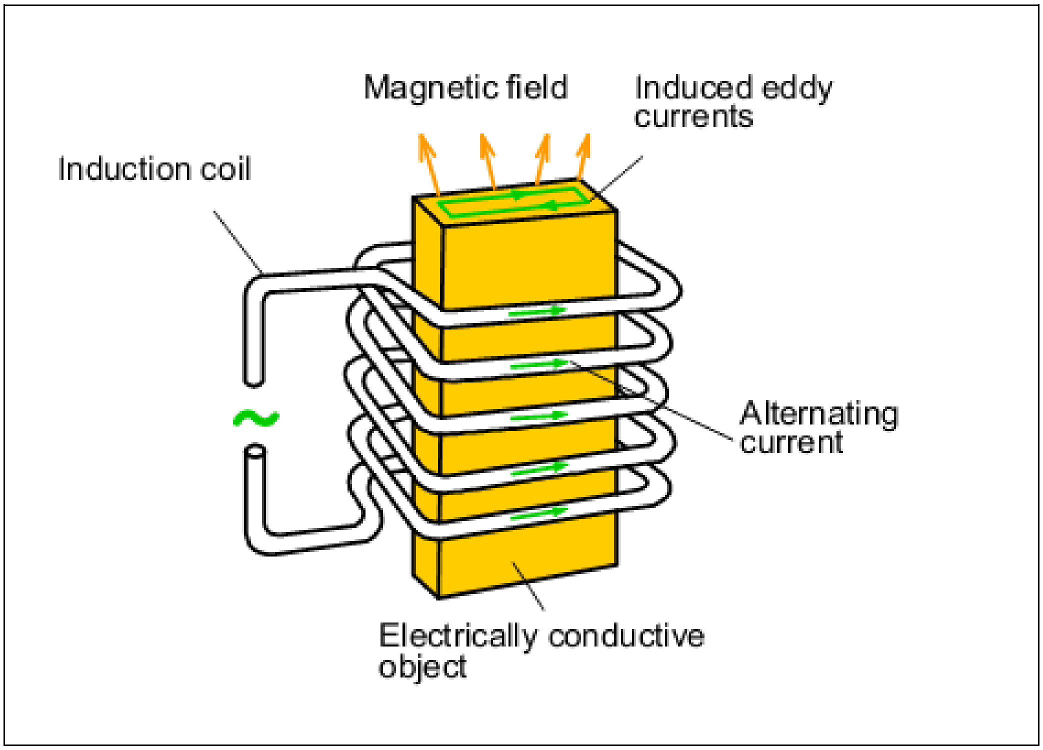
Magnetic field
Induced eddy currents
Induction coil
Alternating current
Electrically conductive object

Figure 2.11 Induction heating system (Larsson, 2005)

Though heat input of the three heat sources are different, the forming mechanisms are the same (Liu *et al.*, 2009).

2.4 Summary

This chapter presented a literature review of topic regarding the state of the art of the roll bending process, investigation techniques for studying it and heat assisted metal forming.

The roll bending process is a process having a long history over one century; it is still the most practical method of producing large cylinders and axisymmetric hollow shapes. Based on the discussions above, some major knowledge gaps can be drawn:

The three-roll asymmetric model produces more accurate final shape, capable of forming a wider range of plate thicknesses, and especially, this kind of machine can be loaded and unloaded much faster than a three-roll pyramidal model. However, most theoretical models, FE simulations and experiment verifications in the literature focused on four-roll model or three-roll pyramidal model but none of them on three-roll asymmetrical model. The parameters that affect the accuracy of the final shape, the bending forces and the residual strains left in the formed plate is only partially understood. Thus, there are many challenges for understanding the forming process with this type of machine.

The forming forces can be reduced by heating the plate. But, to the author's knowledge, up to now, there is no published study about heat assisted roll bending process. In this research, the relationships between the heating plate temperature and the output parameters of roll bending process such as applied forces and final shape quality have been studied by performing FE simulation and analytical computations. These results yield to a better understanding of the mechanism of the process and provide an opportunity for the design of an efficient heating system to control the heat energy to be input in the plate during the roll bending process.

A roll bending process that minimizes the flat areas at the leading and trailing ends of formed plates will produce more accurate and easier to butt joint the bent ends of the plate. There are several methods of minimizing flat areas, but these techniques are costly or difficult to apply for thick plates. Via FE simulations in Ansys/LS-Dyna software package, this study proposes a new, simple approach that reduces these flat areas. This approach includes moving the bottom roll slightly along the feeding direction and adjusting the bottom roll location. The FE results indicate that this new approach not only minimizes the flat areas but also reduces the forming forces.

The analysis and measurement of the residual strain left in a roll bent plate are usually difficult to obtain, and no rigorous study on measuring strains during roll bending has been reported, to our knowledge, in the literature. In this study, strain gauges were mounted on the specimen surface and passed through the rolls without been crushed, thanks to the grooves machined in the bottom and lateral rolls. Finite element results and experiments were compared and analysed for a better understanding of the deformation behaviour of the workpiece before and after passing the bending roll.

CHAPTER 3

ARTICLE #1: ANALYSIS OF THE ASYMMETRICAL ROLL BENDING PROCESS THROUGH DYNAMIC FE SIMULATIONS AND EXPERIMENTAL STUDY

Quan Hoang Tran • Henri Champliaud • Zhengkun Feng • Thien My Dao

Mechanical engineering department, École de technologie supérieure (ÉTS), Montréal (Québec) H3C 1K3, Canada

Article published in International Journal of Advanced Manufacturing Technology,
Volume 75, Issues 5, pp. 1233 - 1244, 2014

3.1 Abstract

Because it is influenced by various processing parameters, predicting the bending force and improving the accuracy of the final shape are significant challenges in the roll bending process when the part to be produced is large and made of high-strength steel. In this paper, a 3D dynamic Finite Element (FE) model of an asymmetrical roll bending process is developed using the Ansys/LS-Dyna software. This model investigates the parameters that affect the accuracy of the final shape, the bending forces and the residual strains left in the formed plate. The simulation results are then compared with experiments performed on an instrumented roll bending machine. Strain measurements are also performed during forming with strain gauges fixed onto plate blanks. A good agreement between the experiments and simulations has been obtained.

Keywords Roll bending process • Dynamic FEM simulation • Ansys/LS-Dyna • Forming process

Résumé

La prédiction de la force de formage et l'amélioration de la précision de la forme finale sont des défis importants dans le processus de cintrage lorsque la pièce à réaliser est de grande dimension et faite d'acier à haute résistance. Dans cet article, un modèle 3D dynamique par éléments finis (FE) d'un processus de formage par roulage asymétrique est développé en utilisant le logiciel Ansys/LS-Dyna. Ce modèle examine les paramètres qui influencent la précision de la forme finale, les forces de flexion et les contraintes résiduelles laissées dans la plaque déformée. Les résultats des simulations sont ensuite comparés aux expérimentations réalisées avec une machine de roulage instrumentée. Les mesures de déformation sont également effectuées pendant le formage avec des jauges de contrainte fixées sur la plaque. Une bonne corrélation entre les mesures expérimentales et les simulations a été obtenue.

Mots-clés: Procédé de roulage • Analyse dynamique par éléments finis • Ansys/LS-Dyna • Procédé de formage

Nomenclature

a	Center location of lateral roll along action line
E	Young's modulus of plate material
I	Moment of inertia of plate
P_t, P_b	Coordinates of the top and the bottom laser dots on the deformed lateral roll
P_{t0}, P_{b0}	Initial coordinates of the top and the bottom laser dots on the lateral roll
t	Plate thickness
R	Radius of the rolled cylinder
r	Radius of the rolls
s	Initial arc length made by two laser beams dotting in lateral roll
x_{os}, y_{os}	Initial location of the lateral roll center
x_{od}, y_{od}	Location of the lateral roll center under force
λ	Angle between the two laser beams

θ	Operating action line angle of offset cylinder
ν	Poisson's ratio of the material
υ	Deflection of the top roll
υ_{lr}	Deflection of the lateral
μ	Friction coefficient

3.2 Introduction

Roll bending is a continuous forming process that uses forming rolls to bend plates, sheets, and even rolled shapes into the desired shape: cylinders, cones or ovals. Given the advantages, such as reducing the setup time, the raw material, and the tooling and equipment costs, the roll bending process is one of the most used techniques for manufacturing axisymmetrical shapes. Moreover, this process is a manufacturing method that is beginning to draw significant attention by industries for producing large, thick parts, such as the thick conical shape of the crown of a Francis turbine runner or of a wind turbine tower.

Many different types of roll bending machines have been developed over the past few decades to adapt to various forming production specifications. However, these roll bending machines can be classified into two major types currently in the market: a three-roll model and a four-roll model. The three-roll model includes pyramidal and asymmetrical models, for which basic principles and operations can be found in Ref.[1]. Generally, an asymmetrical model produces a more accurate final shape. In addition, it can be loaded and unloaded significantly faster than the pyramidal model [2]. Therefore, this type of machine is currently more widely used [3].

Roll bending process seems to be a rather simple process, but the curvature of the bent plate is not that easy to handle by a theoretical analysis [4]. Since 1960s, Bassett [5] performed experiments to measure the upper roll vertical force and the driving torque of the three-roll pyramid type plate bending machine. By assuming the contact point to be shifted at the bottom roll plate interfaces and neglecting the changing of material properties during deformation and the effecting of initial strain, Gandhi et al. [6] proposed an analytical method to estimate the position of the top roll as a function of final radius of curvature for a pyramid type three-roll plate bending machine. Yang et al. [7] simulated deformation of the plate with a U-shaped cross section bent in a pyramid type three-roll bending machine. In this study, based on the properties of the plate, the authors calculated the bending moment and the curvature distribution of the plate in accordance with the displacement of the center roll and the rotation of the side rolls. Cai and Lan [8] analyzed the straight-end problem in a thin-plate formed on a pyramid-type bending machine through the development of an analytical method. Hu et al. [9] applied upper-bound and lower-bound methods to study the mechanism of the roll bending process. In their paper, a new roll bending model was proposed. This model resolves a few inadequacies of traditional roll bending processes and allows more flexibility in the formation of large bending parts.

Most the work of Hua et al. focused on working principle and relevant deformation mechanisms for four-roll model. Hua et al. [10-11] analyzed the working principles and some relevant bending mechanics of the rolls to exploit more fully the potential of the benders on four-roll model. In 1997, Hua et al. [12] proposed a formulation by equilibrium of the internal and external bending moment about the top roll contact to determine the bending force on the rolls in the continuous single pass roll bending process. Hua et al. [13] provided an analytic approach to study the effect of an arbitrary strain hardening plate in an edge bending mode. The mathematical model is developed by solving the governing differential equation for the large deflection of an elasto-plastic thin plate having general strain-hardening law. Influence of material strain hardening on the mechanics relevant to the whole process of four-roll bending machine was then investigated via this mathematical model. Hua et al. [14] developed a mathematical model to determine the internal bending resistance at the top rolls contact for multiple pass process on a four-roll bending model. By separating the bending process into a) the edge preparation bending mode and b) the continuous bending mode, Hua et al. [15] discussed relevant mechanism and its influential parameters for the continuous four-roll model. Some mathematical models have been also established by Hua et al. [16] to simulate the forming of elastic-perfectly plastic plates on a continuous four-roll model bending machine.

3D explicit FE analysis has been used to simulate the roll bending process. However publications focused on four-roll model or three-roll pyramidal model and few of them on three-roll asymmetrical model. Zeng et al. [17] developed 3-D simulations based on the elastic-plastic explicit finite element method with ANSYS/LS-DYNA to study the dynamic process of the three-roll pyramidal model. In this study, the kinematic relationship existing between rolls and workpieces, the geometrical setup and the finite element mode are discussed in detail for manufacturing a conical tube using the conical rolls of a three-roll pyramidal model. Feng et al. conducted a considerable amount of FE modeling and simulation to investigate the three-roll bending process. In 2009, Feng et al. [18] developed a finite element model for studying non-kinematical pyramidal three-roll bending. By using attachments to reduce the velocity at the area close to the top edge of the plate, their FE model can be used to simulate the manufacturing of the conical parts with cylindrical rolls on a pyramidal three-roll bending machine. Based on the same approach, Feng et al. [19] developed a FE model of pyramidal three-roll bending process to produce the conical shapes with conical rolls. In 2011, Feng and Champliaud [20] proposed a three-stage process to improve the geometrical quality of a bent cylinder obtained from FE simulations. In addition, Ktari [21] and Fu [22] used the commercial finite element package, ABAQUS/Explicit environment, to study the forming process of the pyramidal three-roll bending.

The 3D dynamic FE asymmetrical three-roll bending process was also developed by Tran et al. to a) study the relationships between heating input, applied forces and plate thickness [23-24]; b) predict forming forces for manufacturing a conical shape [25]; and c) analyze the workpiece deformation [26] and flat ends areas [27]. Furthermore, Feng et al. [28] simulated the asymmetrical three-roll bending process to increase the productivity by improving the traditional trial and error technique.

According to the literature review, the process parameters that affect the accuracy of the final shape, the bending forces and the residual strains left in the formed plate are only partially understood. In this paper, a 3D dynamic FE model was developed in the ANSYS/LS-DYNA environment for an asymmetrical roll bending machine. The plate material was considered isotropic with an elasto-plastic behavior and friction was taken in account at the interfaces of the plate with the rigid rolls. Investigations were conducted to quantify the influence of process parameters on the forming forces and the accuracy of the final shape. Finally, numerical results were validated with an instrumented roll bending machine. In this paper, it is also proposed a new approach for measuring strain variations in the bent plate during the process. Applying this 3D dynamic FE model in an industrial context may predict the forming forces or the accuracy of the final shape's radius and thus will decrease the setup time before manufacturing.

3.3 Geometric setup of roll bending machine

In this paper, a typical asymmetrical three-roll bending machine is used to shape a plate with a thickness t, as indicated in Figure 3.1

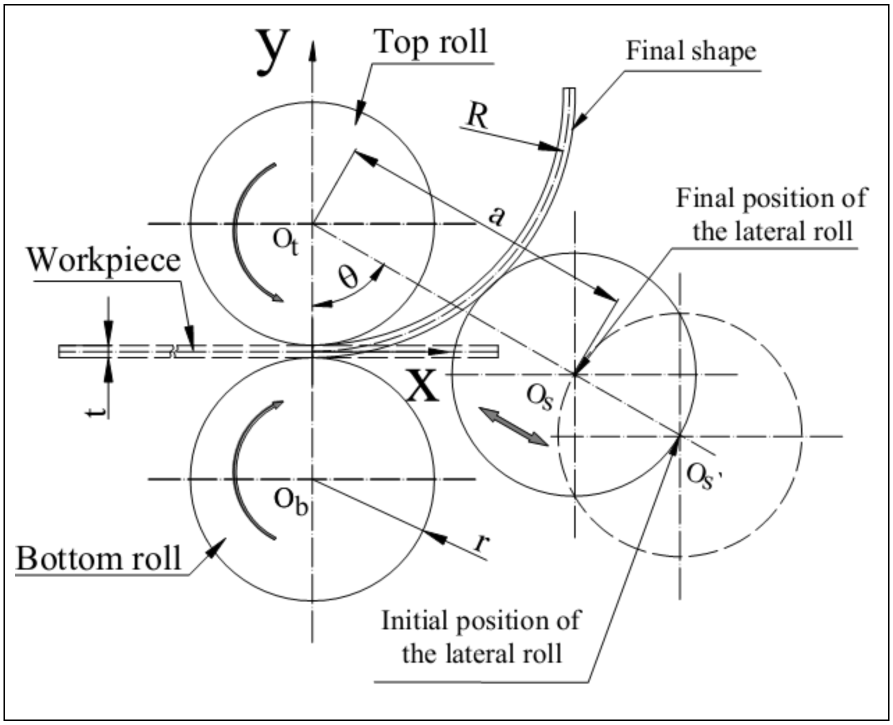
y
Top roll
Final shape
R
a
Final position of
the lateral roll
Workpiece
O_t
θ
X
O_s
O_s'
t
O_b
r
Bottom roll
Initial position of
the lateral roll

Figure 3.1 Asymmetrical three-roll bending machine

The workpiece is fed and "pinched" between the top and bottom rolls while the lateral roll moves up or down to adjust the radius R of the final shape. The top roll is in a fixed position; the up and down displacement of the bottom roll is adjustable to pinch the workpiece, ensure a sufficient grid to feed the plate and allow the removal of the finished workpiece. The final radius R of a formed cylinder depends on the position of the lateral roll center, which is expressed by the center distance "a" from the top roll to the lateral roll. From the elastic relationship between the position of the lateral roll and the final radius R of the formed cylinder [28], the relationship between the final radius R and the center location of the lateral roll along the action line (shown in Figure 3.1) can be expressed by Equation 3.1 as follows:

$$R=\frac{a}{2}\left[\frac{a\sin^2\theta}{2r+t-a\cos\theta}-\cos\theta\right] \tag{3.1}$$

where "a" is the center location of lateral roll along the action line, "r" is the radius of the rolls, "t" is the thickness of the workpiece, and θ is the operating action line angle of the offset cylinder.

3.4 Finite element model

A 3D numerical FE model of the asymmetrical three-roll bending process described in the previous section was developed in the Ansys/LS-Dyna environment [29]. Some assumptions for FE simulations of the bending process are summarized below [20]:

- The plate is considered as a shell since its thickness is small in comparison with its width and length.
- For the plate, the material is isotropic, with bilinear elastoplastic (BISO) behavior described by three constant properties: elastic modulus, yield stress and tangent modulus.
- The static and dynamic friction coefficients are constant.
- The rolls are assumed as rigid bodies.
- The weight of the plate is neglected.

3.4.1 Elements and mesh

In the ANSYS/LS-DYNA environment, when the plate thickness is significantly smaller compared to its width and its length, the geometry can be modeled using the explicit 4-node SHELL163 element with elasto-plastic capabilities. 8000 elements were used to mesh the plate: 50 elements in plate width and 160 elements in plate length. The rolls are considered as rigid bodies in comparison with the deformable plate. The FE model consists of four main components: three rigid rolls and one flexible plate, which are illustrated in Fig. 2.

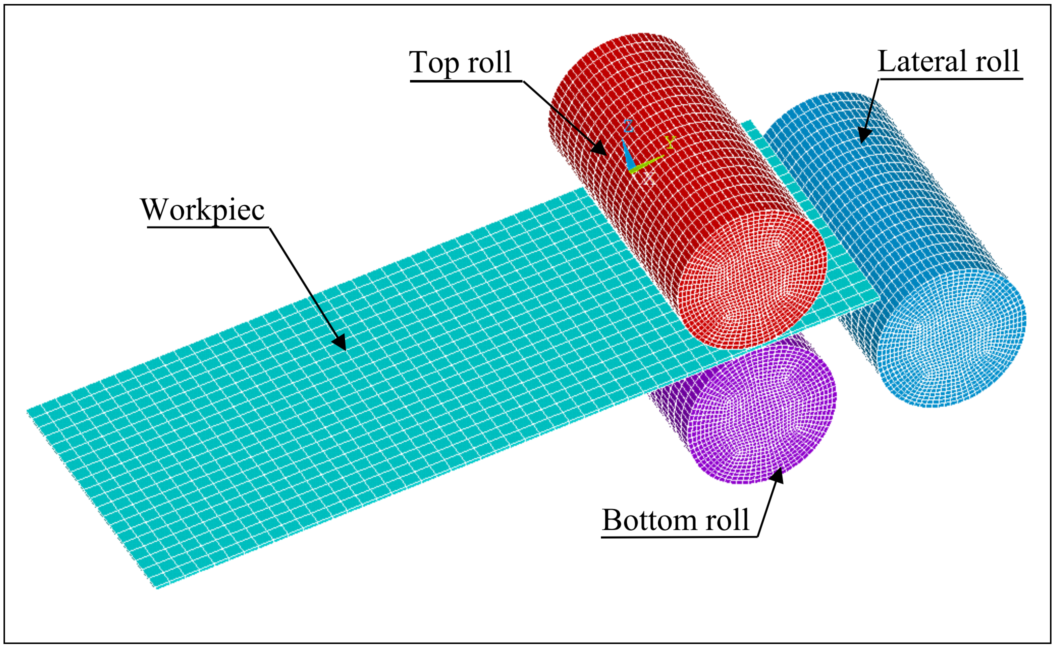

Figure 3.2 FE simulation model of asymmetrical three-roll bending machine

AISI-304 stainless steel plates of various thicknesses with a Young's modulus E of 195 GPa and a Poisson's ratio ν of 0.29 were used for the experiments in this study. The material constants E and nu were measured using tensile testing with dog-bone specimens cut with a water jet into shapes with dimensions based on ASTM-E8 testing standards. Figure 3.3 illustrates the results of a tensile test run using a 2.5 mm thick specimen. A bilinear isotropic (BISO) material model defined in Ansys/LS-Dyna was used to represent the elasto-plastic behavior obtained from uniaxial tensile tests.

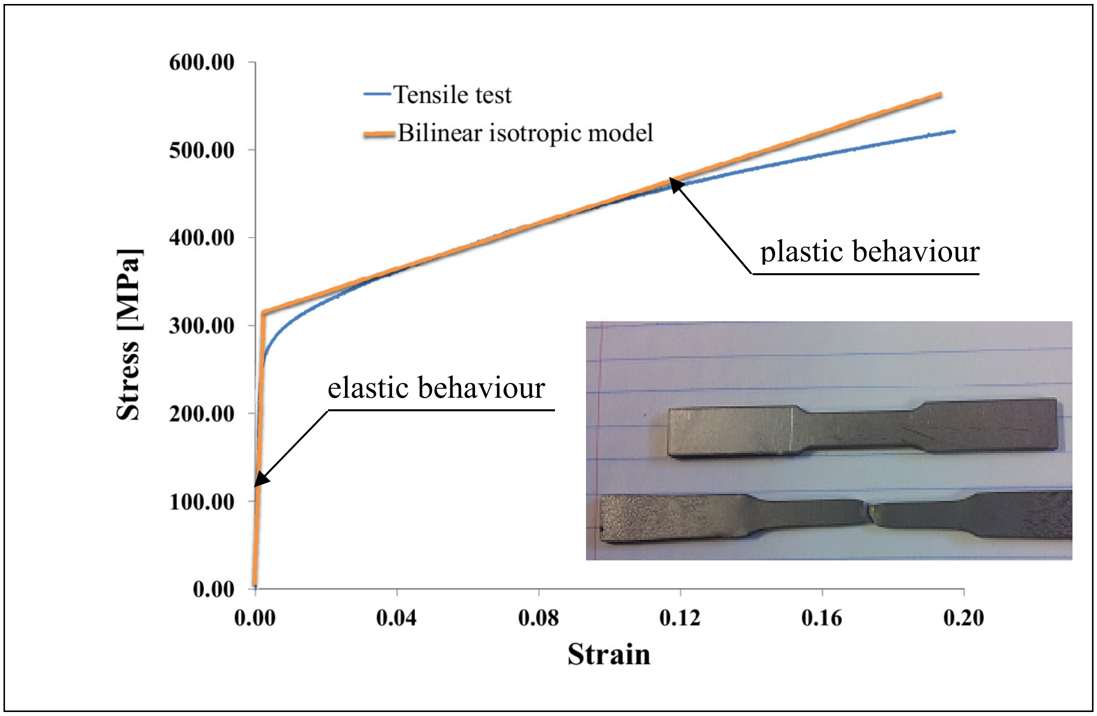

Figure 3.3 Tensile testing curves and dog-bone specimen

Table 3.1 FE model and material properties parameters

FE model parameters of the plate	
Type of element	SHELL-163
Type of interaction	Automatic node to surface
Number of element	8000
Static friction coefficient	0.2
Material properties of plate	
Material model	Bilinear isotropic
Young’s modulus (GPA)	195
Yield stress 0.2% proof (MPa)	274
Tangent modulus (GPA)	1.90
Poisson’s ratio	0.29
Density (kg/m^3)	7830

3.4.2 Contact surface and friction

The interaction between components is characterized through contact surfaces. In the roll bending process model, the surface of the roll is smaller than the surface of the workpiece. Although Ansys/LS-Dyna supports a large selection of contact options to define the interaction between surfaces in the explicit analysis, the automatic node to surface algorithm is used for the interaction between the rolls and the plate. This type of surface contact is efficient when a smaller surface comes into contact with a larger surface [30]. The workpiece is driven and deformed to its final shape through these contact surfaces. Furthermore, the static friction coefficient μ of 0.2 between the plate and the rolls is directly measured experimentally.

3.4.3 Loading

In the numerical simulations, the top and bottom rolls are driven in rotation and fixed in translation. The lateral roll is constrained in translation and experiences no self-rotation to press the forming plate against the top roll. The plate is only constrained by the rolls through contacts.

3.5 Experimental validation and measuring methodologies

A three-roll asymmetric model machine with a roll radius r of 50.0 mm, a roll length of 1500.0 mm and an operating action line angle of lateral roll θ of 60° (see Figure 3.1) was available in our lab and used to validate the FE simulation model.

A series of experiments and FE simulations using the same forming conditions, machine parameters, workpiece dimensions, etc., were conducted to investigate the bending force variations and factors that may affect the accuracy of the final shape. Additionally, to ensure qualitative experimental results, different measuring devices were used to verify the same output quantities.

3.5.1 Verifying the final shape

Examining the radius of the final shape is the first step in experimentally evaluating the FE models. A hand-held device called an EXAscan laser scanner (Figure 3.4) is generally used for scanning and measuring the formed plate without the inconvenience of setting up tools or tracking arms. Using an auto positioning system of targets ticked on the final shape's surface, this system allows a quick and accurate data acquisition to investigate the forming characters of the workpiece and the final shape.

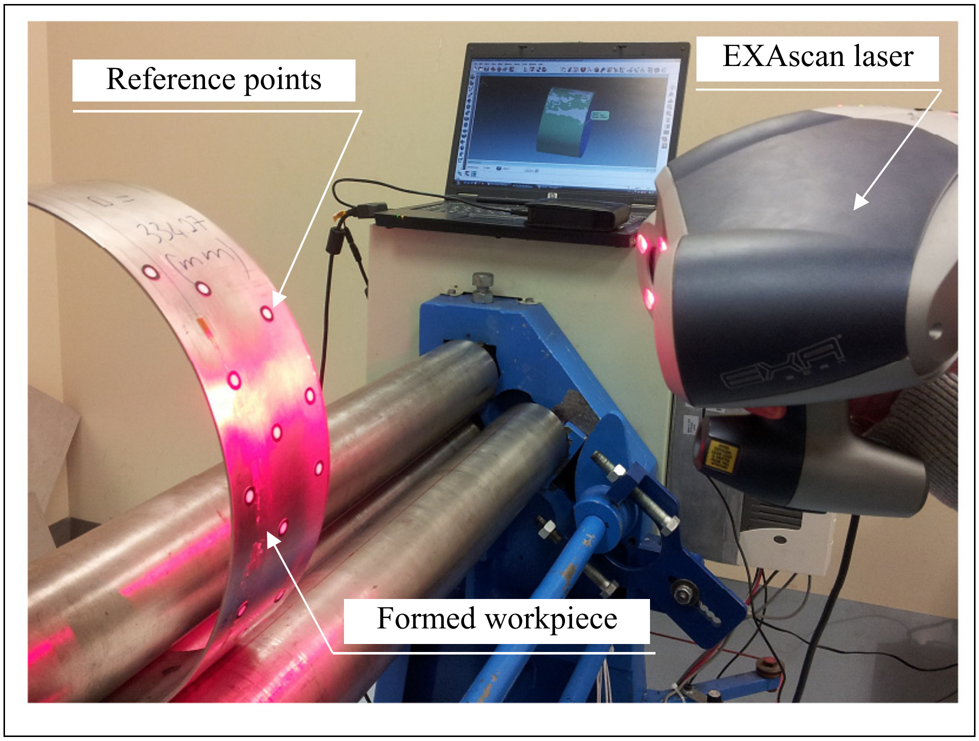

Figure 3.4 Final shape radius verification

3.5.2 Recording and computing the bending force acting on the lateral roll

Two differential apparatuses are combined to measure the deflection of the lateral roll. It includes two indicators placed at the two ends of the lateral roll and two laser distance sensors fixed on the frame at the middle of the lateral roll. This measurement is necessary for two reasons: first, laser sensors can record the deflection of the lateral roll during the roll bending process, and second, the sensors examine the possible backlash at the two ends of the lateral roll. Two lasers, based on optical displacement sensors using an extremely small spot (with 0.5 µm resolution and ±0.1% linearity), are attached to a prototype part that was designed to keep the angle λ constant, as indicated in Figure 3. 5.

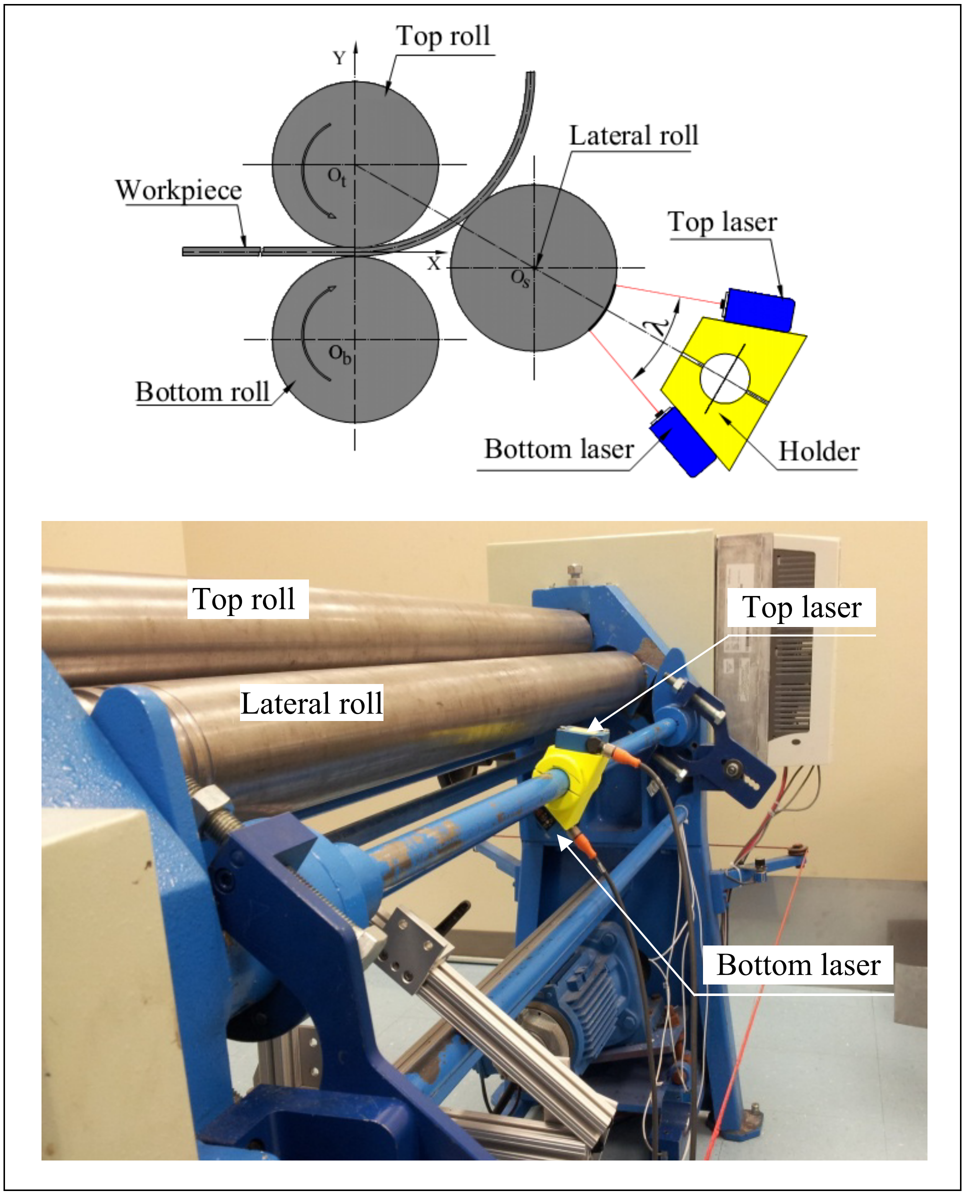
Top roll
Y
Lateral roll
Workpiece
O_t
Top laser
X
O_s
λ
O_b
Bottom roll
Bottom laser
Holder
Top roll
Top laser
Lateral roll
Bottom laser

Figure 3.5 Recording deflection of the lateral roll with laser sensors

The deflection information of the lateral roll before and during the forming process is obtained via the reflection of the laser beam. With “s” defined as the initial arc length formed by two laser beam dots on the lateral roll, let λ = s/r be the angle of two laser beams produced from the top and bottom lasers (see Figure 3.6); the initial coordinates of the top and bottom laser dots on the lateral roll are expressed at point P_{t0} (x_{t0}, y_{t0}) and P_{b0} (x_{b0}, y_{b0}), respectively, as follows:

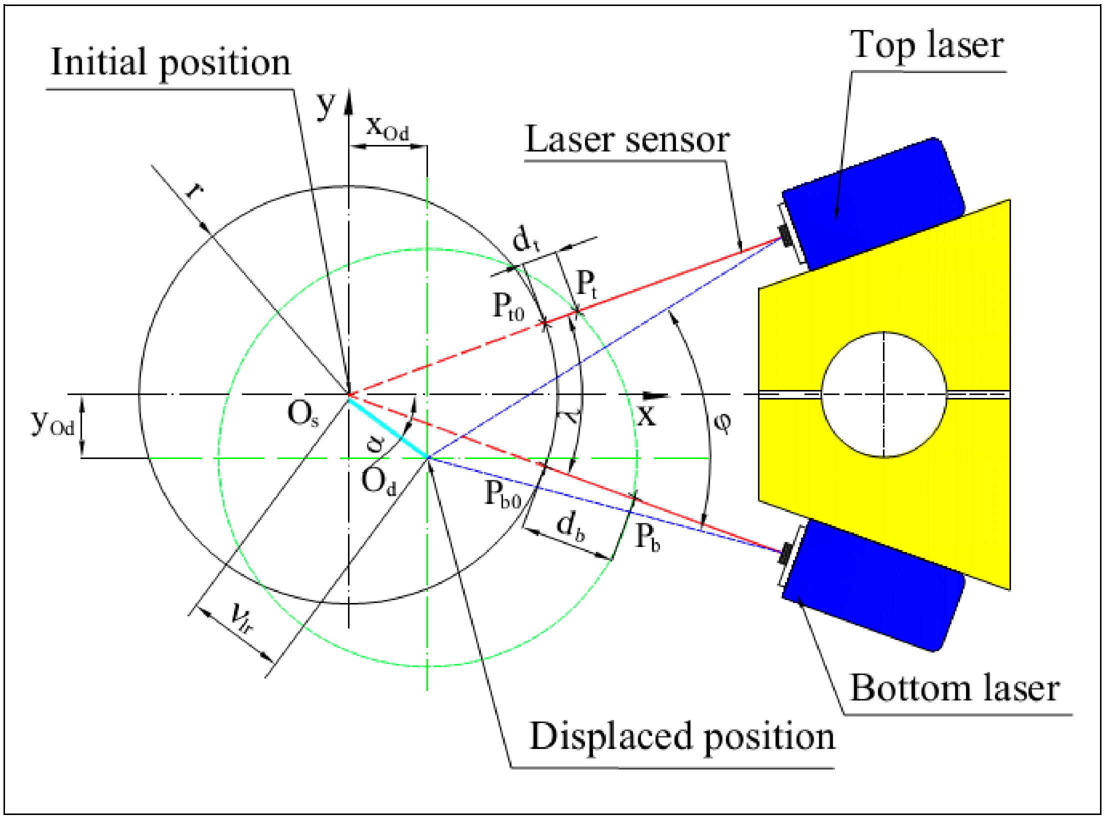
Initial position
Top laser
y
x_{Od}
Laser sensor
r
d_t
P_t
P_{t0}
y_{Od}
O_s
x
λ
φ
α
O_d
P_{b0}
d_b
P_b
v_{lr}
Bottom laser
Displaced position

Figure 3.6 Diagram of deflection checking by laser system

$$x_{t0} = r\cos\frac{\lambda}{2} \tag{3.2a}$$

$$y_{t0} = r\sin\frac{\lambda}{2} \tag{3.2b}$$

$$x_{b0} = x_{t0} \tag{3.3a}$$

$$y_{b0} = -\,y_{t0} \tag{3.3b}$$

Under bending forces, the lateral roll will be deflected in the direction of the applied force. Because the laser system is fixed to a prototype part with a constant angle λ, the dots of the two laser beams on the lateral roll at initial positions P_{t0} (x_{t0}, y_{t0}) and P_{b0} (x_{b0}, y_{b0}) are located at two new coordinates P_t (x_t, y_t) and P_b (x_b, y_b) after roll deflection.

$$x_t = x_{t0} + d_t \cos\frac{\lambda}{2} \tag{3.4a}$$

$$y_t = y_{t0} + d_t \sin\frac{\lambda}{2} \tag{3.4b}$$

$$x_b = x_{b0} + d_b \cos\frac{\lambda}{2} \tag{3.5a}$$

$$y_b = y_{b0} - d_b \sin\frac{\lambda}{2} \tag{3.5b}$$

With d_t and d_b, which are the recorded distances provided by the top and bottom laser sensors, respectively, the new center of the lateral roll $O_d(x_{Od}, y_{Od})$ under bending forces is computed as follows:

$$x_{Od} = x_m - r\cos\frac{\varphi}{2}\cos\alpha \tag{3.6a}$$

$$y_{Od} = y_m + r\cos\frac{\varphi}{2}\sin\alpha \tag{3.6b}$$

Where

$$x_m = \frac{x_t + x_b}{2} \tag{3.7a}$$

$$y_m = \frac{x_t + x_b}{2} \tag{3.7b}$$

and

$$\alpha = \arctan\left(\frac{x_t - x_b}{\mathrm{y_t - y_b}}\right) \tag{3.7c}$$

Then, the mid-distance deflection $\overline{O_sO_d}$ of the lateral roll center under bending force is expressed by Equation 3.8 as follows:

$$\upsilon_{\mathrm{lr}} = \sqrt{x_{\mathrm{Od}}^2 + y_{\mathrm{Od}}^2} \tag{3.8}$$

The potential "backlash" at the two ends of the lateral roll is examined using two indicators with 0.001 mm resolution and 25.0 mm maximum displacement.

Along with the laser systems and the supporting indicators to define the bending force acting on the lateral roll via its deflections as mentioned above, two load cells are also designed to directly measure the bending force, as indicated in Figure 3.7. These compression strain gauge load cells, LC-321-500, have a capacity of 2200 N. The initial value of the load-cells are set to zero when both ends of the lateral roll are just in contact with the bearings without any applied bending load. This procedure is used to eliminate dead weight effects of the lateral roll bearing reaction measurements. The bending force acting on the lateral roll is calculated using the sum of all individual force values recorded by each load-cell as follows (see Figure 3.7):

$$F_{\mathrm{lr}} = \sum_{i=1}^{4} F_i \tag{3.9}$$

where i is the number of load-cells.

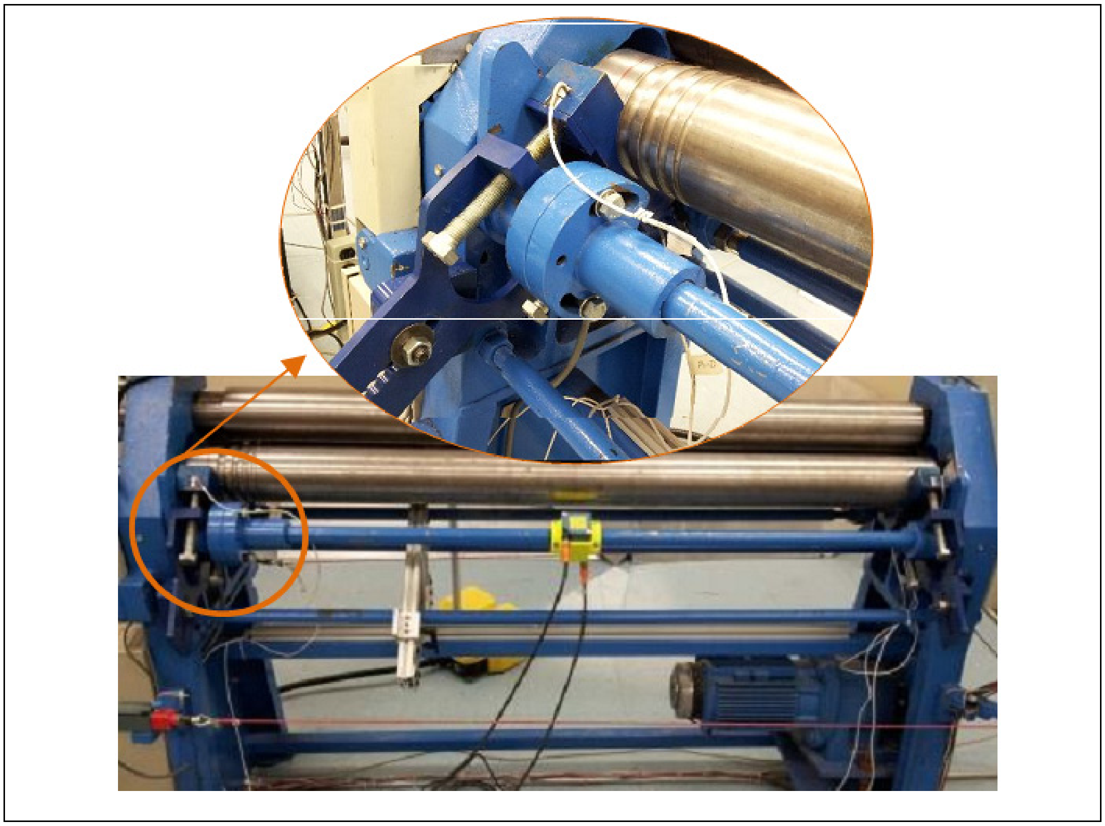

Figure 3.7 Measuring the bending force of the lateral roll

3.5.3 Computing the bending force acting on the top roll

The method that measures the total deflection resulting from an applied load is also used to compute the bending force acting on the top roll. Three digital indicators are rigidly clamped on magnetic bases mounted on the machine frame, as presented in Figure 3.8.

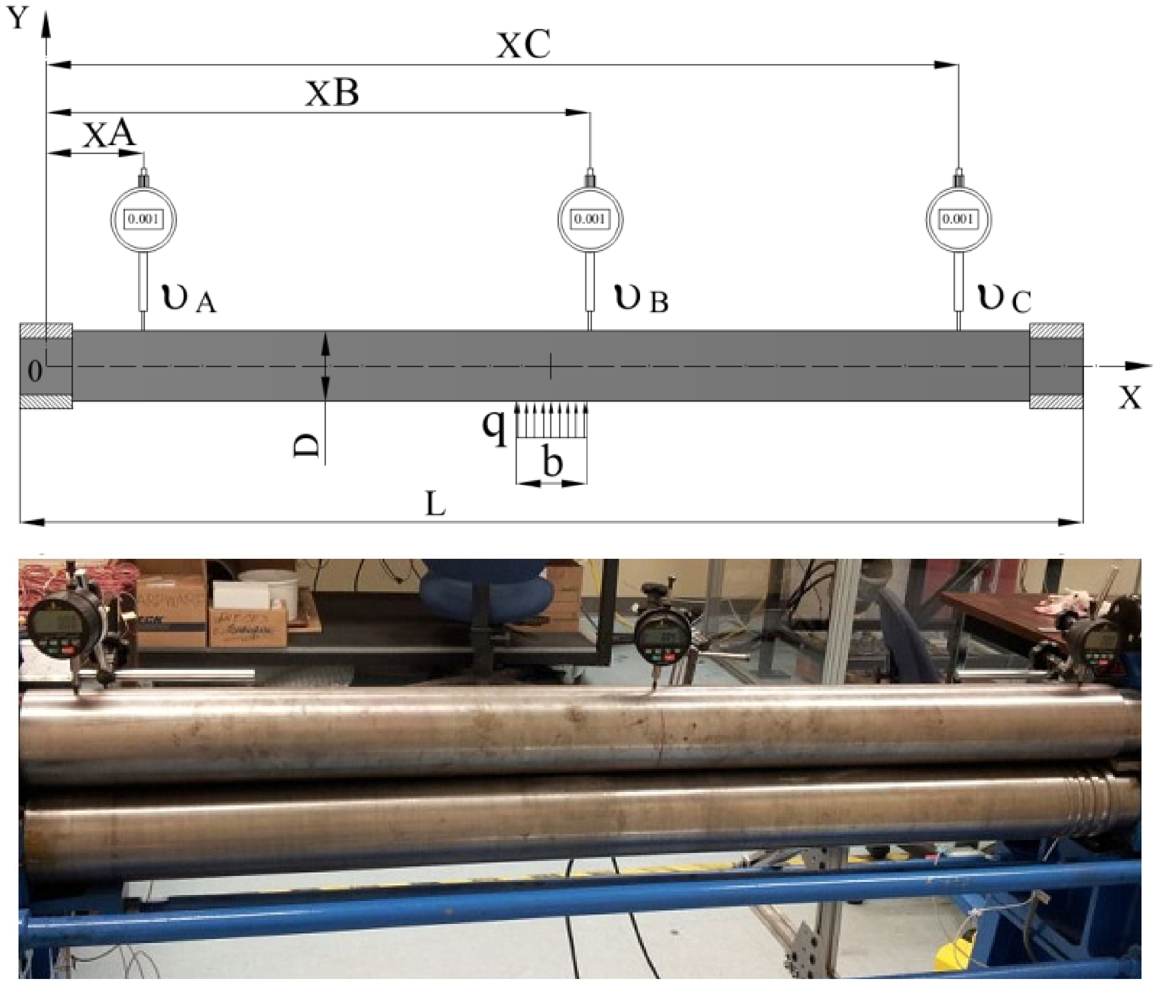

Figure 3.8 Measurement of the top roll deflection

The free body diagram of the system, including the deflection at points A, B and C, is shown in Figure 3.9. The deflection curve υ depending on the length x of the top roll is expressed as follows:

$$\upsilon(x) = -\frac{R_0 x^3}{6EI} + \frac{q}{24EI}\left[x - \left(\frac{L}{2} - \frac{bq}{2}\right)\right]^4 - \frac{q}{24EI}\left[x - \left(\frac{L}{2} + \frac{bq}{2}\right)\right]^4 + \theta_0 x + \upsilon_0 \tag{3.10}$$

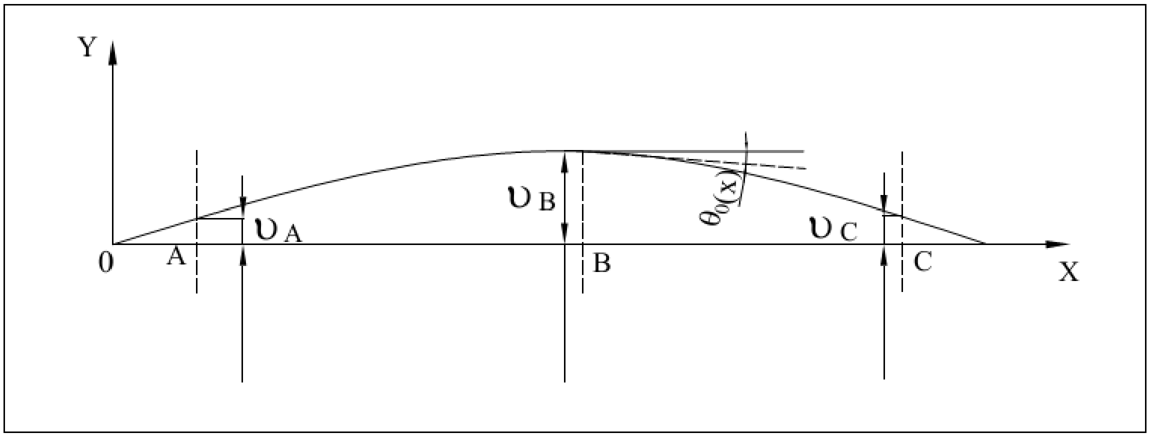

Figure 3.9 Free body diagram of deflection

where R_0 and υ_0 are the reaction force and the deflection of the top roll at position zero, respectively; b is the width of the plate; q is the applied force acting on the top roll; and θ_0 is the possible deflection angle of the top roll. It should be noted that in the following equations, it is assumed that the force exerted by the plate on the roll is uniformly distributed over the contact line of length b (see Figure 3. 8). Using the least squares method, it can be determined that:

$$\begin{aligned}
&\sum_{i=1}^{n} \frac{\partial\, \upsilon(x_i)}{\partial\, q}(\upsilon(x_i)-\upsilon_i)=0 \\
&\sum_{i=1}^{n} \frac{\partial\, \upsilon(x_i)}{\partial\, \upsilon_0}(\upsilon(x_i)-\upsilon_i)=0 \qquad (3.11) \\
&\sum_{i=1}^{n} \frac{\partial\, \upsilon(x_i)}{\partial\, \theta_0}(\upsilon(x_i)-\upsilon_i)=0
\end{aligned}$$

By solving Equation 3.11, the three unknown variables q, θ_0 and ν_0 can be determined.

3.5.4 Strain variation and deformed behavior of the plate

To measure the strain variations left in the formed plate and the residual strain, a strain gauge is used to record the strain variations during the bending process. The strain gauges are directly fixed onto the plates. Special care is given at the beginning of the process to avoid any damages to strain gauges while handling blanks and feeding them between rolls. Three strain gauges J_1, J_2 and J_3 with equal resistance of 120 Ohms ±0.4% were mounted on the specimen surface. They were equally distributed, as shown in Figure 3.10. When the plate deformed, the strain variations were recorded with an acquisition system programmed with Labview® [31].

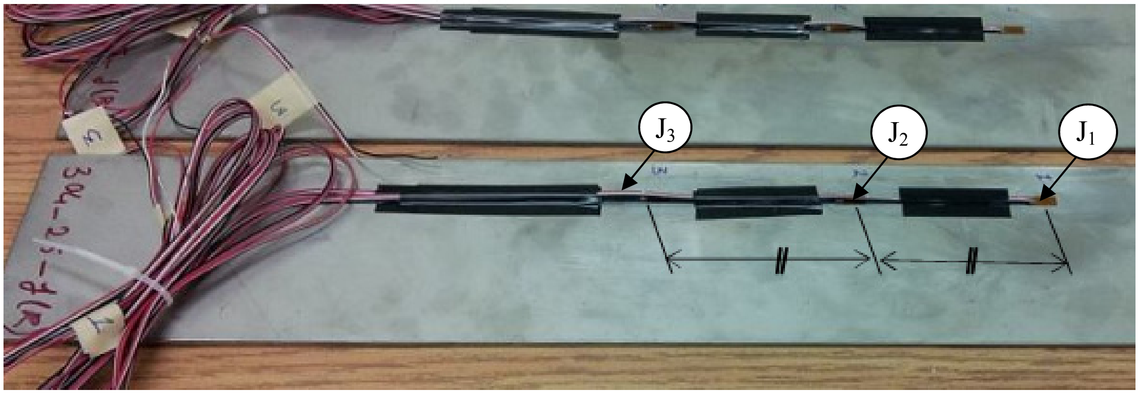

Figure 3.10 Strain gauges fixed onto workpieces

3.5.5 Examining the rotational speed and supplied power of the roll bending machine

An encoder is used to determine the rotational speed of the rolls during the roll bending process. This is an electromechanical component with a shaft that converts its rotation to an analog signal. By directly connecting the rolls of the machine to the rotating shaft of the encoder, this measurement can provide high precision results, even for a slow rotational speed, and stable measurements. Furthermore, the amount of supplied power (W) during the roll bending process is recorded. With features such as RS-232/communication, all measurement equipment outputs are saved in a file with Labview®.

3.6 Results and discussion

The precision of the radius of any final shape R of the roll bending process depends on many factors, such as the thickness “t” of the plate, the position “a” of the lateral roll, the dimension “R” of the final shape and even the skills of the machine operators.

3.6.1 Geometric verification model

To verify the geometry of the final shapes of the forming plate obtained from FE simulations in Ansys/LS-Dyna, a numerical check is applied. The successive shape of the forming plate using FE simulations is plotted at various steps, as depicted in Figure 3.11 and Figure 3.12.

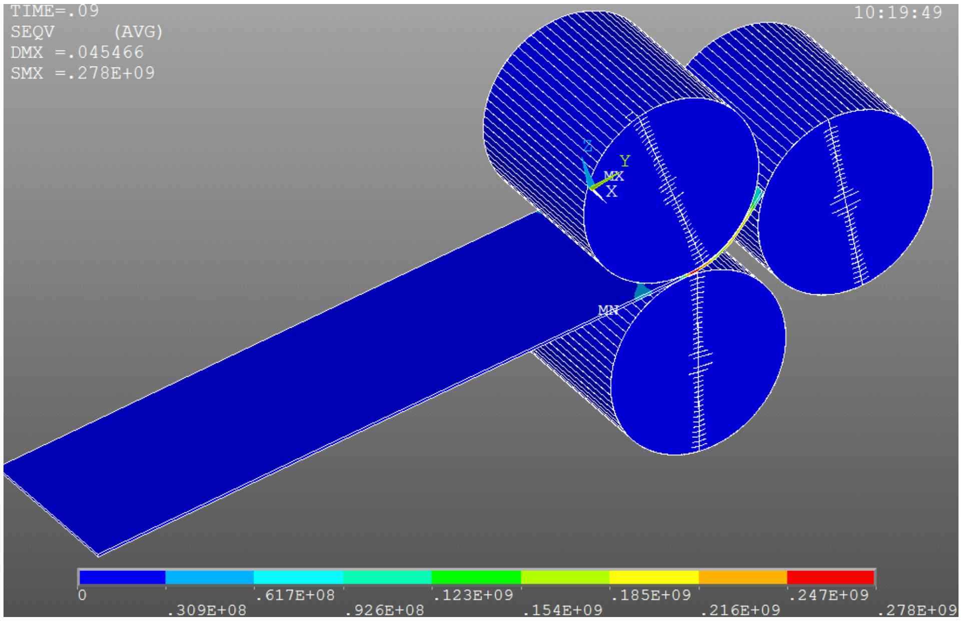
TIME=.09
SEQV (AVG)
DMX =.045466
SMX =.278E+09
10:19:49
Z
Y
MX
X
MN
0
.309E+08
.617E+08
.926E+08
.123E+09
.154E+09
.185E+09
.216E+09
.247E+09
.278E+09

Figure 3.11 FE simulations of roll bending process at beginning of the process

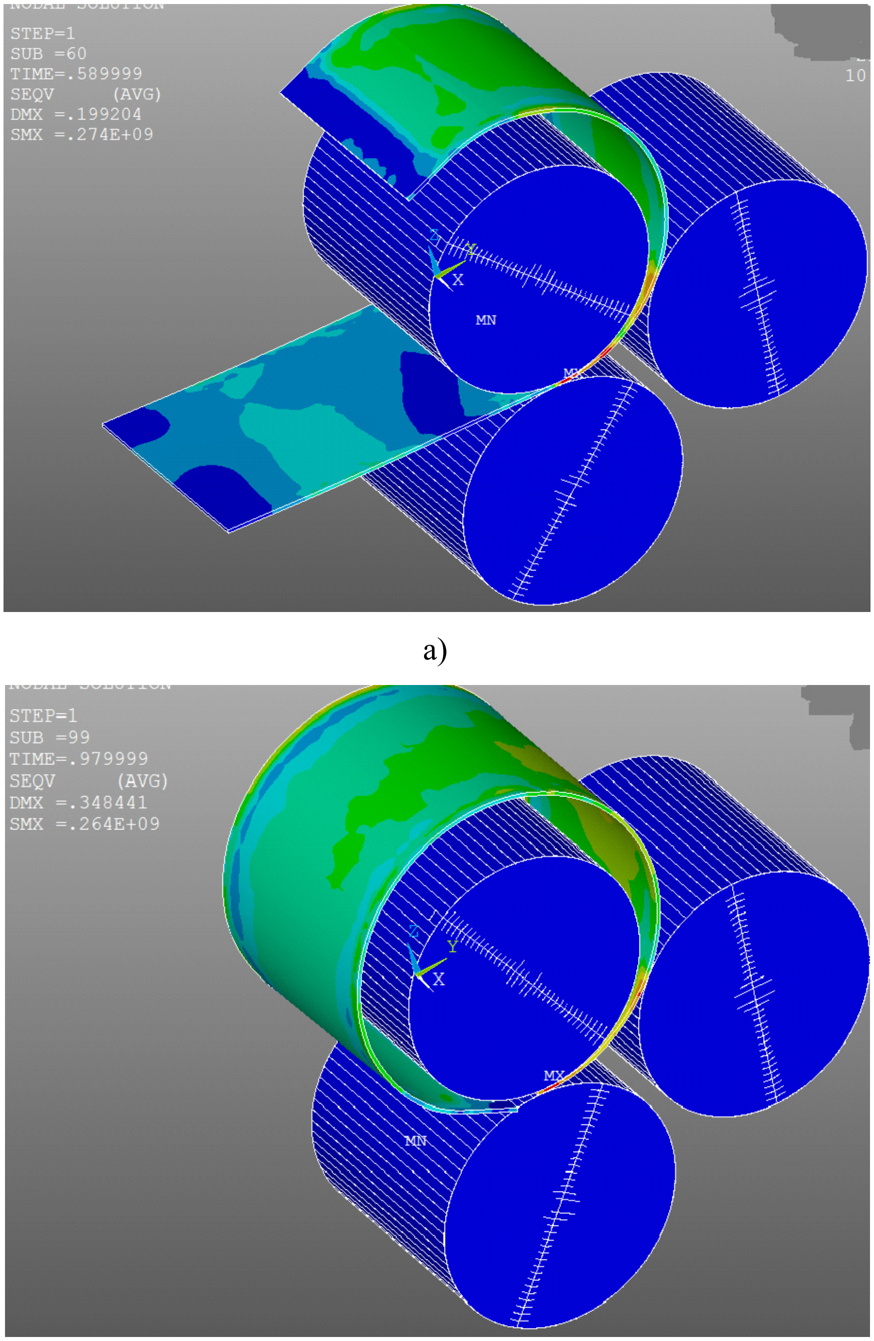
STEP=1
SUB =60
TIME=.589999
SEQV (AVG)
DMX =.199204
SMX =.274E+09
10
Z
Y
X
MN
MX
STEP=1
SUB =99
TIME=.979999
SEQV (AVG)
DMX =.348441
SMX =.264E+09
Z
Y
X
MX
MN

a)

b)

Figure 3.12 FE simulations of roll bending process at a) midpoint of the process and b) completion of the process

When the process is completed, as illustrated in Figure 3.11c, the coordinates of the center of the circle xC, yC and its radius R, assuming that the nodes of the formed plate are distributed along a cylindrical geometry, are determined using the following objective function:

$$\min F(x_c, y_c, R) \tag{3.12a}$$

$$\text{with } F = \Sigma\,(R - R_i)^2$$

Where

$$R = \sqrt{[(x_i - x_c)^2 + (y_i - y_c)^2]} \tag{3.12b}$$

$$\text{with } x_i = x^{(0)} + ux \text{ and } y_i = y^{(0)} + uy$$

With grad(F) = 0, three nonlinear equations are solved simultaneously for x_C, y_C and R. Because these equations are differentiable, a Newton-Raphson scheme was applied to determine the circle parameters. Only the initial coordinates $x^{(0)}$, $y^{(0)}$ and displacements ux and uy of nodes located at the mid-width of the plate are imported into Matlab® [32] for processing, as indicated in Figure 3.13.

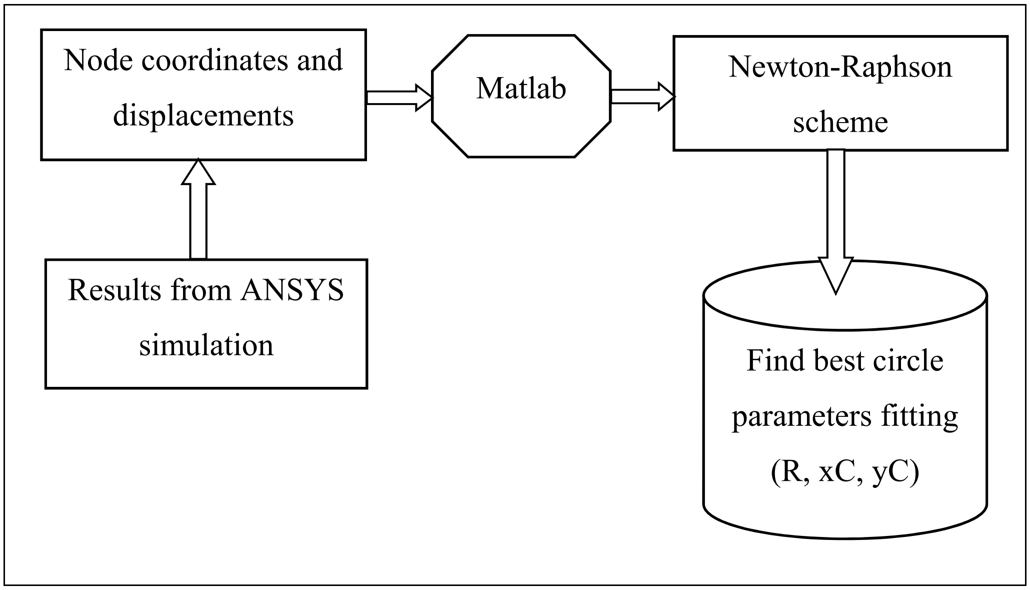
Node coordinates and displacements
Matlab
Newton-Raphson scheme
Results from ANSYS simulation
Find best circle parameters fitting (R, xC, yC)

Figure 3.13 Geometric verification model

3.6.2 Influence of plate thickness (t) and center location of lateral roll (i.e., a) on final shape radius (R)

As mentioned above, among the many workpiece parameters that affect formability of the roll bending process, the plate thickness may have the highest influence. Therefore, it is necessary to capture the effects of plate thickness on the radius of the final shape of the workpiece. To compare with the FE model simulations, the same sheet material properties, machine parameters and workpiece dimensions are used in the experimental process. Figure 3.14 provides a comparison of the FE simulation and experimental results for roll bending of flat plates with thicknesses of t = 1.0 mm, 1.5 mm, 2.0 mm, 2.5 mm at four different locations along the lateral roll of a = 110.0 mm, 115.0 mm, 120.0 mm and 125.0 mm. The positions of the lateral roll are defined by the length of value a, as provided in Figure 3.1.

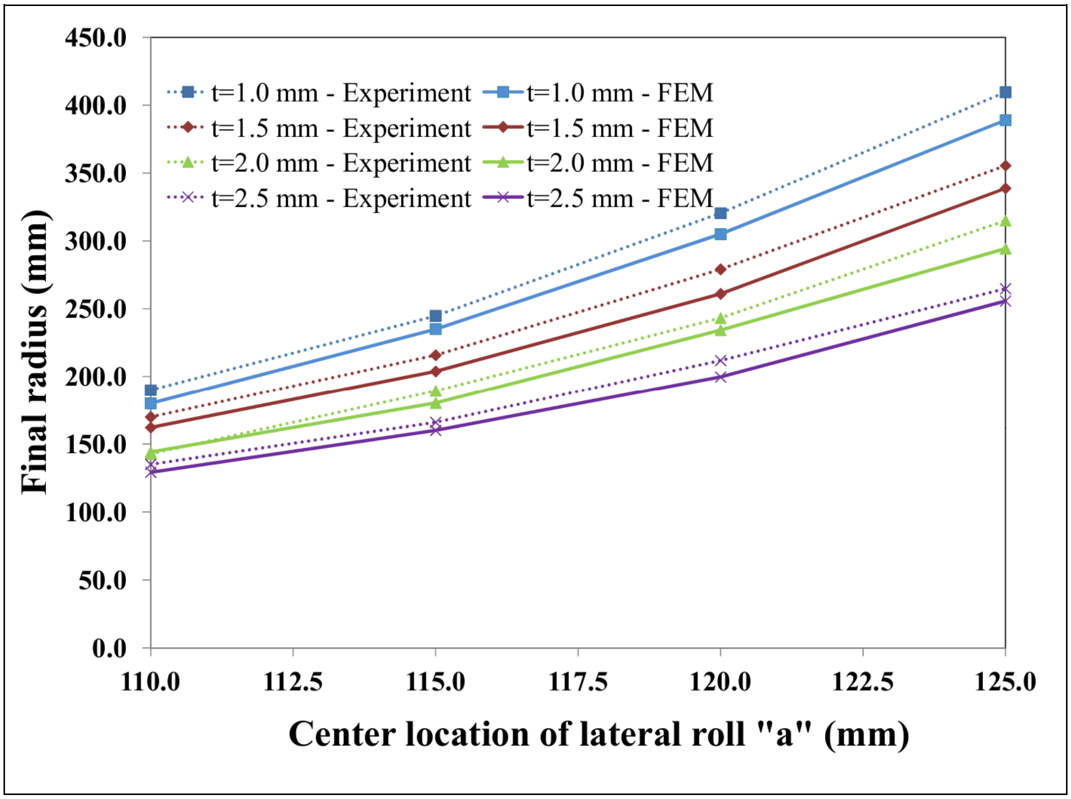

Figure 3.14 Final radius depending on the plate thickness and the lateral roll center location

A good agreement between the FE simulations and the experimental results over the entire range of all lateral positions and all plate thicknesses is observed in Figure 3.14. However, with the same forming conditions and location of the center of the lateral roll, the final shape's radius from the FE simulation is slightly smaller compared to that of the experimental results. The maximum difference between the FE simulation and the experimental result is less than 10%. This difference may result from the assumption that the rolls are considered to be rigid in our numerical model. Moreover, experiments showed that the rolls actually deform under bending forces, which affects the final shape radius.

The radius of the final shape is also dependent on the plate thickness. Figure 3.14 shows the resulting radius for the same location of the lateral roll (i.e., a) in comparison with the plate thickness. FE simulations and experimental results indicate the same trend; however, there is a slight difference in the resulting radii. The reason behind this result is that for exactly the same geometric configuration of rolls, the amount of plastic deformation through the thickness increases with the thickness of the rolled plate. Then, the final radius of the cylinder is dependent on the amount of plasticity built in through the thickness.

In an industrial context, the radius of the final shape in the roll bending process is generally determined based on "trial-and-error" or an empirical approach, which requires several attempts. Therefore, applying these results in manufacturing plants will be beneficial in providing the accuracy of the final shape's radius. Additionally, using this FE model will considerably reduce the setup time before manufacturing.

3.6.3 Deformation characteristics of the forming plate

To verify strain variations dependent on the radius of the shape, several FE simulations varying the value of the center location of the lateral roll (i.e., a) at 115.0 mm, 120.0 mm, 122.0 mm and 125.0 mm were performed and then compared to experimental results using the same plate dimensions. Figure 3.15 presents how the strain gauges pass the rolls through the grooves at the bottom and lateral rolls.

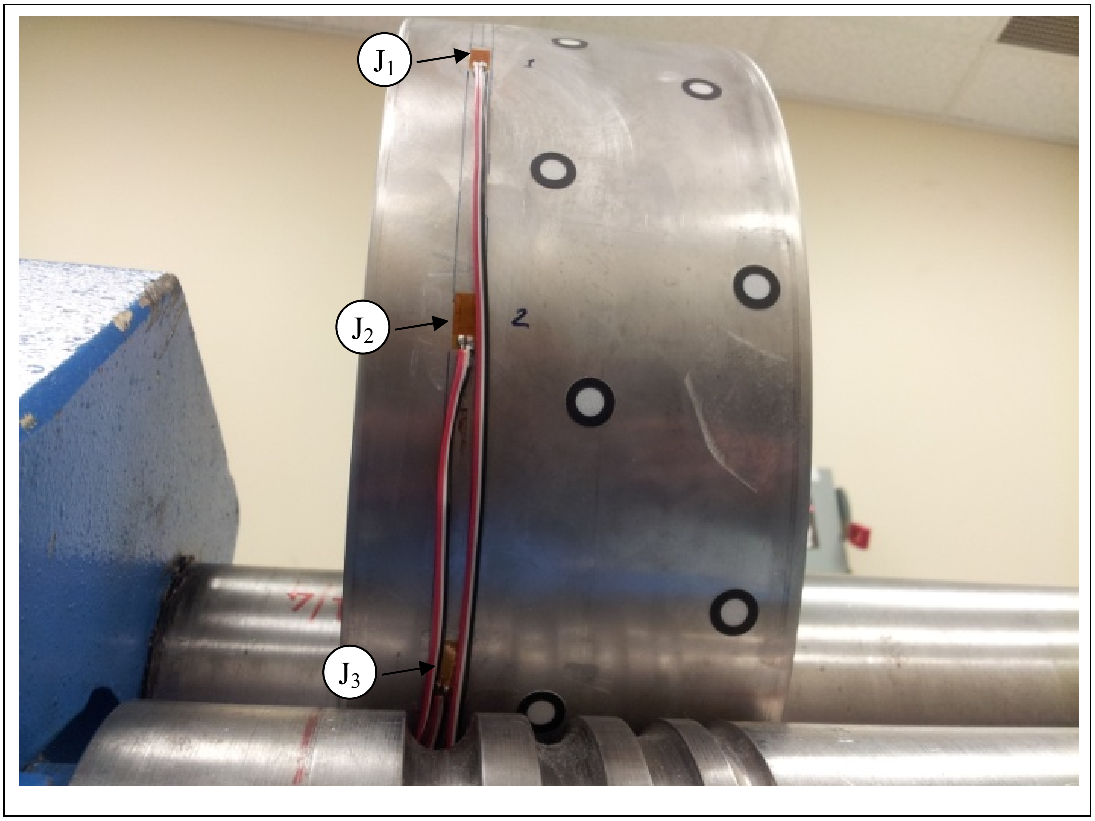

Figure 3.15 Strain gauges setup for rolling

The strain variations recorded by strain gauges J_1, J_2 and J_3 are provided in Figure 3. 16. The strains at A, B and C are close from one strain gauge Ji to another.

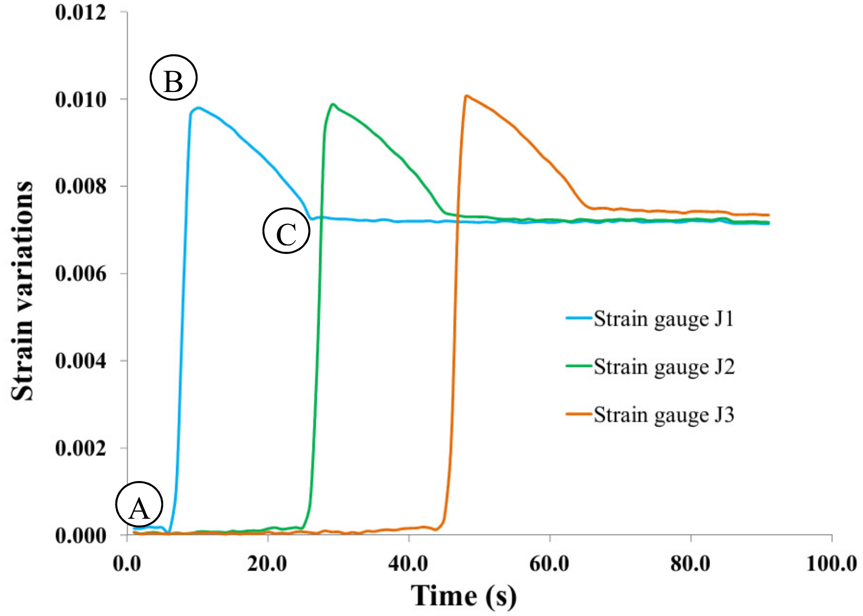

a)

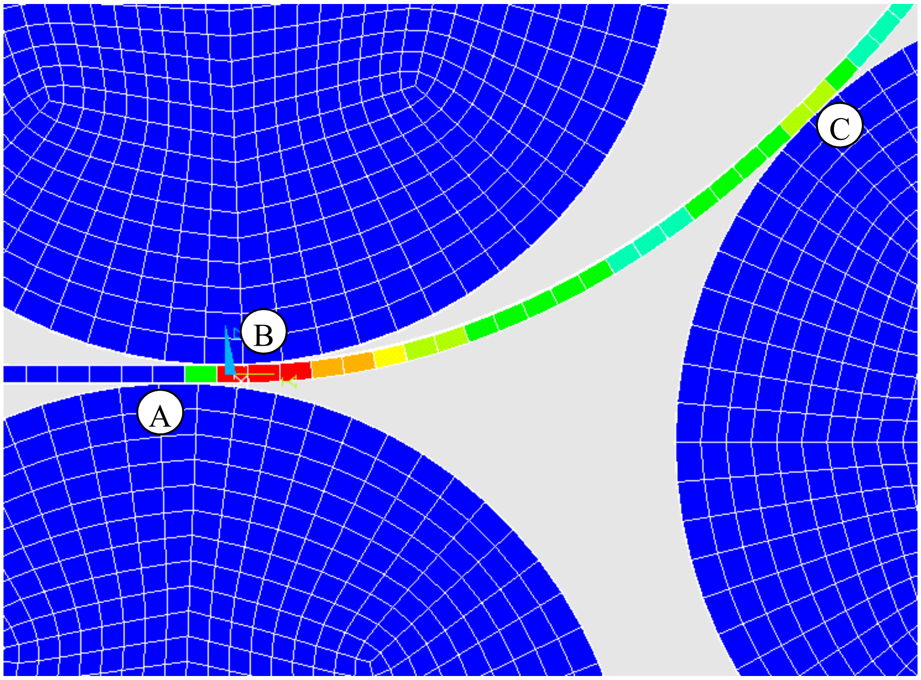

b)

Figure 3.16 Strain variation at locations of strain gauges J_1, J_2 and J_3 a) experiments; b) typical location of A, B and C

A good agreement between the FE simulations and experimental studies is shown in Figure 3.17. As expected, the maximum strain variation was obtained for the smallest value of ”a”. It is clear that a smaller radius of curvature provides a larger value of strain.

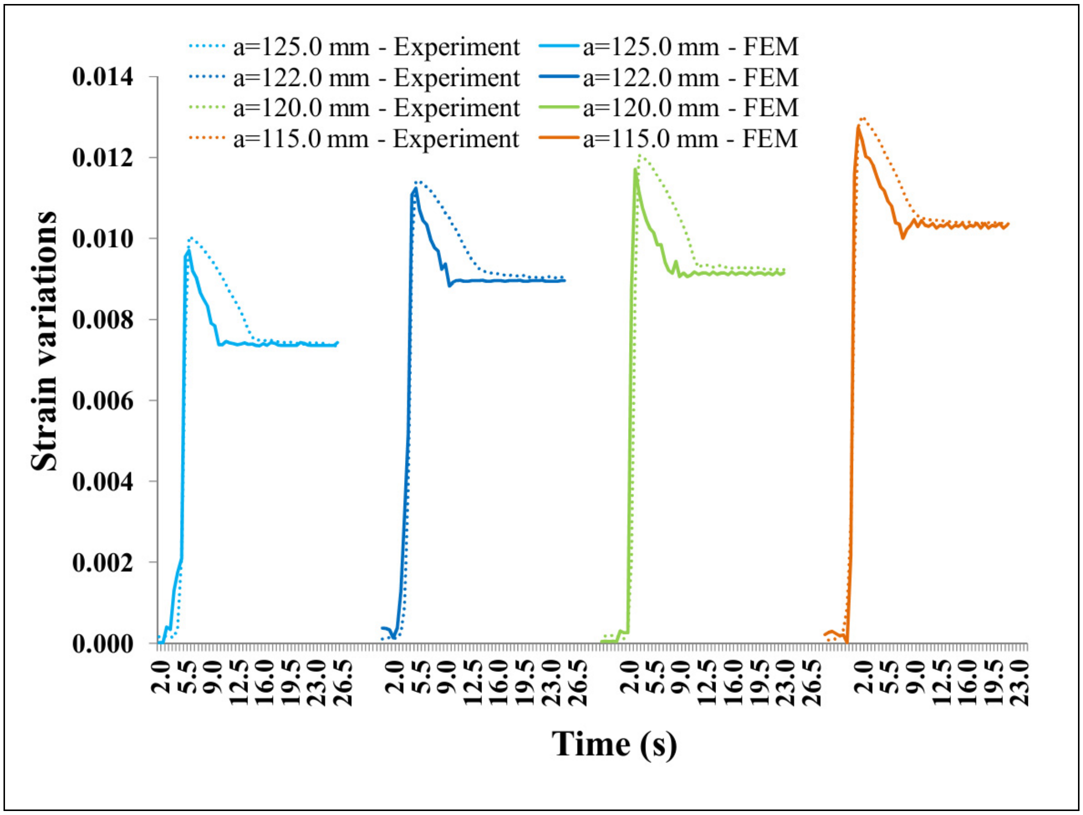

Figure 3.17 Strain variations depending on center location “a” of the lateral roll

Figure 3.18 shows the strain gauge measurements during forming and the strains computed at the same locations as the FE model for four different plate thicknesses with the same position “a” (see Figure 3.1) for the lateral roll. The strain variations are plotted from when the strain gauge enters the gap between the top and bottom rolls until it passes the contact point of the lateral roll.

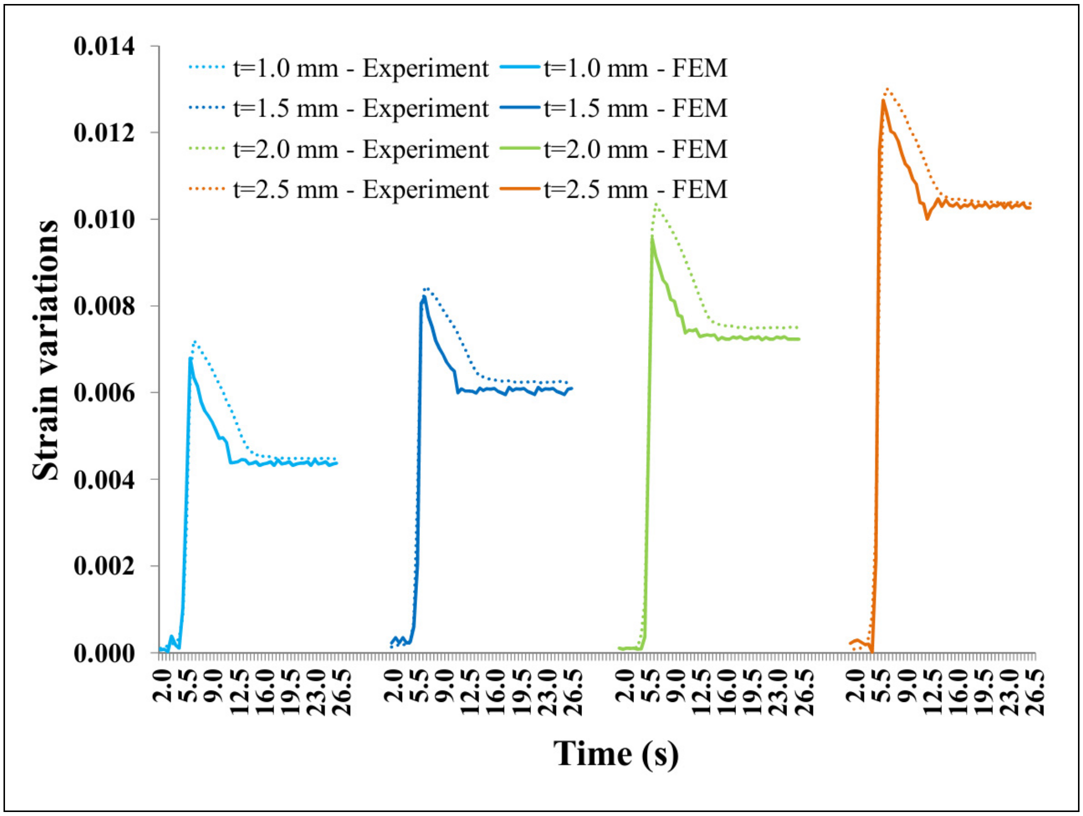

Figure 3.18 Strain variations depending on the plate thickness

As expected, the thicker workpiece will obtain a higher strain value at the same value of a. The trends in strain variation are well captured by the FE simulations and experimental results that were recorded using strain gauges.

Furthermore, it can be observed from Figure 3.17 and 3.18 that the strain variation curves end with a lower and constant value after the strain gauge passes the contact point on the lateral roll. This result illustrates the spring back of the plate, and the final radius can be obtained just seconds after the strain sensor records the peak value. The overall residual strain pattern is nearly the same, with a maximum difference of approximately 10 % in comparison with the peak of each strain.

The analysis and measurement of the residual strain left in a roll bent plate are usually difficult to obtain, and no rigorous study on measuring strains during roll bending has been reported in literature to our knowledge. Therefore, this FE simulation model evaluated by experiments is not only a new approach for a better understanding of the deformation behavior of the workpiece before and after passing the bending roll but also provides an accurate residual strain measurement procedure that relates the workpiece properties, final shape dimensions and process parameters.

3.6.4 Influence of plate thickness "t" and center location "a" of lateral roll on bending forces F

A series of simulations and experiments were performed with various final shape radii R (expressed by the center distance "a" from the top roll to the lateral roll, with a = 110.0 mm to 125.0 mm) and different plate thicknesses (from 1.0 mm to 2.5 mm) to study their effects on bending forces acting on the rolls.

In Figure 3.19, the reaction forces applied on the top roll depending on final shape radius R and plate thickness t are displayed. The top roll forces are function of the final shape radius R and the plate thickness t: when R increases, the forming forces decrease because less bending is necessary for shaping the plate; when t decreases, the forming forces also decrease because the plate strength in bending decreases. This has been observed with FEM results and confirmed with experiments. It should be noted that experiment results are not displayed for larger R (i.e., a=120.0 mm, or 125.0 mm) and thinner plates (i.e., t=1.0 mm or 1.5 mm) because the deflections of the top roll cannot be measured accurately.

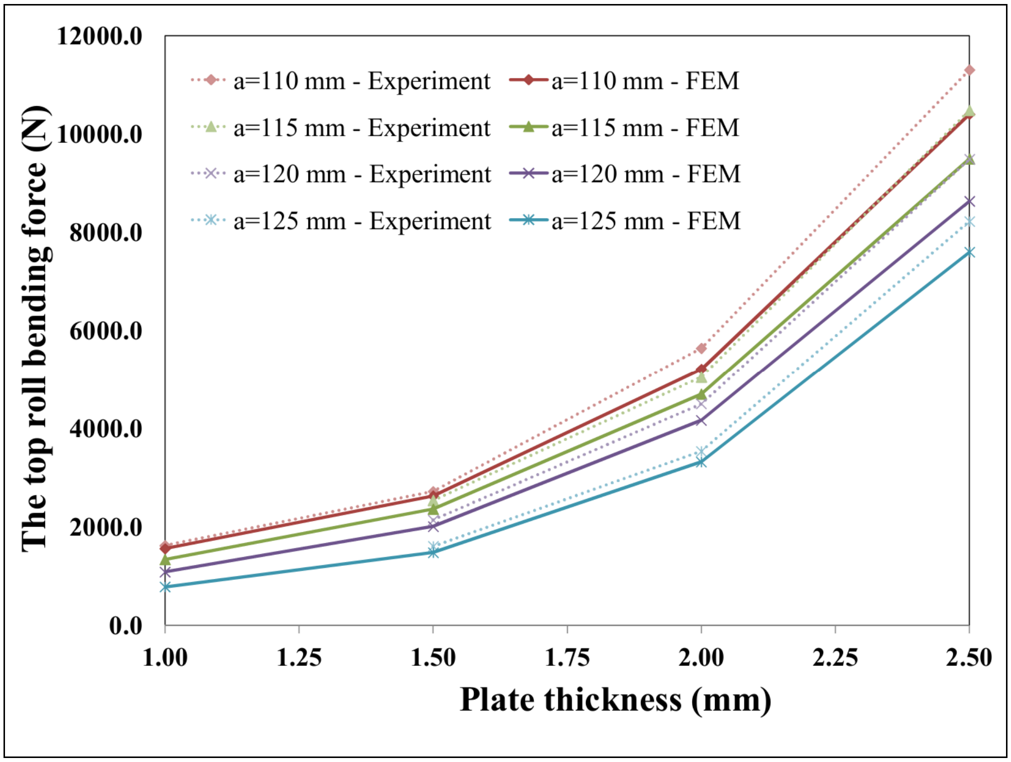

Figure 3.19 Top roll bending force based on the plate thickness and center location of the lateral roll

Figure 3.20 shows the comparison between FE simulations and experimental results for bending forces acting on the lateral roll for different plate thicknesses t and different final radii R of the roll bent cylinder. The FE simulation results (solid line in the graph) are evaluated using two sources of experimental results: a laser system for computing the bending force via deflection of roll (single-dotted line in the graph); and load-cell systems for directly verifying the bending force (double-dotted line in the graph).

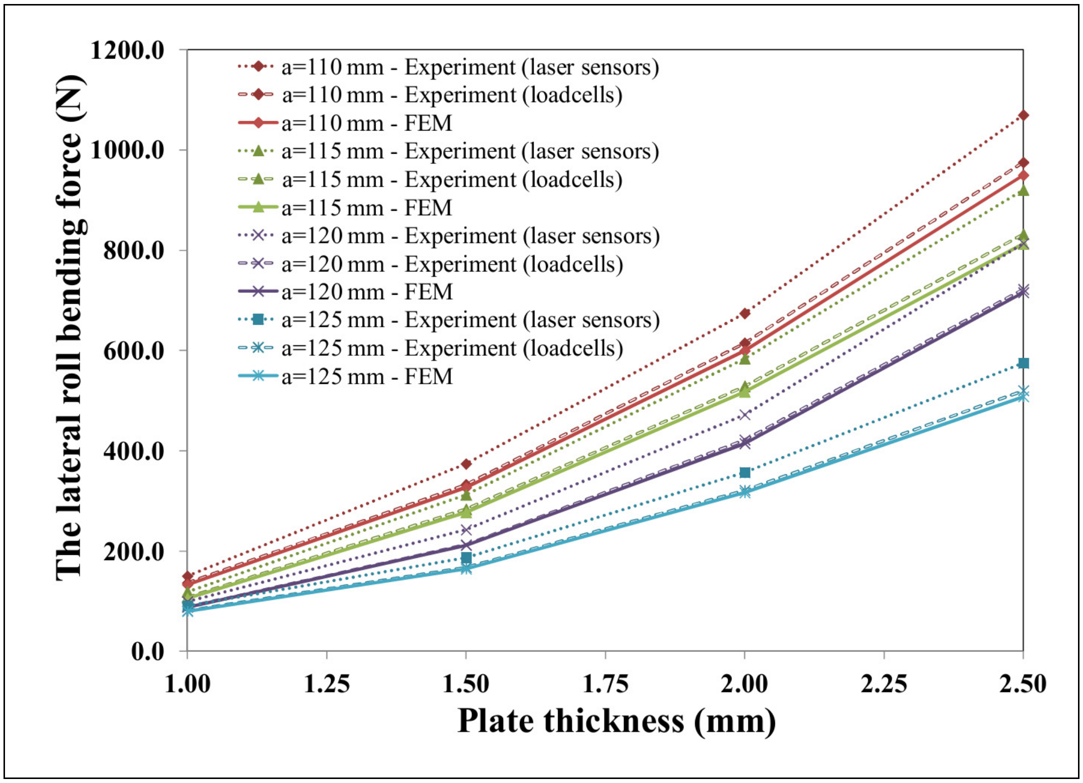

Figure 3.20 Lateral roll bending force depending on the plate thickness and center location of the lateral roll

Overall, Figure 3.20 indicates that the FE simulation results are in good agreement with the experimental results (from both sources). The value of the applied force for a 1.0 mm thick sheet was found to be less compared to those in a 1.5 mm, 2.0 mm and 2.5 mm thick metal plate at the same final shape radius R. Typically, it is clear that the roll bending machine applies a larger force for bending thicker plates. Furthermore, the final radius directly influences the reaction forces of the lateral roll. The results confirmed that the reaction forces acting on the lateral roll increase with a decreasing final shape radius R.

In comparison with other rolls, the top roll always yields the highest bending force. Therefore, this study not only provides a better understanding for selecting or designing a machine capacity based on the plate thickness and the final shape radius but is also the first step towards finding the best strategy for a heat assisted roll forming process to soften the workpiece.

3.6.5 Influence of the plate widths (H) on the bending force

The influence of the plate width H on bending force acting on the top roll is shown in Figure 3.21. Analyses were performed for various plate widths (80.0 mm, 100.0 mm, 120.0 mm, 140.0 mm, and 155.0 mm) with the other input parameters, such as the plate thickness, final radii, process parameters and material properties, remaining constant. The bending forces acting on the top roll increase when the width of the final shape is increased.

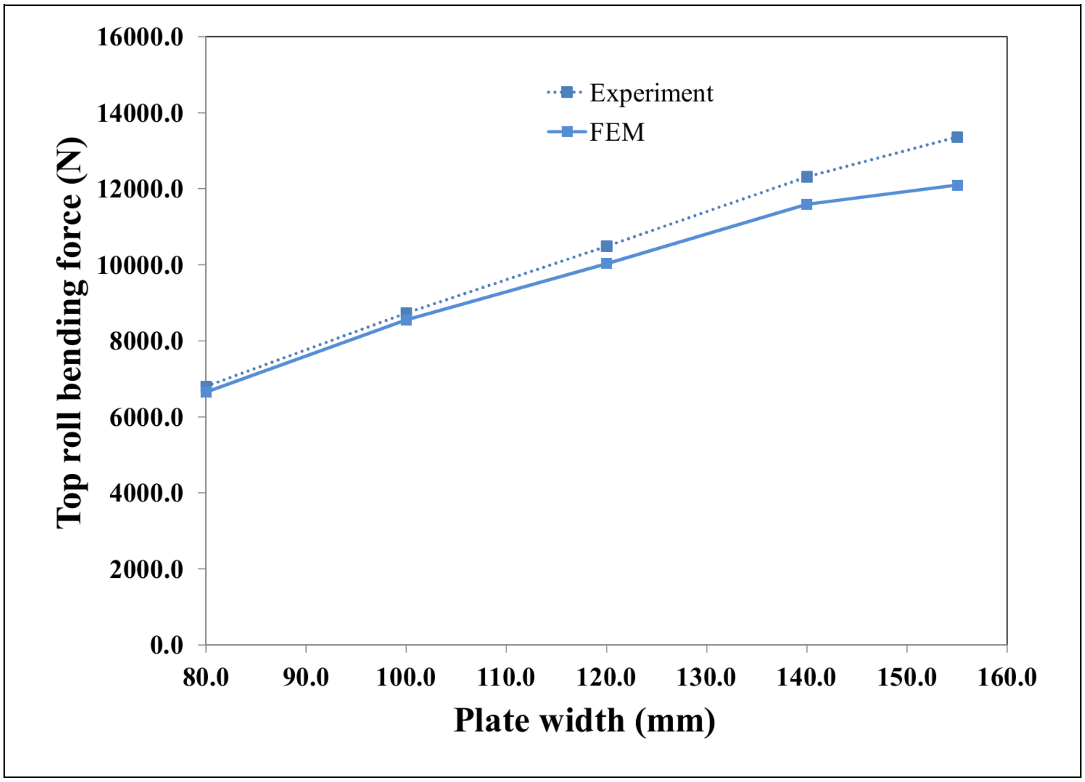

Figure 3.21 Top roll bending force depending on the plate width

Figure 3.22 indicates that the forces exerted by the lateral roll vary nearly linearly with an increase in the plate thickness.

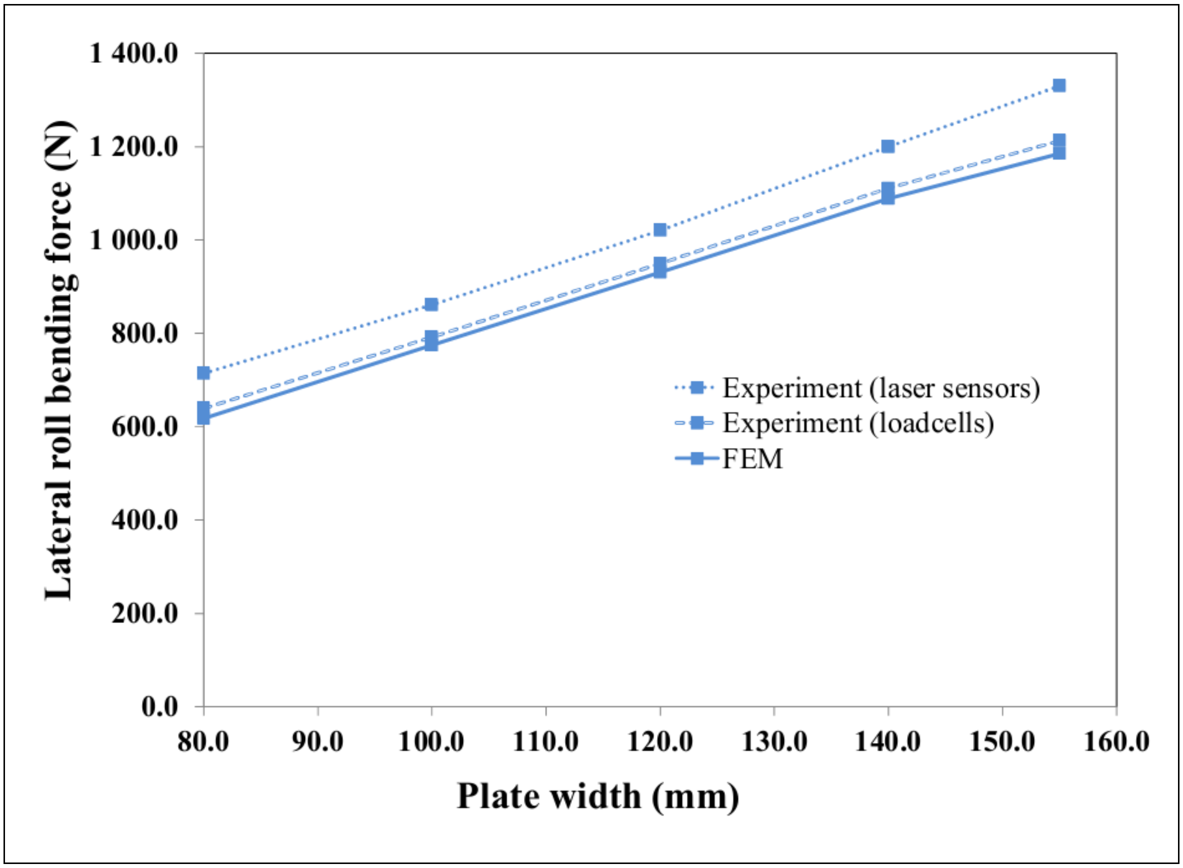

Figure 3.22 Lateral roll bending force depending on the plate width

3.6.6 Influence of the plate thickness (t) on supplied power (W) and rotational speed (RPM) of the rolls

The rotational speed of the rolls is an important but not well-known parameter that can affect the roll bending machine’s life and the mechanical properties of the final product. Therefore, it would have been interesting to study the effect of the rotational speed of the rolls on the formed shape. However, it is difficult to handle the large amount of experiments that are required to study this parameter’s effect. Therefore, only the relationship between the power supplied and the plate thickness for the same position of the lateral roll is provided here. An increase in the plate thickness was associated with an increase in the supplied power, as indicated in Figure 3. 23.

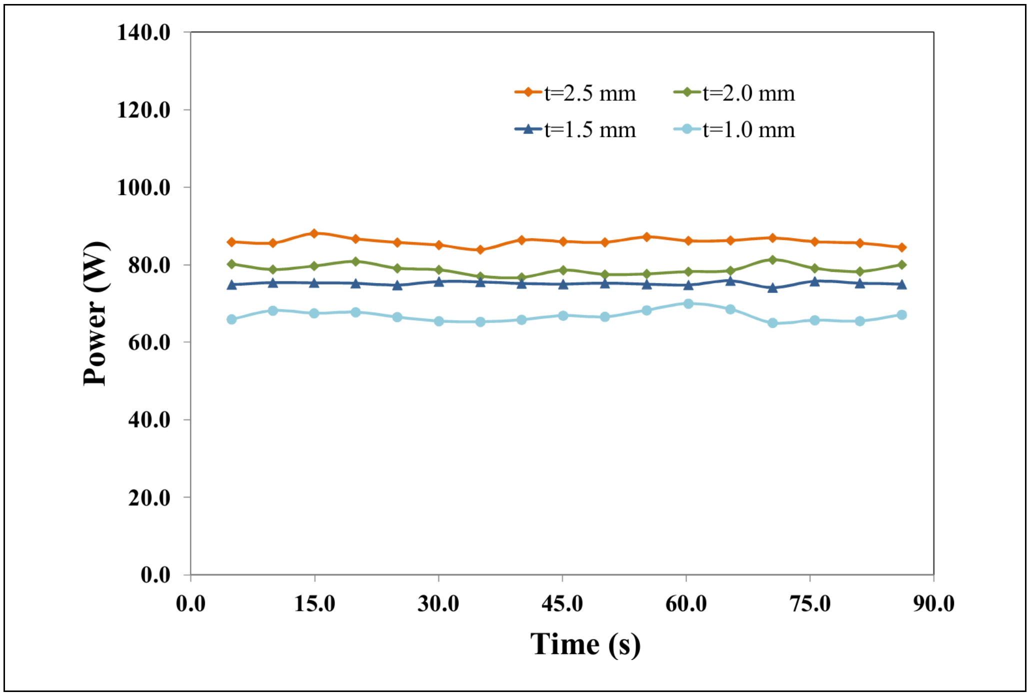

Figure 3.23 Supplied power depending on plate thickness

For the same forming parameters and material conditions, the supplied power for a 1.0 mm thick sheet was found to be less compared to those in metal plates with thicknesses of 1.5 mm, 2.0 mm and 2.5 mm.

3.7 Conclusions

A 3D-dynamic FE model of a roll bending process verified using experiments was developed in this paper. This model allowed the authors to identify the primary processing parameters of the roll bending process and to investigate the influence of these process factors on the precision of the final shape. The influence of several forming parameters, such as plate thickness, final shape radius, and width of final shape, on reaction forces were studied in detail. Furthermore, a new experimental approach for measuring strains with strain gauges to obtain the strain variation left in the formed plate is proposed. This comprehensive analysis will be beneficial in the industrial context for an accurate prediction of the final shape or reaction forces acting on bending rolls to increase the effectiveness of an existing asymmetrical roll bending machine.

3.8 Acknowledgements

The authors express their thanks to the Natural Sciences and Engineering Research Council (NSERC) of Canada for its financial support during this research.

3.9 References

1. DeGarmo E, Black JT, Kohser R (2003) Materials and Processes in Manufacturing. J. Wiley, Volume 9, New York.
2. Semiatin SL (2006) ASM Handbook: metalworking sheet forming. ASM international, Volume 14B, Ohio.
3. Lascoe O (1998) Handbook of fabrication processes. ASM International, Ohio.
4. Hansen NE, Jannerup O (1979) Modelling of elastic-plastic bending of beams using a roller bending machine. Journal of Manufacturing Science and Engineering Vol.103(No.03):pp.304-310.
5. Bassett M, Johnson W (1966) The bending of plate using a three roll pyramid type plate bending machine. The Journal of Strain Analysis for Engineering Design Vol.1(No.5):pp.398-414.
6. Gandhi AH, Raval HK (2008) Analytical and empirical modeling of top roller position for three-roller cylindrical bending of plates and its experimental verification. Journal of Materials Processing Technology Vol.197(No.1-3):pp. 268–278.
7. Yang M, Shima S (1988) Simulation of pyramid type three-roll bending process. International Journal of Mechanical Sciences Vol. 30(No.12):pp.877-886.
8. Cai ZY, Lan YW (2011) Analysis on the straight-end problem in thin-plate three-roll bending. Applied Mechanics and Materials Vol.80-81:pp.585-590.
9. Hu W, Wang ZR (2001) Theoretical analysis and experimental study to support the development of a more valuable roll-bending process. International Journal of Machine Tools and Manufacture Vol.41(No.5):pp.731-747.

10. Hua M, Baines K, Cole I (1995) Bending mechanisms, experimental techniques and preliminary tests for the continuous four-roll plate bending process. Journal of Materials Processing Technology Vol.48(No.1-4):pp.159-172.
11. Hua M, Baines K, Cole IM (1999) Continuous four-roll plate bending: a production process for the manufacture of single seamed tubes of large and medium diameters. International Journal of Machine Tools and Manufacture Vol.39(No.6):pp.905–935.
12. Hua M, Cole IM, Baines K et al. (1997) A formulation for determining the single-pass mechanics of the continuous four-roll thin plate bending process. Journal of Materials Processing Technology Vol.67(No.1-3):pp.189–194.
13. Hua M, Lin YH (1999) Effect of strain hardening on the continuous four-roll plate edge bending process. Journal of Materials Processing Technology Vol.89-90:pp.12-18.
14. Hua M, Sansome DH, Baines K (1995) Mathematical modeling of the internal bending moment at the top roll contact in multi-pass four-roll thin-plate bending. Journal of Materials Processing Technology Vol.52(No.2-4):pp.425–459.
15. Hua M, Sansome DH, Rao KP et al. (1994) Continuous four-roll plate bending process: Its bending mechanism and influential parameters. Journal of Materials Processing Technology Vol.45(No.1-4):pp.181–186.
16. Hua M, Lin YH (1999) Large deflection analysis of elastoplastic plate in steady continuous four-roll bending process. International Journal of Mechanical Sciences Vol.41(No.12):pp.1461-1483.
17. Zeng J, Liu Z, Champliaud H (2008) FEM dynamic simulation and analysis of the roll-bending process for forming a conical tube. Journal of Materials Processing Technology Vol.198(No.1-3):pp.330–343.
18. Feng Z, Champliaud H, Dao TM (2009) Numerical study of non-kinematical conical bending with cylindrical rolls. Simulation Modelling Practice and Theory Vol.17(No.10):pp.1710–1722.
19. Feng Z, Champliaud H (2012) Investigation of non-kinematic conical roll bending process with conical rolls. Simulation Modelling Practice and Theory Vol.27:pp.65–75.
20. Feng Z, Champliaud H (2011) Three-stage process for improving roll bending quality. Simulation Modelling Practice and Theory Vol.19(No.2):pp.887–898.

21. Ktari A, Antar Z, Haddar N et al. (2012) Modeling and computation of the three-roller bending process of steel sheets. Journal of Mechanical Science and Technology Vol.26(No.1):pp.123-128.
22. Fu Z, Tian X, Chen W et al. (2013) Analytical modeling and numerical simulation for three-roll bending forming of sheet metal. The International Journal of Advanced Manufacturing Technology Vol.69(No.5-8):pp.1639-1647.
23. Tran HQ, Champliaud H, Feng Z et al. (2011) FE simulation of heat assisted roll bending process for manufacturing large and thick high strength steel axisymmetric parts. Modelling, Identification, and Simulation 755-041.
24. Tran HQ, Champliaud H, Feng Z et al. (2013) Heat assisted roll bending process dynamic simulation. International Journal of Modelling and Simulation Vol.3(No.1):pp.54–62.
25. Tran HQ, Champliaud H, Feng Z et al. (2012) Analytical modeling and FE simulation for analyzing applied forces during roll bending process. ASME-DETC2012:p207-215.
26. Tran HQ, Champliaud H, Feng Z et al. (2012) Dynamic analysis of a workpiece deformation in the roll bending process by FEM simulation. 24th European Modeling and Simulation Symposium:p477-482.
27. Tran HQ, Champliaud H, Feng Z et al. (2013) Dynamic FE analysis for reducing the flat areas of formed shapes obtained by roll bending process. ASME-2013 International Mechanical Engineering Congress & Exposition IMECE-63302.
28. Feng Z, Champliaud H (2011) Modeling and simulation of asymmetrical three-roll bending process. Simulation Modelling Practice and Theory Vol.19(No.9):pp.1913–1917.
29. ANSYS (2012) Ansys LS-dyna Version 14. ANSYS, Inc.
30. ANSYS (2012) Ansys LS-dyna user's guide ANSYS, Inc.:p14-52.
31. LABVIEW (2010) LABVIEW Version 2010. National Instruments.
32. MATLAB (2011) MATLAB Version 2011a. MATHWORKS.

CHAPTER 4

ARTICLE #2: HEAT ASSISTED ROLL BENDING PROCESS DYNAMIC SIMULATION

Quan Hoang Tran • Henri Champliaud • Zhengkun Feng • Jamel Salem • Thien My Dao

Mechanical Engineering Department, École de Technologie Supérieure (ÉTS), Montréal (Québec) H3C 1K3, Canada

Article published in International Journal of Modelling and Simulation, Volume 3, Issues 1, pp. 54 - 62, 2013

4.1 Abstract

The forming forces during roll bending process can be reduced by heating the workpieces. Heat assisted roll bending is a promising alternative to the costly and time consuming casting process that is usually selected for manufacturing large and thick axisymmetric parts made of high strength steel. In this paper, a computer aided simulation program has been built in the Ansys/LS-Dyna environment to study the relationships between temperature, applied forces and plate thickness. The finite element modelling of the formed geometry is sequential with first a thermal simulation followed by a structural one. The numerical results are then compared to analytical ones. The analyses of the process with numerical simulations yield to a better understanding of the mechanism of the process and provide an opportunity for the design of an efficient heating system to control the heat energy to be input in the workpiece during the roll bending process.

Key Words Roll bending process, FEM, Ansys/Ls-dyna, hot forming

Résumé

Les forces de formage pendant le processus de cintrage peuvent être réduites par chauffage des pièces à former. Le cintrage assisté par chauffage est une alternative prometteuse à l'opération de coulée longue et coûteuse qui est généralement choisie pour la fabrication de pièces axisymétriques de grandes dimensions, épaisses et faites en acier à haute résistance. Dans cet article, un programme de simulation assistée par ordinateur a été construit dans l'environnement Ansys / LS-Dyna pour étudier les relations entre la température, les forces appliquées et l'épaisseur de la plaque. La modélisation par éléments finis de la géométrie formée est séquentielle avec une première simulation en thermique suivie d'une simulation structurale. Les résultats numériques sont ensuite comparés à ceux analytiques. Les analyses du procédé avec des simulations numériques donnent une meilleure compréhension du mécanisme du processus et fournissent une opportunité pour la conception d'un système de chauffage efficace afin de contrôler l'énergie thermique devant être transmise à la pièce à former pendant le processus de cintrage.

Mots-clés: Procédé de roulage, analyse dynamique par éléments finis, Ansys/LS-Dyna, formage à chaud

Nomenclature

a	Center location of lateral roll along action line
E	Young's modulus of plate material
I	Moment of inertia of plate
k_1, k_2, k_3	Curvature of plate at region P_1P_e, P_eP_2 and P_2P_3
k_e	The maximum elastic curvature
K_p	The stiffness coefficient of system at P_1
M_1, M_2, M_3	Bending moment of plate at P_1, P_2 and P_3
M_e	The maximum elastic moment
q_1, q_2, q_3	Contact forces at their respective angle θ_1, θ_2 and θ_3
Q_1, Q_2, Q_3	The applied forces by the respective top, bottom and lateral roll

R	Radius of the rolled cylinder
r	Radius of the rolls
s_1, s_2, s_3	Arc length coordinate of P_1P_e , P_eP_2 and P_2P_3
s	Initial arc length made by two laser beams dotting in lateral roll
t	Plate thickness
Y	The yield stress of plate
θ_1, θ_2, θ_3	Inclined angle of plate at P_1, P_2 and P_3
θ	Operating action line angle of offset cylinder
δ	The deflection of the roll at contact point P_1
ν	Poisson's ratio of the material

4.2 Introduction

High grade stainless steel is widely used in the manufacturing of parts dealing with heavy cyclic loads and corrosive environments. High grade steel are hard to shape and for some applications like the thick conical shape of the crown in a Francis turbine runner tooling is dedicated to one single part. Some of the Francis turbine runners installed in the dam basement are 10 meters in diameter with more than 5 meters in height, while plate thickness can exceed 100 millimeters. The manufacturing technique currently applied in forming the crown of Francis turbine consists of a combination of several metal forming techniques, such as the foundry and welding, punching and welding or forging…Choosing one or more manufacturing processes for delivering a thick and heavy parts like a crown in due time and at a reasonable cost is a hard to solve problem. Here, the roll bending process can make the difference, because bending a plate around a linear axis could be feasible under specific conditions on a roll bending machine.

Rolling plates into cylinders, cones or cylindrical segments is carried out on machines usually with three roll [1] and in some cases, four-rolls, and even two-rolls that rotate and bend the metal as it passes between them. With the advantages such as reducing the setting up time and material, lowering the cost in tooling investment and equipment and to achieve high final shape quality, the roll bending process is one of the fundamental forms used in metalworking. The description of the basic principle and operation for the roll bending process can be found in [2, 3]. Bouhelier [4] gives the formulas for calculating the spring-back, applied forces and the essential required power. Unfortunately, the author does not discuss the mechanism of this process clearly; the final shape is thus difficult to estimate using these formulas. Yang [5] constructed a model for estimating deformation during the various steps of the roll bending process. Hua et al [6-12] have done a considerable amount of work for studying the four-roll model bending process and for understanding the bending mechanism. Hu [13] applied FEM to the study of the mechanism of the roll bending process and proposed a new model which separated the top or bottom rolls into two parts. Analyses of pyramidal three-roll model bending process [5, 14-18] and asymmetrical three-roll model bending process [19] can also be found in some publications, but none of them deals with FE dynamic simulation of heat assisted roll bending process for manufacturing hollow cylindrical or conical parts. It is therefore important to study the roll bending process in hot conditions in order to reduce the force needed to bend a thick plate when manufacturing an axisymmetric part made from high strength steel, for which no rigorous study has been reported.

4.3 Analytical model

The heat assisted roll bending process model in this research consists of four main components: three roll and a plate. The initial and final position of roll and plate are plotted in Figure 4.1.

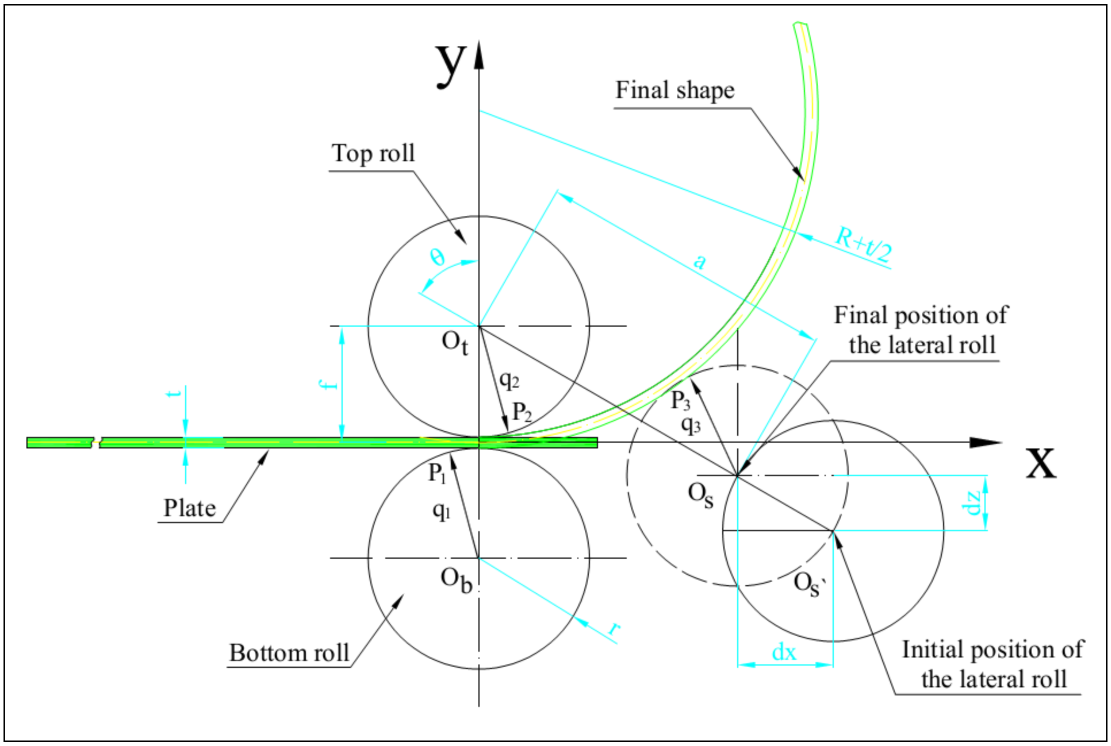
y
Final shape
Top roll
θ
a
R+t/2
Final position of the lateral roll
O_t
f
q2
P2
t
P3
q3
X
Plate
P1
q1
O_s
dz
O_b
O_s`
r
Bottom roll
dx
Initial position of the lateral roll

Figure 4.1 Asymmetrical three-roll bending machine geometry setup

Roll bending machine is used to shape the plate with thickness t indicated in Figure 4.1. The radius R of the plate is computed based on the dimension and the position of rolls and is expressed in equation 4.1

$$R = \frac{a^2 + f^2 - (r + \frac{t}{2})^2 - 2\ a\ f \cos\theta}{2\left(r + \frac{t}{2} + f - a \cos\theta\right)} \tag{4.1}$$

where “a” is the center location of lateral roll along the action line; “f” is the distance from the top roll center to the mid-plate (see Figure 4.1); “r” is the radius of the rolls; “t” is the thickness of the workpiece; and “θ” is the operating action line angle of the offset cylinder.

Equation 4.1 is based only on geometrical consideration; it gives the formula of the geometric setup independently of the material properties and temperature. It helps to compute the setup location of the rolls depending on the desired radius of the final shape. In practice, because of plastic deformation and spring-back effect, the setup is slightly corrected by trial and error to get the right shape.

As seen in Figure 4.2, the plate between P_1P_3 is restricted by contacts with top roll, bottom roll and lateral roll during continuous roll bending mode. Therefore, the following assumptions about the deformation state of the material are made in this region: P_1P_e encounters elastic deformation; P_eP_2 encounters elastic-perfectly plastic deformation, while P_2P_3 encounters elasto-plastic deformation. The free body diagram of the system, including the contact forces q_1, q_2, q_3 and their respective angle θ_1, θ_2, θ_3 is shown in Figure 4.2.

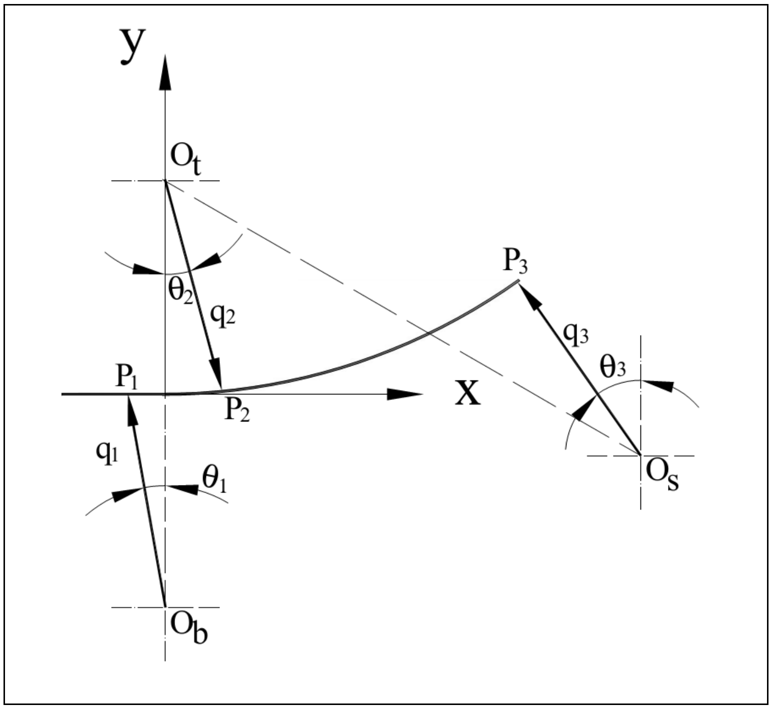

Figure 4.2 Free body diagram of system

Applying equilibrium of forces for each zone of bending plate are shown as in Figure 4.3

$$q_2 \sin\theta_2 = q_1 \sin\theta_1 + q_3 \sin\theta_3 \tag{4.2}$$

$$q_2 \cos\theta_2 = q_1 \cos\theta_1 + q_3 \cos\theta_3 \tag{4.3}$$

where the inclined angle at P_3 is define as $\theta_3=\arcsin[\frac{a \sin\theta}{\left(R+\frac{t}{2}+r\right)}]$. Other inclined angle at P_2, P_1 and the normal contact forces q_1, q_2, q_3 by the respective forces applied at P_1, P_2 and P_3 correspondingly is found out by analyzing each zone of the deformed deformation of the plate as following

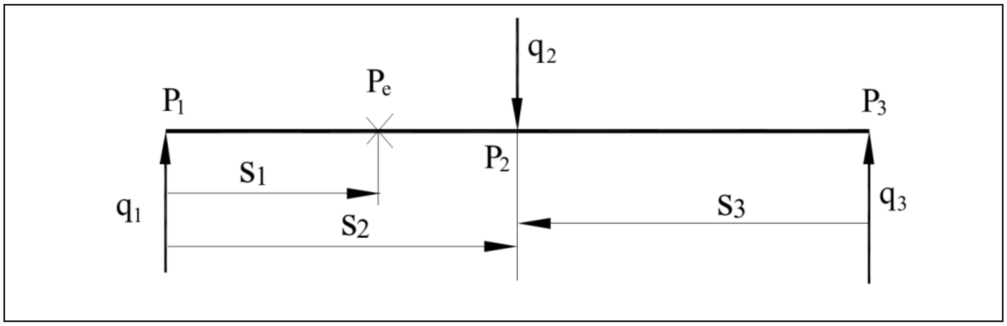

Figure 4.3 Equilibrium of forces of deformation

4.3.1 Elastic deformation P_1P_e

Figure 4.3 is equilibrium of forces of deformation zone. This equilibrium of forces is established based on free body diagram of system in Figure 4.2. It includes 3 contact forces at their respective angle θ_1, θ_2 and θ_3. The maximum elastic moment of the bent plate in the elastic deformation zone are determined by applying engineering beam theory.

$$M_1 = EIk_x \tag{4.4}$$

where $I=\frac{3t}{12}$ is the moment of inertia of plate section per unit width and E is the Young's modulus of plate material

Equilibrium of moments in this zone (Figure 4.3) leads to the $M_1 = q_1 s_1$. Substituting the value of equation $M_1 = EIk_x$ into equation $M_1 = q_1 s_1$ thus gives as an infinitesimal form

$$ds_1 = \frac{EI}{q_1} dk_x \tag{4.5}$$

Integrating both side of equation 4.5 at specific points (from θ_1 to θ_e and from 0 to k_e) with the replacement of $ds_1 = \frac{1}{k_x} d\theta_x$, the inclined angle of plate at P_e is obtained by solving the equation $\int_{\theta_1}^{\theta_e} d\theta_x = \frac{EI}{q_1} \int_0^{k_e} k_x dk_x$

$$\theta_e = \frac{EI}{2q_1} k_e^2 + \theta_1 \tag{4.6}$$

where $k_e = 2Y/Et$

Y is the yield stress of plate

Let y be the y-coordinate of contact point with $ds_1 = \frac{1}{\theta_x} dy_x$. Substituting $ds_1 = \frac{1}{\theta_x} dy_x$ into equation 4.5 with θ_x from equation 4.6, integrating both side to specific points (from y_3 to y_e and from 0 to k_e) and then solving the equation $\int_{y_1}^{y_e} dy_x = \frac{EI}{q_1} \int_0^{k_e} \left(\frac{EI}{2q_1} k_x^2 + \theta_1 \right) dk_x$ thus gives

$$y_e - y_1 = \frac{EI}{q_1} \left(\frac{EI}{6q_1} k_e^3 + \theta_1 k_e \right) \tag{4.7}$$

4.3.2 Elastic-perfectly plastic deformation P_eP_2

In the region of P_eP_2 (see Figure 4.2) moment M_2 and curvature k_2 are following the assumptions of an elastic-perfectly plastic behaviour as discussed by Hua [12]. The governing constitutive equation can be expressed as $M_2 = M_e\left[\frac{3}{2} - \frac{1}{2}\left(\frac{k_e}{k_x}\right)^2\right]$. Equilibrium of moments in this zone (see Figure 4.3) leads to the expression:

$$M_2 = q_1 s_2 \tag{4.8}$$

Upon substitution of equation $M_2 = M_e\left[\frac{3}{2} - \frac{1}{2}\left(\frac{k_e}{k_x}\right)^2\right]$ into equation 4.8, equation 4.8 may be written in an infinitesimal form

$$ds_2 = M_e \frac{k_e^2}{q_1}\frac{1}{k_x^3}\, dk_x \tag{4.9}$$

With $ds_2 = \frac{1}{k_x} d\theta_x$, integrating both sides of equation 4.9 to specific points (from θ_e to θ_2 and from k_e to k_2) and then solving equation $\int_{\theta_e}^{\theta_2} d\theta_x = \frac{M_e k_e^2}{q_1}\int_{k_e}^{k_2} \frac{1}{k_x^2} dk_x$ leading to

$$\theta_2 = M_e \frac{k_e^2}{q_1}\left(\frac{1}{k_e} - \frac{1}{k_2}\right) + \theta_e \tag{4.10}$$

In addition, the equation 4.9 is also expressed as an infinitesimal form $dy_x = \frac{M_e k_e^2}{q_1}\frac{1}{k_x^3}\theta_x dk_x$, with $ds_2 = \frac{1}{\theta_x} dy_x$. Substituting θ_x from equation 4.10 into equation $dy_x = \frac{M_e k_e^2}{q_1}\frac{1}{k_x^3}\theta_x dk_x$, integrating both side to specific points (from y_e to y_2 and from k_e to k_2) and then solving equation $\int_{y_e}^{y_2} dy_x = \int_{k_e}^{k_2}\left(\frac{\theta_e M_e k_e^2}{k_x^3 q_1} - \frac{M_e^2 k_e^4}{k_x^4 q_1^2} + \frac{M_e^2 k_e^3}{k_x^3 q_1^2}\right) dk_x$ gives

$$y_2 - y_e = \frac{M_e^2 k_e}{q_1^2}\left(\frac{k_2^3 + 2k_e^3 - 3k_e^2 k_2}{6k_2^3}\right) + \frac{\theta_e M_e}{2q_1}\left(\frac{k_2^2 - k_e^2}{k_2^2}\right) \tag{4.11}$$

4.3.3 Elasto-plastic deformation P_2P_3

Under large deflection condition, the plate displacement in region of P_2P_3 is assumed as an elastoplastic deformation. The free body diagram is illustrated in Figure 4.3. The equilibrium of moment for this zone is expressed by equation 4.12, where $s_3 = \cos(\theta_1 - \theta_x)\overline{P_2P_3}$

$$M_3 = q_3 s_3 \tag{4.12}$$

The governing constitutive equation has been established in [9] as $M_3 = M_2 + EI(k_x - k_2)$. Substituting equation $M_3 = q_3\cos(\theta_1 - \theta_x)\overline{P_2P_3}$ into $M_3 = M_2 + EI(k_x - k_2)$ and solving this equation after integrating both side to generic points (from θ_2 to θ_3 and from k_2 to k_3), $\int_{\theta_3}^{\theta_2} \cos(\theta_1 - \theta_x)d(\theta_1 - \theta_x) = \frac{EI}{q_3}\int_{k_3}^{k_2} k_x dk_x$ gives

$$q_3 = \frac{EI}{2\sin(\theta_3 - \theta_2)}\left(k_2^2 - k_3^2\right) \tag{4.13}$$

By substituting equation 4.6 into equation 4.10, the relationship between θ_2 and θ_1 is shown as

$$\theta_2 - \theta_1 = M_e \frac{k_e^2}{q_1}\left(\frac{1}{k_e} - \frac{1}{k_2}\right) + \frac{EI}{2q_1}k_e^2 \tag{4.14}$$

Based on the geometric setup, the arc length s_2 can be expressed by $s_2 = \frac{r+t}{2}(\theta_2 + \theta_1)$. Therefore, substitution this value of s_2 into equation 4.8, thus gives an equation for showing the relationship between θ_1 and θ_2 as:

$$\theta_1 = \frac{2M_2}{q_1(r+t)} - \theta_2 \tag{4.15}$$

The equation $q_1 = \frac{P_0}{2\theta_2}$ is established by substituting $\theta_1 = \frac{2M_2}{q_1(r+t)} - \theta_2$ into the above equation $\theta_2 - \theta_1 = M_e \frac{k_e^2}{q_1}\left(\frac{1}{k_e} - \frac{1}{k_2}\right) + \frac{EI}{2q_1}k_e^2$, where $P_0 = k_e^2\left[M_e\left(\frac{1}{k_e} - \frac{1}{k_2}\right) + \frac{EI}{2}\right] + \frac{2M_2}{(r+t)}$

Again, solving equation 4.15 for θ_1 with the value of q_1 given from $q_1 = \frac{P_0}{2\theta_2}$ leads to a simply form

$$\theta_1 = D_0\theta_2 \tag{4.16}$$

in which $D_0 = 1 - \frac{2k_e^2\left[\frac{EI}{2} + M_e\left(\frac{1}{k_e} - \frac{1}{k_2}\right)\right]}{P_0}$

Substituting the equation 4.7 for y_e into equation 4.11 gives the following equation as

$$y_2 - y_1 = M_e^2\frac{k_e}{q_1^2}\left(\frac{k_2^3 + 2k_e^3 - 3k_e^2k_2}{6k_2^3}\right) + M_e\frac{\theta_e}{2q_1}\left(\frac{k_2^2 - k_e^2}{k_2^2}\right) + \frac{EI}{q_1}\left(\frac{EI}{6q_1}k_e^3 + \theta_1 k_e\right) \tag{4.17}$$

Consequently, the substitution of $\theta_e = \frac{EI}{2q_1}k_e^2 + \theta_1$, $q_1 = \frac{P_0}{2\theta_2}$ and $\theta_1 = D_0\theta_2$ into equation 4.17 thus gives a $y_2 - y_1$ relation as

$$y_2 - y_1 = \frac{(A_0 + A_1)\theta_2^2}{3k_2^3P_0^2} \tag{4.18}$$

where $A_0 = 3P_0D_0k_2\left(M_ek_e^2 - M_ek_e^2 + 2EIk_ek_2^3\right)$

and $A_1 = 2E^2I^2k_e^3k_2^3 + 2M_e^2k_e\left(k_2^3 + 2k_e^3 - 3k_e^2k_2\right) + 3EIM_ek_e^2k_2\left(k_2^2 + k_e^2\right)$

Let $\delta = \frac{q_1}{K_p}$ be the deflection of the roll at contact point P_1. By geometry analysis, plate deflection at contact P_1 and P_2 in y direction will be y_1 and y_2 respectively, as $y_1 = -\delta - r\left(1 - \cos\theta_1\right) \approx -\delta - r\frac{\theta_1^2}{2}$ and $y_2 = \delta + r\left(1 - \cos\theta_2\right) \approx \delta + r\frac{\theta_2^2}{2}$ or $y_2 - y_1 = 2\delta + \frac{r\left(\theta_2^2 - \theta_1^2\right)}{2}$. Applying value or $(y_2 - y_1)$ into equation $y_2 - y_1 = \frac{(A_0 + A_1)\theta_2^2}{3k_2^3P_0^2}$ and then substituting above value of $\delta = \frac{q_1}{K_p}$, $\theta_1 = D_0\theta_2$ and $q_1 = \frac{P_0}{2\theta_2}$, the value of θ_2 is determined as:

$$\theta_2 = \frac{\sqrt[3]{6}P_0 k_2}{\sqrt[3]{K_p}\sqrt[3]{2(A_0 + A_1) - 3k_2^3 r(1 + D_0^2)}} \tag{4.19}$$

The relationship between k_2 and k_e was developed by Salem et al [20] and expressed as $k_2 = \frac{k_e}{\sqrt{3 - 2\gamma}}$, where

$$\gamma = \frac{(2k_f + 3)\sin\left[\frac{\arctan\left(\frac{\sqrt{6}\left(8k_f^3 + 36k_f^2 + 54k_f - 27\right)}{36\sqrt{k_f}\sqrt{4k_f^2 + 18k_f + 27}}\right)}{3} + \frac{\pi}{3}\right]}{3} - \frac{4k_f - 3}{6} \tag{4.20}$$

with $k_f = \frac{1}{Rk_e}$

The equation 4.13 is used to determine for q_3, where $k_3 = 1/R$. Then q_1 and θ_1 can be evaluated by the above equation $q_1 = \frac{P_0}{2\theta_2}$ and $\theta_1 = D_0\theta_2$ respectively. Applying equilibrium of forces in equation 4.2, the value of q_2 can be computed.

The above system of equations is programmed in Matlab® [21] software to study the variation of the applied forces in the roll bending process depending on the various parameters. Numerical predictions were conducted for high strength steel plate having dependent thermal properties shown in Figure 4.6.

4.4 Computational modeling of heat forming technique

Line heating method is used for softening the material in this simulation. By this process, the heating system is added directly on the spinning machine as shown in Figure 4.4.

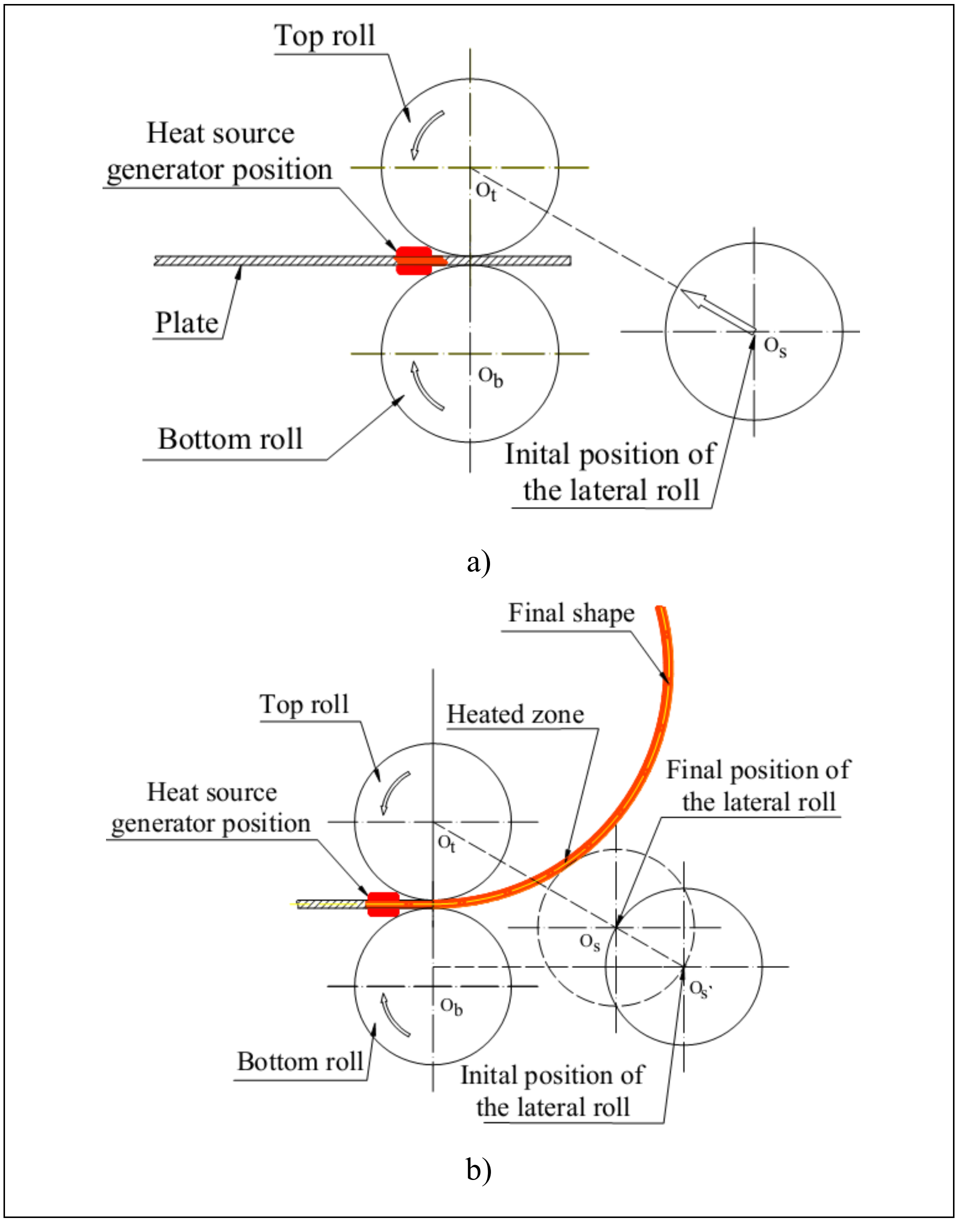
Top roll
Heat source generator position
O_t
Plate
O_s
O_b
Bottom roll
Inital position of the lateral roll
a)
Final shape
Top roll
Heated zone
Final position of the lateral roll
Heat source generator position
O_t
O_s
O_s'
O_b
Bottom roll
Inital position of the lateral roll
b)

Figure 4.4 Heating approach a) at the early stage of heating up; b) during the forming process

During the forming process, the heat source that scans from left-hand to right-hand (Figure 4.4) with a constant speed to generate necessary thermal gradient required for forming. The plate is heated directly and then bent in the same time steps. Through the plate thickness, the temperature gradient makes a different expansion. The numerical modeling of this heat forming technique has been discussed and established in a previous article [22].

4.5 Finite element model

Thermo-mechanical simulation of hot roll bending process includes two-step process. The nonlinear transient thermal analysis is done firstly with three dimensional heat conductions to determine the temperature distribution in the workpiece. Then results in the previous step are applied at various nodes of the mesh and used as the thermal loading for structural analysis and consequent effects of plastic deformation. The finite element model consists of four main components: three roll and a plate which are illustrated in Figure 4.5. All configuration of the model such as the geometry, material properties, mesh size, contacts and loading conditions are defined in the input file.

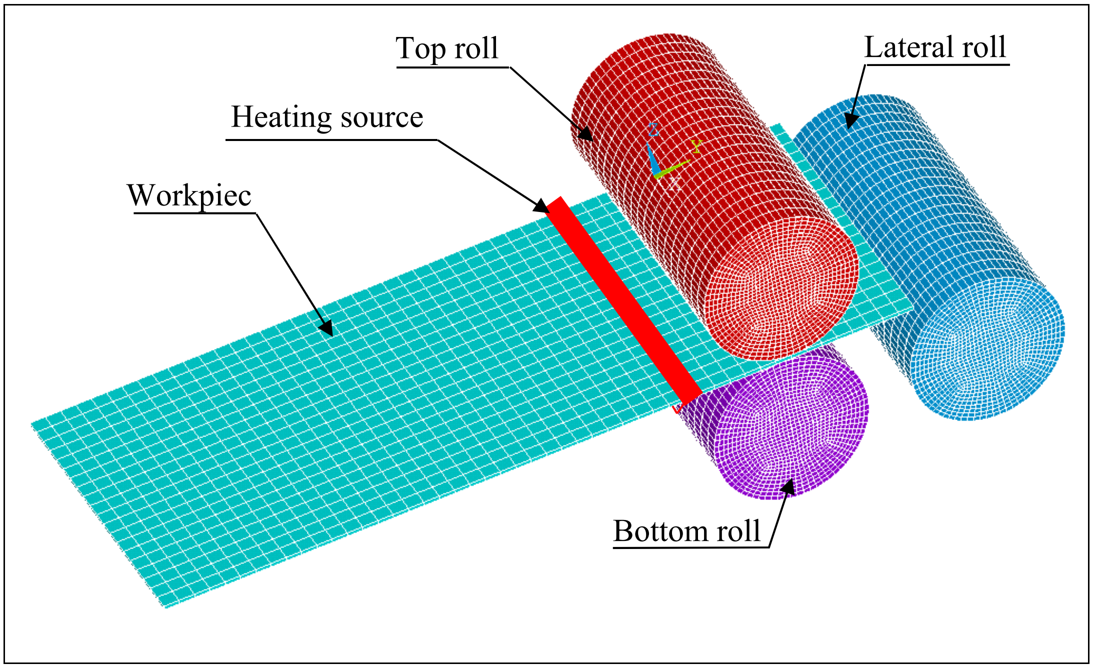

Figure 4.5 FE simulation model of heating assisted roll bending process

4.5.1 Element and mesh

When the plate thickness is very much less than its width and its length, it is commonly modeled with shell elements giving a smaller FE model to solve. For thermal analysis, the 4-

node 3D thermal shell element SHELL57 with a single degree of freedom of temperature at each node is used. Following the thermal solving at each step, these elements are automatically converted into SHELL163 structural shell elements in Ansys/LS-Dyna [23] for explicit dynamic analyses. This process helps in maintaining the same geometrical and mesh of the model for both thermal and structural analysis. The rolls are considered as rigid in comparison with the elasto-plastic deformable plate.

The stainless steel is commonly selected for turbines and hydraulic accessories. Simulation work is done with the stainless steel by using the data provided in reference [24]. The materials properties i.e. Young's modulus, yield stress and thermal expansion coefficient as shown in Figure 4.6 and Figure 4.7 are taken as dependent thermal properties to determine the temperature distribution and the amount of plastic deformation induced in the model.

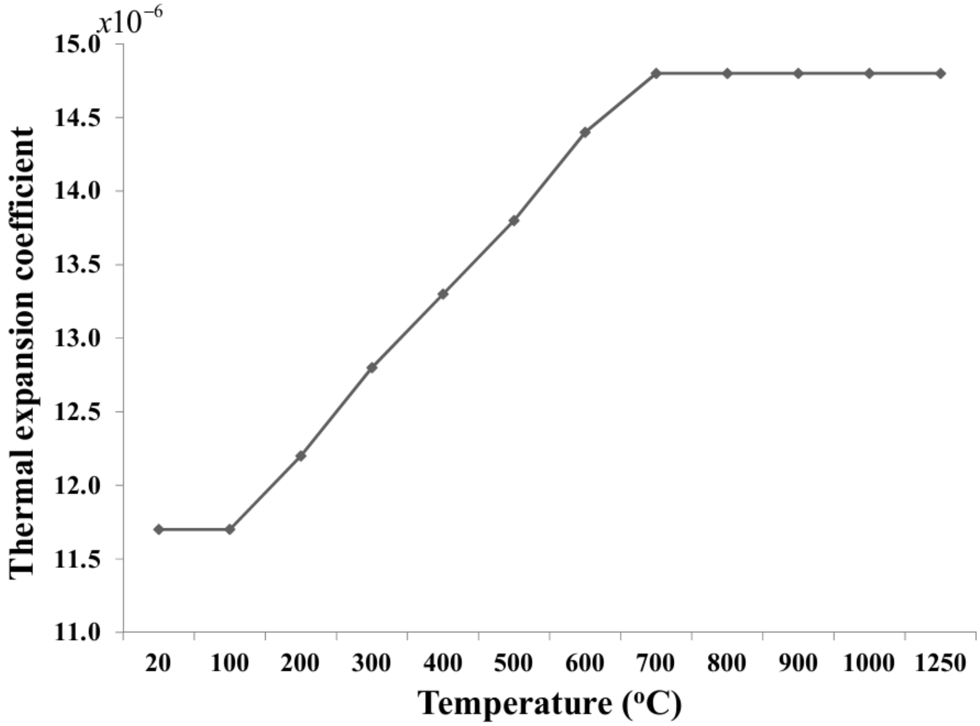

Figure 4.6 Material properties: thermal expansion coefficient [24]

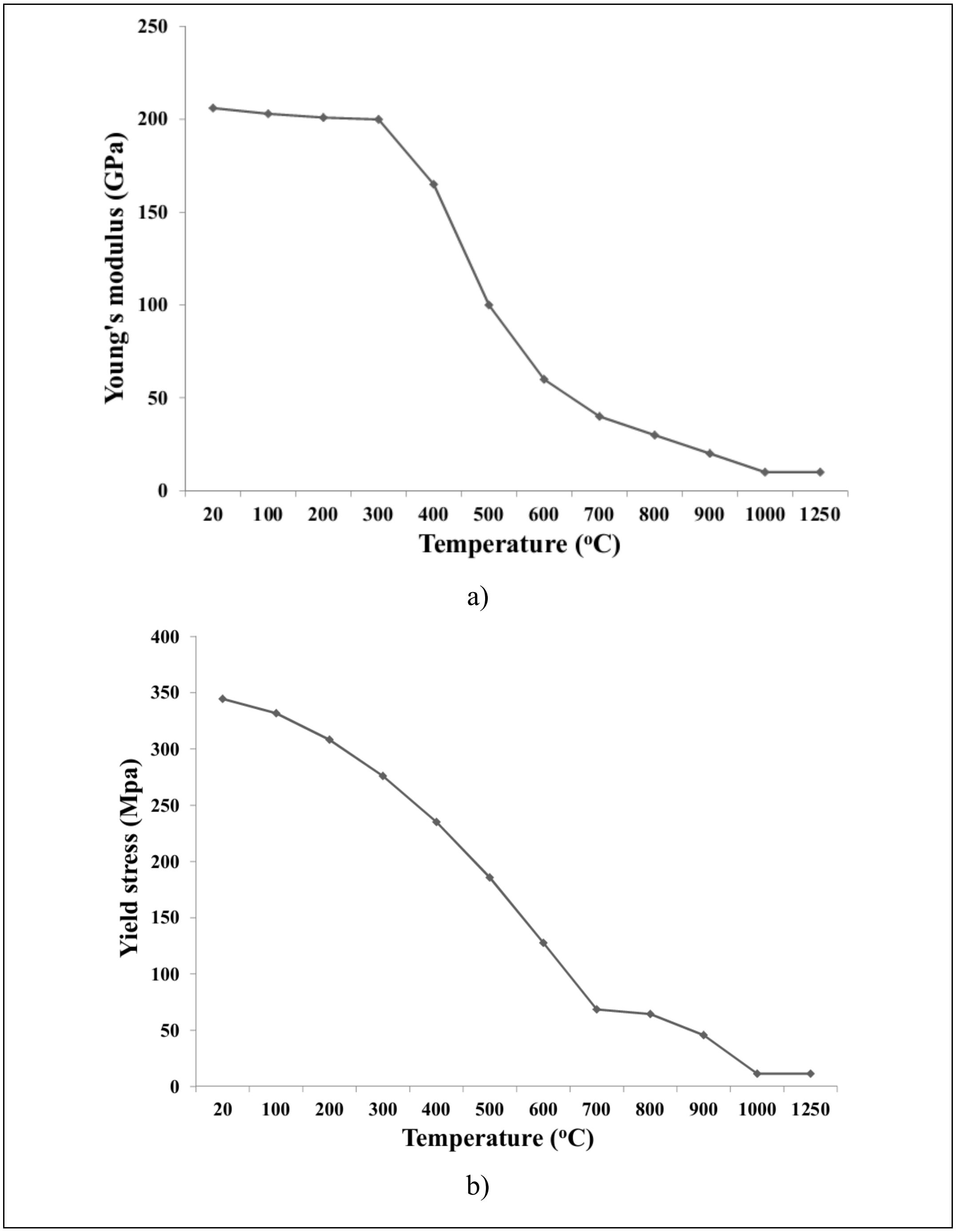

a)

b)

Figure 4.7 Material properties: a) Young's modulus and b) Yield stress [24]

The constitutive property of the material is characterized by a temperature dependent bilinear isotropic model (BISO), an extensive library of material models of Ansys/LS-Dyna that uses two slopes (elastic and plastic) to represent the behaviour of many different materials under numerous conditions. Young’s modulus is used for the elastic slope. The plastic slope is given by the tangent modulus, which in this case was chosen very low (0.1 (Pa)) and temperature independent. The stress-strain relationship is specified at four different temperatures. This model is robust because of its adaptability and flexibility in a FE analysis. For the plate, a mapped mesh is used with quadrilateral shaped element in order to avoid triangular elements.

4.5.2 Contact surface and friction model

The interaction between components is defined by contact surface. Although Ansys/LS-Dyna support a large choice of contact options to define the interaction between surfaces in an explicit analysis but it should be noticed that the contact plays an important role in the modeling of explicit analyses. In general, for most typical analysis, three basic contact algorithms are available: single surface contact, nodes to surface contact and surface-to-surface contact. In our roll bending process model, the surface of the roll is smaller than the surface of workpiece. Therefore, the automatic node to surface was used to define interaction between roll and plate. This kind of surface contact is efficient when a smaller surface come into contact with a larger one. There are three main contact surfaces defined between the plate and rolls for our roll bending FE model. The workpiece is driven and deformed to its final shape via these contact surfaces.

Besides, two coefficients of friction include static friction and dynamic friction that must be defined for the contact model when defining the contact surface. The values of the two coefficients of friction are available in the current literature [18].

4.5.3 Loading

In this simulation, the top and the bottom rolls are constrained as rotation and no translation. The lateral roll yield tool paths as no self-rotation and translate to press the forming plate against the top roll (Figure 4.5). The plate is not typically constrained, but by the rolls through contacts in this simulation.

4.6 Simulations and numerical results

A series of simulations were performed on stainless steel with various heat fluxes and plate thicknesses (from 0.001 m to 0.008 m). While the width of workpiece always remains at 0.20 m, its length (along its scanning direction) is found out by equation 4. 1 that depends on the plate thickness.

To examine the effects of heat flux on temperature induced on the surface of the plate, thermal analyses were performed for various heat fluxes and plate thicknesses with other input parameters remaining unchanged. The temperature induced on the surface of the workpiece is dependent on heat flux power, heat source velocity and the thickness of workpiece. Temperature histories on the top surface of the plate during the moving time of heat flux at three selected times: time = 1 sec when heat source is at the early stage of heating up; time = 30 sec and when the process is completed are plotted in Figure 4.8 and Figure 4.9.

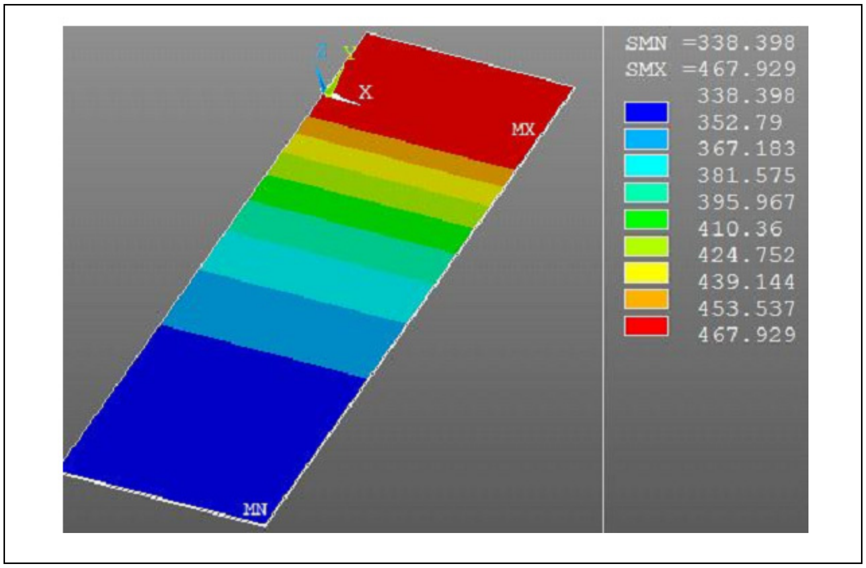

Figure 4.8 Temperature distributions at 1 sec

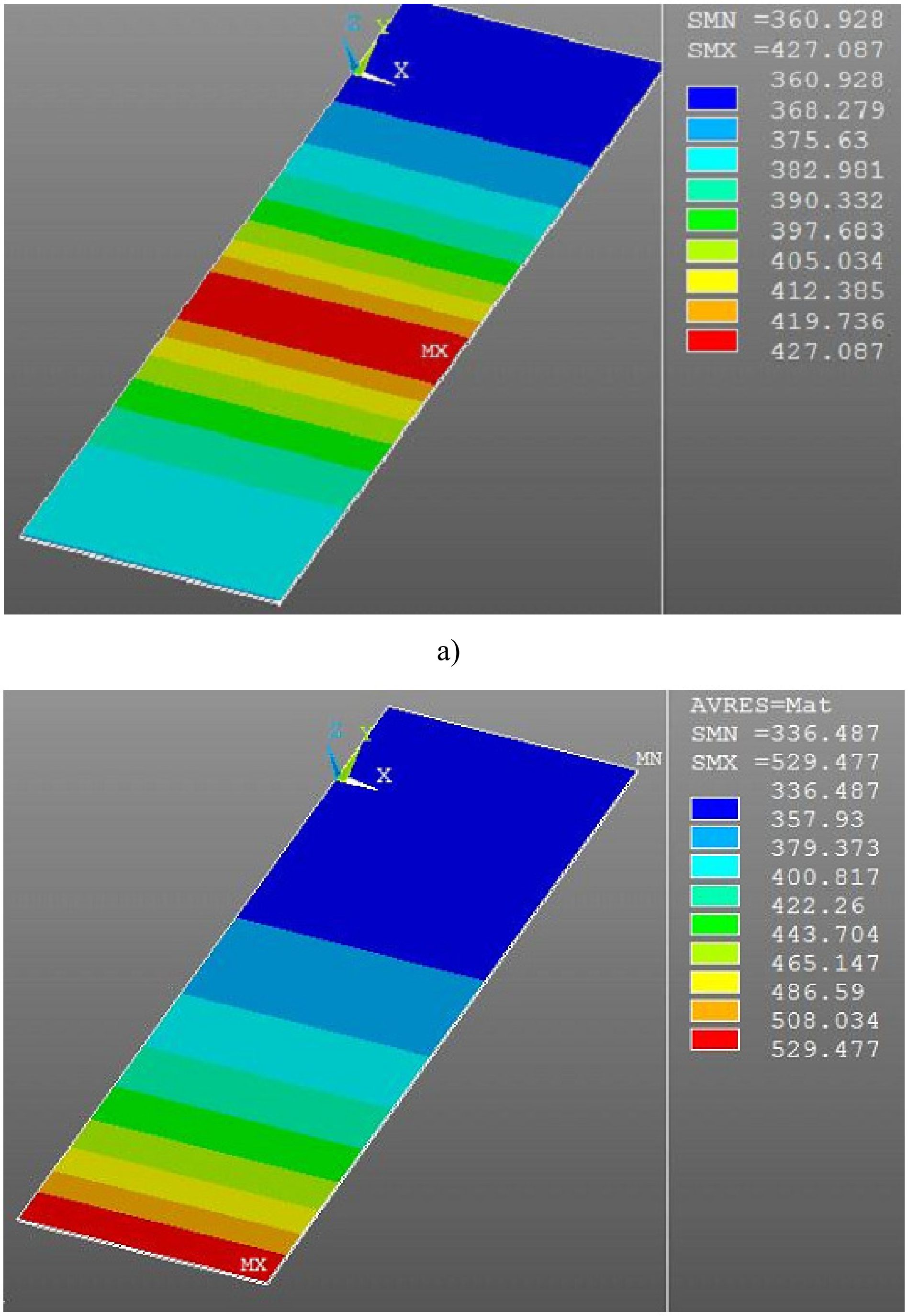

a)

b)

Figure 4.9 Temperature distributions at: a) 30 sec and b) the process is completed

Figure 4.10 shows the temperature distributions at various heat flux for case of plate thickness equals 0.001 m, 0.002 m, 0.004 m and 0.008 m. Thermal gradient increases rapidly with an increasing heat flux.

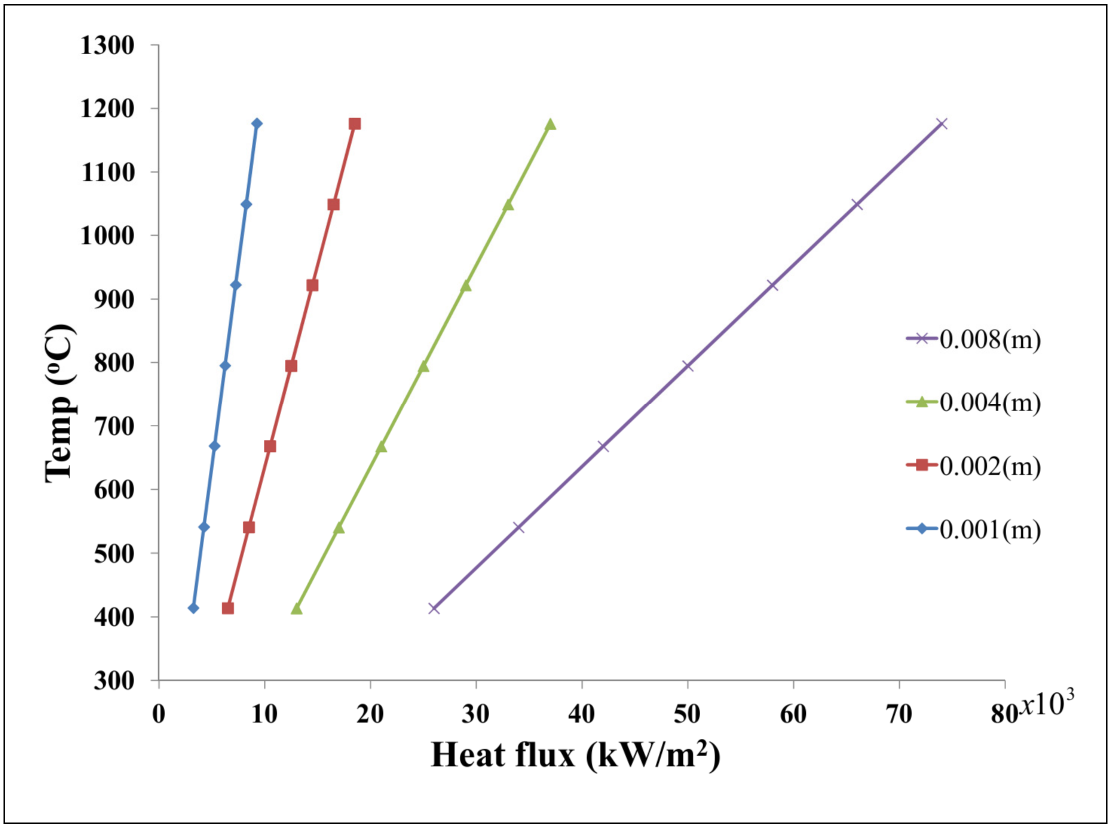

Figure 4.10 Temperature distributions at various heat flux values and plate thickness

In order to heat up the surface of the plate from 415°C to 1175°C, a 0.001 m thick plate required a heat flux from 3.25e3 to 9.25e3 kW/m2. This value increases from 6.5e3 to 18.5e3 and from 13.0e3 to 37.0e3 kW/m2 with 0.002 m and 0.004 m thick sheets, respectively. While surface temperature of a plate with thickness of 0.008 m is maximum for hot forming (1175°C) at 74e3 kW/m2 of heat flux input. The thicker plate needs higher heat flux inputs to produce a required temperature for hot forming. These results will help in selecting a heat flux that does not exceed the melting point of the material for various plate thicknesses.

In order to evaluate the difference in formability between hot and cold forming conditions, reaction force (or called applied force) is measured during the roll bending process. This force is given by total forces of the lateral roll required to form a plate.

As expected, Figure 4.11 and Figure 4.12 shows a decrease in the reaction force when heat flux value is increased. For sheet of greater thickness, increase temperature leads to increases of heat flux input. This means that the greater thickness plate needs more energy to heating up to an acceptable forming temperature in comparison with less thick plate. However, the bending force in hot forming is very much less than in cold forming, especially for thick plate. This is considered as an interesting alternative to apply to hot roll bending process for shaping the thick high strength steel axisymmetric part.

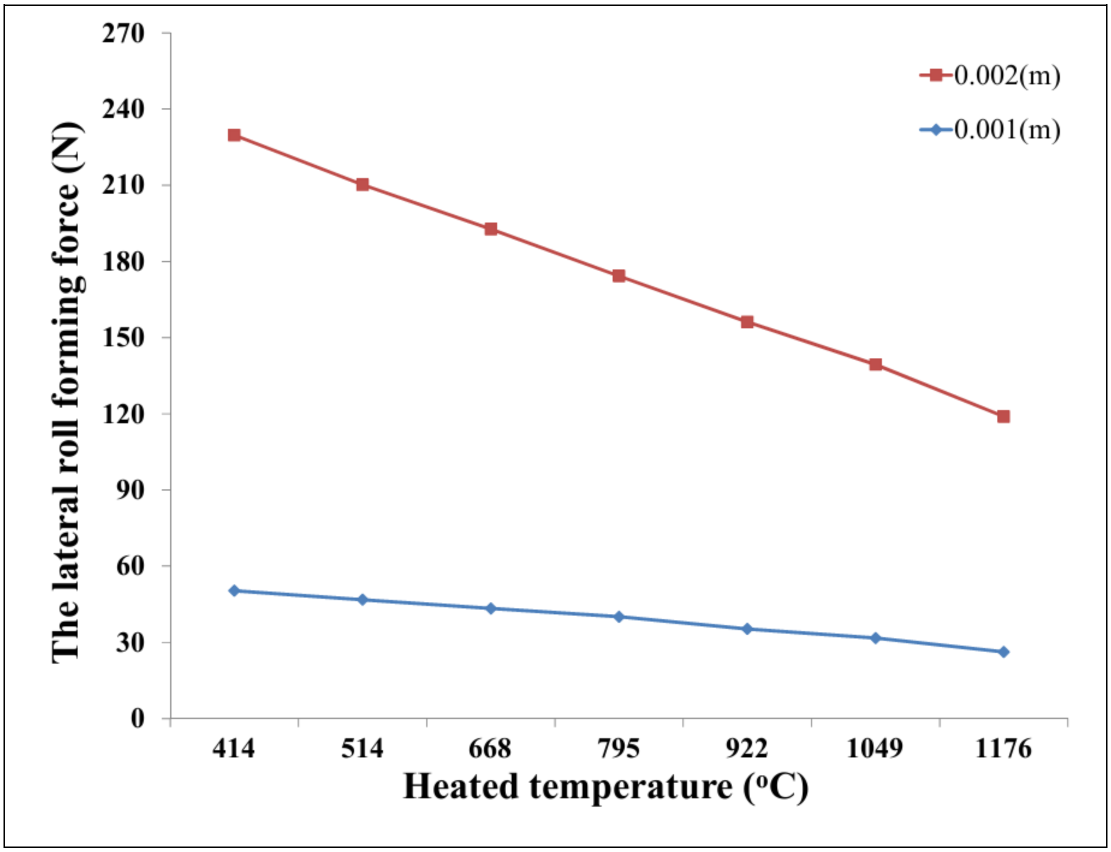

Figure 4.11 Applied force as a function of heat input: t = 0.001 m and 0.002 m

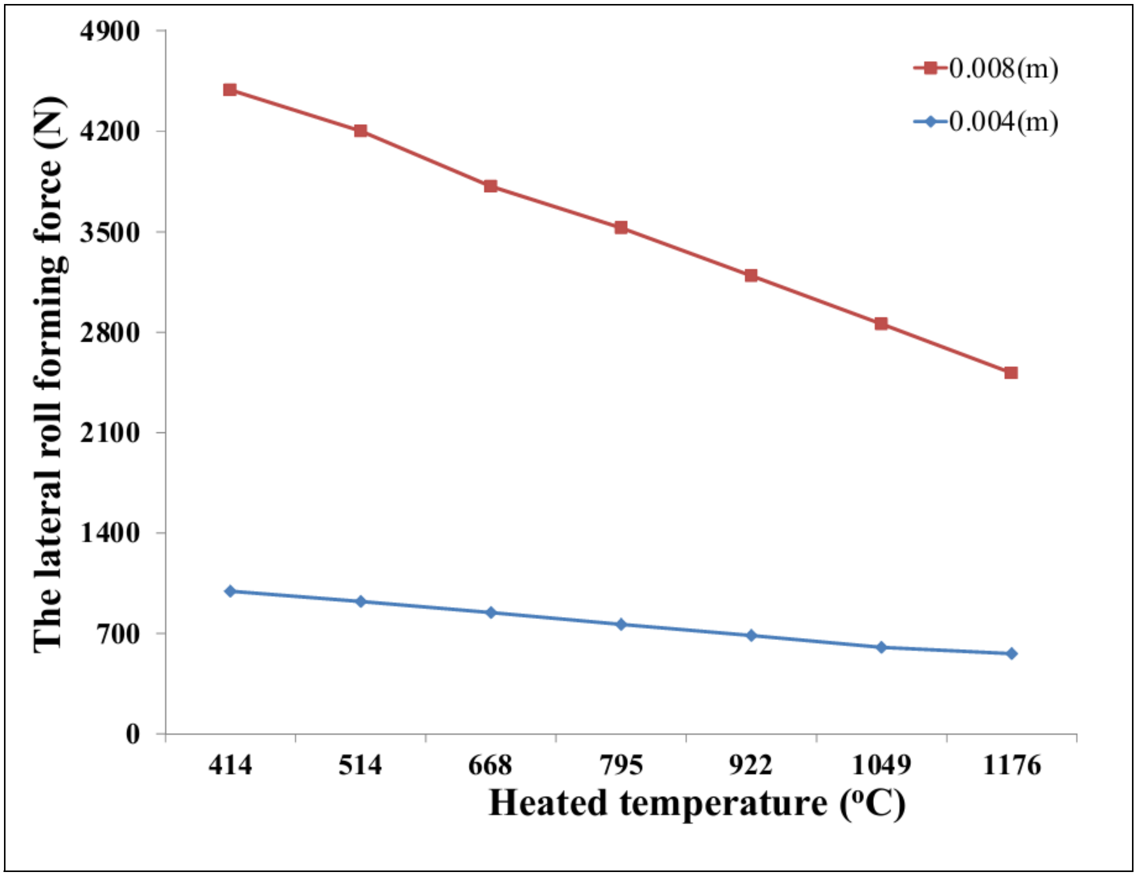

Figure 4.12 Applied force as a function of heat input: t = 0.004 m and 0.008 m

Figure 4.13 shows the comparison between FEM and analytical results of bending force for different plate thicknesses at the room temperature. In general, the increasing trend of reaction force of the analytical results is in a quite good agreement in comparison to the FEM results when the plate thickness is increasing. However, the analytical solution in Matlab® is considered as static modeling while FEM is performed as dynamic simulation. Therefore, the reaction force value from analytical model is quite smaller than FEM results. The value of the applied force for a 0.001 m thick sheet was found to be less than in a 0.002 m and 0.004 m thick metal plate at the same temperature. Typically this is because with the larger thickness of plate, the roll bending machine needs more force to form the shape.

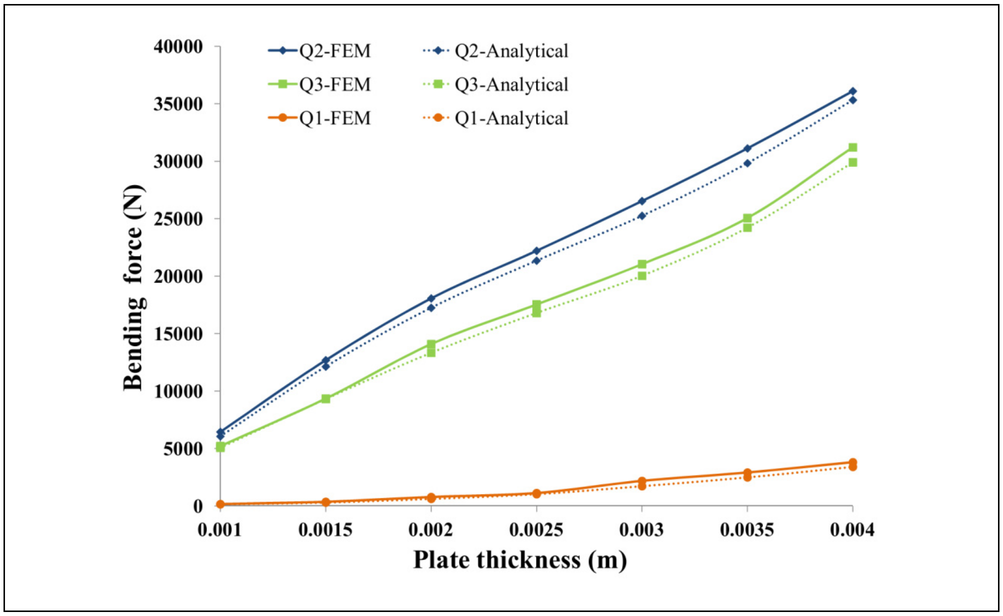

Figure 4.13 Applied force for plate thicknesses at room temperature

From the results of simulations in Ansys/LS-Dyna, the bending quality such as stress distribution, displacement and reaction forces can be plotted directly as shown in Figure 4.14 and Figure 4.15. However, a numerical check must be performed to verify the geometric and radius of the final shapes.

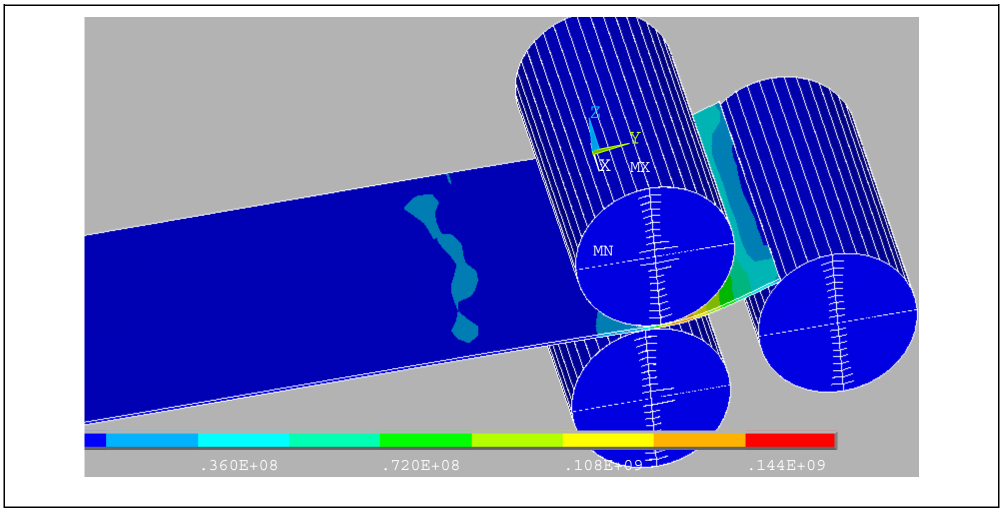

Figure 4.14 Stress distribution at 1 sec

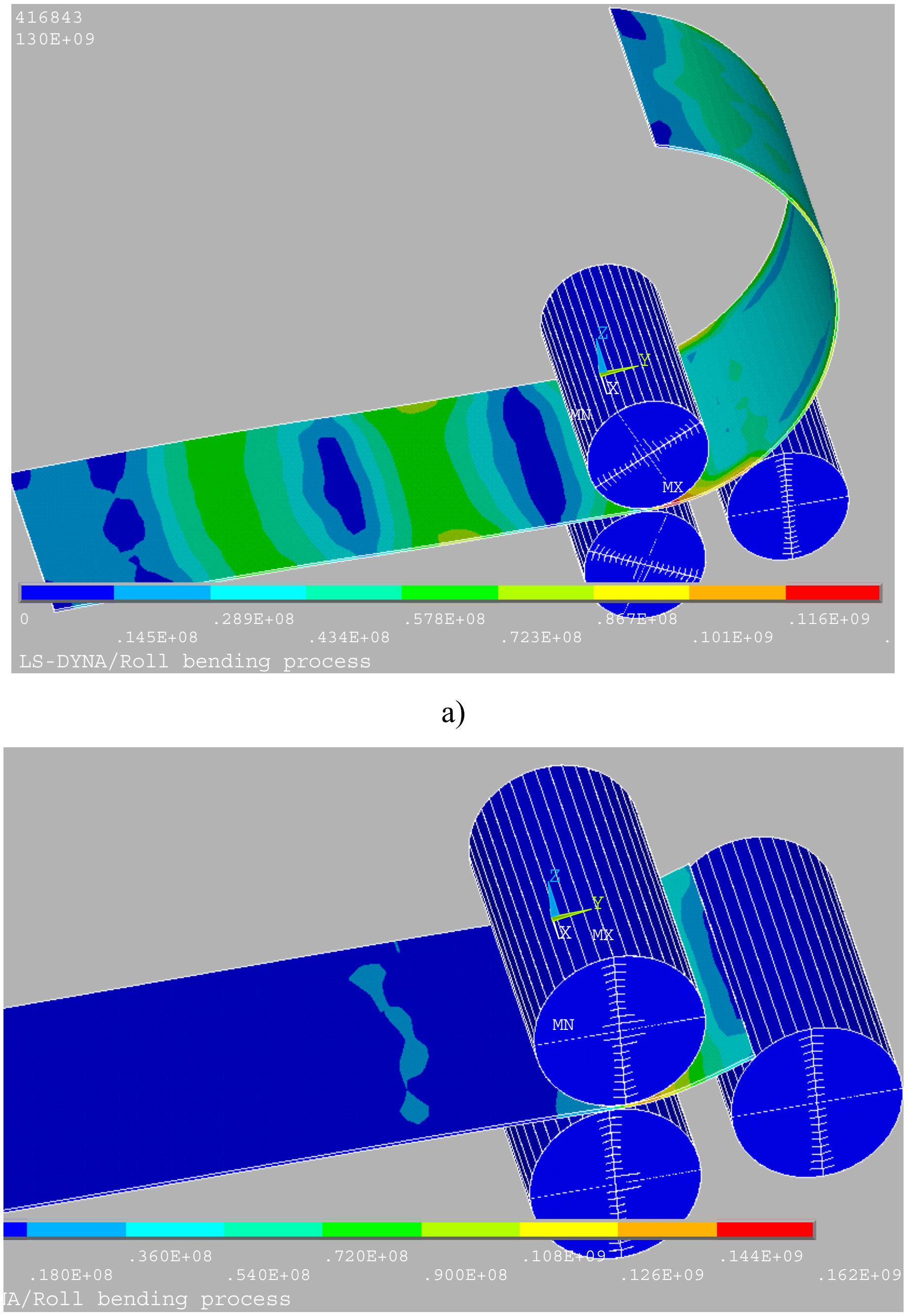
416843
130E+09
Z
Y
X
MN
MX
0
.145E+08
.289E+08
.434E+08
.578E+08
.723E+08
.867E+08
.101E+09
.116E+09
LS-DYNA/Roll bending process
Z
Y
X
MX
MN
.180E+08
.360E+08
.540E+08
.720E+08
.900E+08
.108E+09
.126E+09
.144E+09
.162E+09
A/Roll bending process

a)

b)

Figure 4.15 Stress distribution at: b) 30 sec and c) the process is completed

The purpose of geometric verification is to define bending quality i.e. the radius of the final shape computed from FE results. The coordinates of the center of the circle xC, yC and its radius R, assuming that the nodes of the formed plate are distributed along a cylindrical geometry, are found using the following objective function:

$$\min F(x_c, y_c, R), \text{ with } F=\Sigma (R - R_i)^2 \tag{4.21}$$

Where

$$R_i = [(x_i-x_C)^2 + (y_i-y_C)^2]^{1/2}, \text{ with } x_i= x^{(0)}+ ux \text{ and } y_i= y^{(0)}+ uy \tag{4.22}$$

With grad(F) = 0, three nonlinear equations are solved simultaneously for xC, yC and R. Because these equations are differentiable, a Newton-Raphson scheme was applied to determine the circle parameters. Only the initial coordinates x(0), y(0) and displacements ux and uy of nodes located at the mid-width of the plate are imported into Matlab® for processing, as indicated in Figure 4.16.

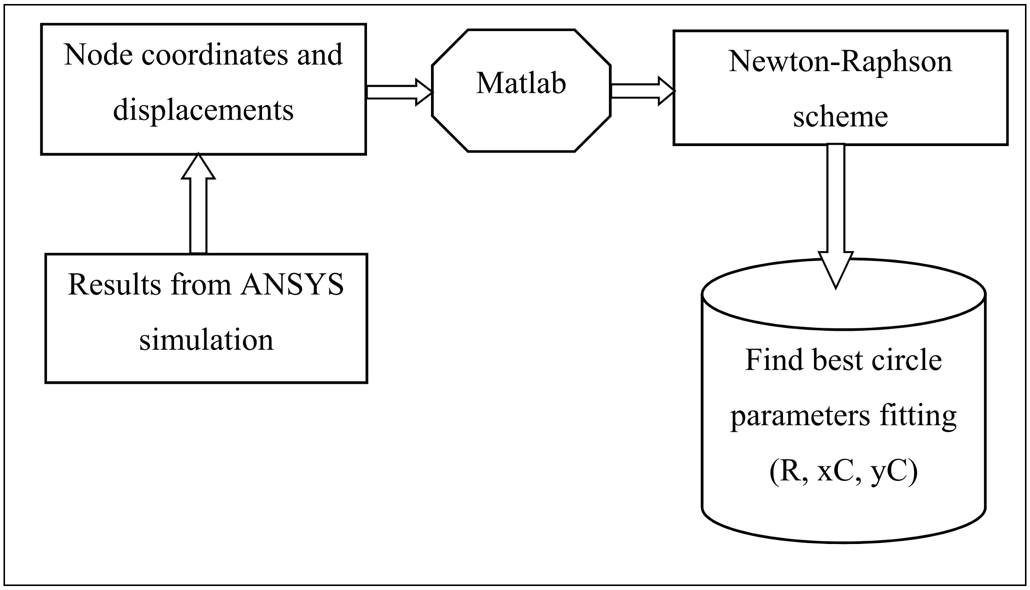
Node coordinates and displacements
Matlab
Newton-Raphson scheme
Results from ANSYS simulation
Find best circle parameters fitting (R, xC, yC)

Figure 4.16 Geometric verification procedure

Different shapes are obtained depending on the forming temperature. Figure 4.17 illustrates radius values of the final shape depending on the heating temperatures. When temperature increases, this value becomes smaller and smaller.

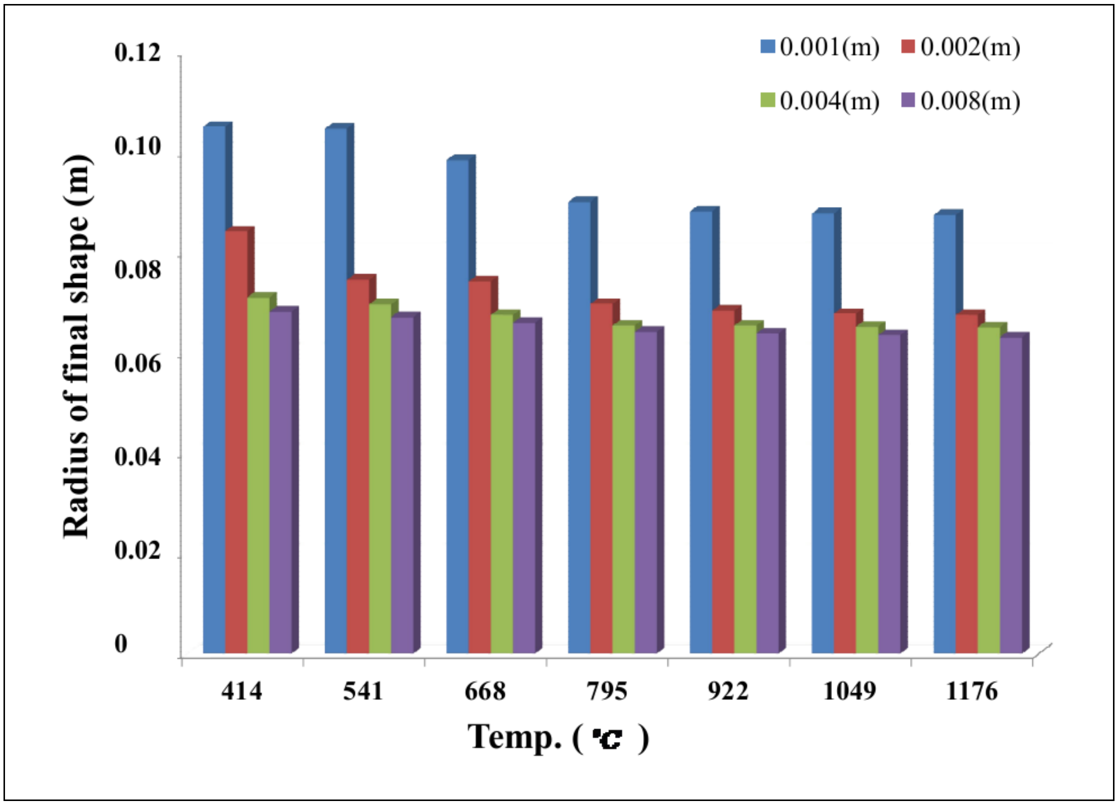

Figure 4.17 Radius of final shape on the different of heating temperature

It is clear that a significant change of the radius occurs at lower thicknesses but when the thickness is increased the radius tends to converge to a constant value, if we plot the resulting radius in comparison with the plate thickness. The reason is that for exactly the same geometric configuration of rolls the amount of plastic deformation through the thickness increases with the thickness of the rolled plate. The final radius of the cylinder is dependent of the amount of plasticity built in through the thickness. When the thickness of the plate increases the plastic zone increases too and the radius tends to converge to a constant value. The material properties change with the temperature but still there is an elastic part and a plastic part in the overall behavior. When the temperature goes over 800°C, the elastic limit is very low and the plate plastifies through nearly all over its thickness leading again the resulting radius to stabilize to a constant value. Again, this shows that the heat energy input can be controlled to get a better bending quality.

4.7 Conclusion

In this research, a three-dimensional FEM shell elements of Ansys and Ansys/LS-Dyna for three-dimensional thermo-mechanical simulation of hot roll bending process has been developed. The analytical model is established based on equilibrium of forces approach and developed in Matlab® programming. As expected, the greater thickness plate needs more energy to heating up to an acceptable temperature for hot condition in comparison with smaller thick plate. However, the bending force in hot forming is very much less than in cold forming, especially for thicker plate. Different radius of final shape is obtained at different heating temperature that may give a chance in order to get better roll bending final shape quality.

4.8 Acknowledgements

The authors are extremely grateful to NSERC of Canada for their support during this research.

4.9 References

1. Wick C., Benedict J.T., Veilleux R.F. (1984). Tool and manufacturing engineers handbook, SME Fourth Edition Volume II.
2. DeGarmo E. P., Black J. T., Kohser R. A. (2002). Materials and Processes in Manufacturing, John Wiley & Sons.
3. Couture P. (2004). Simulation du roulage de tôles fortes, Department of Mechanical Engineering, École de technologie supérieure, Université du Québec, Montreal.

4. Bouhelier C. (1982). Le formage des tôles fortes, CETIM.
5. Yang M. & Shima S. (1988). Simulation of Pyramid Type Three-roll Bending Process, International Journal of Mechanical Sciences, 30:12, 877-886.
6. Hua M., Baines K. & Cole I.M. (1995). Bending Mechanisms, Experimental Techniques and Preliminary Tests for the Continuous Four-roll Plate Bending Process, Journal of Material Processing Technology, 2nd Asia Pacific Conf. on Mat. Proc., 48:1-4, 159-172.
7. Hua M., Baines K. & Cole I.M. (1999). Continuous Four-roll Plate Bending: a Production Process for the Manufacture of Single Seamed Tubes of Large and Medium Diameters, Int. J. of Machine Tools and Manufacture, 39:6, 905-935.
8. Hua M. & al. (1997). A Formulation for Determining the Single-pass Mechanics of the Continuous Four-roll Thin Plate Bending Process. Journal of Materials Processing Technology, Proceedings of the International Conference on Mechanics of Solids and Materials Engineering, 67:1-3, 189-194.
9. Hua M. & Lin Y.H. (1999). Effect of Strain Hardening on the Continuous Four-roll Plate Edge Bending Process, Journal of Materials Processing Technology, 89-90, 12.
10. Hua M., Sansome D.H., Baines K. (1995). Mathematical Modeling of the Internal Bending Moment at the Top Roll Contact in Multi-pass Four-roll Thin-plate Bending, J. of Materials Processing Tech., 52:2-4, 425.
11. Hua M. & al. (1994). Continuous Four-roll Plate Bending Process: Its Bending Mechanism and Influential Parameters, Journal of Materials Processing Technology, 45, 181-186.
12. Hua M., Lin Y. H. (1999). Large deflection analysis of elastoplastic plate in steady continuous four-roll bending process, International Journal of Mechanical Sciences, 41, 1461-1483.
13. Hu W., Wang Z.R. (2001). Theoretical Analysis & Experimental Study to Support the Development of a more Valuable Roll bending Process. Int. J. of Machine Tools and Manufacturing, 41:5, 731-747.
14. Bassett M. B., Johnson W., (1966). The bending of plate using a three roll pyramid type plate bending machine. J. Strain Anal., I(5) 398-414.

15. Hansen N. E., Jannerup O. (1979). Modelling of elastic-plastic bending of beams using a roller bending machine, Journal of Engineering for Industry, Transactions of the ASME, 101(3) 304-310.
16. Roggendorff S., Haeusler J. (1979). Plate bending: three-rolls and four rolls compared, Welding and Metal Fabrication, v 47(6) 353-357.
17. Zeng J., Liu Z., Champliaud H. (2008). Dynamic Simulation and Analysis By Finite Element Method for Bending Process of a Conical Tube and Geometric Inspection, Journal of Materials Processing Technology, 198(1-3) 330-343.
18. Feng Z., Champliaud H., Dao T. M. (2009). Numerical Study of Non-Kinematical Conical Bending with Cylindrical Rolls, Simulation Modelling Practice and Theory, 17(10) 1710-1722.
19. Feng Z., Champliaud H. (2011). Modeling and Simulation of Asymmetrical Three-Roll Bending Process, Simulation Modelling Practice and Theory, 19 (9) 1913-1917.
20. Jamel Salem (2012). Influences des paramètres du roulage à trois rouleaux asymétriques sur la qualité de la pièce formée, Master thesis, École de technologie supérieure.
21. Matlab, 2011, version 7.12.0.365, Release 2011a.
22. Tran Hoang Quan, Henri Champliaud, Zhengkun Feng and Dao Thien-My (2011). FE simulation of heat assisted roll bending process for manufacturing large and thick high strength steel axisymmetric parts, Proceedings of the IASTED International Conference on Modelling, Simulation, and Identification (MSI 2011), November 7 – 9, 2011, Pittsburgh, USA.
23. ANSYS, 2011, ANSYS, Version 13.
24. Lu Zhang (2004). Investigation of Lagrangian and Eulerian finite element methods for modeling the laser forming process, Finite elements in analysis and design, 40, 383-405.

4.10 Biographies

	Tran, Hoang Quan is a PhD student in the Department of Mechanical Engineering, École de technologie supérieure (ÉTS), University of Québec (Canada) under the supervision of Prof. Henri Champliaud and Prof. Thien My Dao. Before coming to ÉTS, he received his Msc in Mechanical engineering at National Kaohsiung University of Applied Sciences (KUAS), Taiwan in 2009. Before that, he completed a B. Eng in Mechanical engineering from Cantho University, Vietnam in 2005. His research focused on simulation of manufacturing processes. He is particularly interested in analysing metal forming process by Finite Element Method.
	Dr Henri Champliaud is a Professor in the Department of Mechanical Engineering, École de technologie supérieure (ÉTS), University of Québec (Canada). He received a Bachelor's Degree from ÉTS, Master's Degree from Sherbrooke University and PhD in Mechanical Engineering from ÉTS in 1991, 1994 and 2000 respectively. He is specialized in the following fields: stress analysis (assemblies and mechanisms), theory and application of the Finite Element Method (static and dynamic analysis in structural, numerical simulation of the non linear behavior of metals and rubber like materials). His research interests are mainly FE simulation of manufacturing processes including forming and welding.
	Dr Zhengkun Feng is a Researcher in the Department of Mechanical Engineering of École de technologie supérieure. Prior to his current position, he was a professor in school of Mechanical Engineering of Guangxi University, China. He received his Bachelor's Degree in automatic control engineering from Xi'an Jiaotong University, China, a DEA in mechanical engineering from Université Pierre & Marie Curie, France and a PhD in mechanical engineering from École de technologie supérieure. He worked for many years in several industries. His research interests include solid and fluid mechanics.

	Dr Thiên-My DAO is a Professor in the Department of Mechanical Engineering, École de technologie supérieure (ÉTS), University of Québec (Canada). He received a Bachelor's Degree, Master's Degree and PhD in Mechanical Engineering (Design option) from Sherbrooke university in 1969, 1971 and 1974 respectively. After four (4) years in industry sector, he joined the Department of Mechanical Engineering of École de technologie supérieure, University of Québec, in 1976 where he is teaching particularly production and operations management, quality management and design of manufacturing systems. His research interests are in optimization of the design, the reliability and the management of manufacturing systems.
	Jamel Salem is a PhD student in the Department of Mechanical Engineering, École de technologie supérieure (ÉTS), University of Québec (Canada) under the supervision of Prof. Henri Champliaud. He received a Bachelor's Degree from École normale supérieure d'enseignement technique (ÉNSET), University of Tunis (Tunisia) in 1995 and a Master's Degree from ÉTS in 2012. He was a professor of mechanical engineering, École technique, Tunisia. His research focused on spot welding process and roll bending of an asymmetrical setup. He is particularly interested in analyzing metal spinning process by Finite Element Method.

CHAPTER 5

ARTICLE #3: FE STUDY FOR REDUCING FORMING FORCES AND FLAT END AREAS OF CYLINDRICAL SHAPES OBTAINED BY ROLL BENDING PROCESS

Quan Hoang Tran • Henri Champliaud • Zhengkun Feng • Thien My Dao

Mechanical Engineering Department, École de Technologie Supérieure (ÉTS), Montréal (Québec) H3C 1K3, Canada

Article published in Journal of Mechanics Engineering and Automation, Volume 4, Issues 6, pp. 467 - 475, 2014

5.1 Abstract

A roll bending process that minimizes the flat areas on the leading and trailing ends of formed plates will produce more accurate and easier to assemble final shapes. There are several methods of minimizing flat areas, but they are costly or difficult to apply for thick plates. This study proposes a new, simple approach that reduces these flat areas. This approach includes moving the bottom roll slightly along the feeding direction and adjusting the bottom roll location. Sensitivity analyses were performed using a developed 3-D dynamic finite element (FE) model of an asymmetrical roll-bending process in the Ansys/LS-Dyna software package. Simulations were validated by experiments run on an instrumented roll bending machine. The FE results indicate that this new approach not only minimizes the flat areas but also reduces the forming forces.

Key words: Roll bending process, flat end areas, dynamic FEM simulation, Ansys/LS-Dyna

Résumé

Un processus de cintrage qui minimise les zones plates aux extrémités avant et arrière des plaques formées produira des formes finales plus précises et plus facile à assembler. Il existe plusieurs méthodes pour minimiser l'étendue des zones plates, mais elles sont coûteuses ou difficiles à appliquer pour les plaques épaisses. Cette étude propose une approche nouvelle et simple qui permet de réduire ces zones plates. Cette approche consiste à déplacer le rouleau inférieur légèrement le long de la direction d'alimentation de la tôle et d'ajuster l'emplacement du rouleau inférieur. Des analyses de sensibilité ont été effectuées en utilisant un modèle d'éléments finis (FE) 3D dynamique développé pour un processus de cintrage axisymétrique avec le logiciel ANSYS / LS-Dyna. Les simulations ont été validées par des expériences exécutées sur une machine de roulage instrumentée. Les résultats par éléments finis indiquent que cette nouvelle approche non seulement minimise les zones plates, mais réduit également les forces de formage.

Mots clés: Procédé de roulage, étendue de plaque non-cintrée, analyse dynamique par éléments finis, Ansys/LS-Dyna

5.2 Introduction

Roll bending is an efficient metal forming technique, where plates are bent to a desired curvature using forming rolls. This type of sheet forming process is one of the most widely used techniques for manufacturing axisymmetric shapes. Moreover, this process is beginning to be taken into serious consideration by industries for producing large, thick parts such as the thick, conically shaped crown of a Francis turbine runner or of a wind turbine tower [1].

Over the past few decades, several bending machines were developed to adapt to various forming production specifications. However, these can be classified into two major types of roll bending machines in the current market: three-roll models and four-roll models. For three-roll models, depending upon the setup location of the forming rolls, they can be

arranged in two groups: three-roll pyramidal models and three-roll asymmetric models. The roll bending process is a continuous type of three-point bending, where the basic principles and operations can be found in Ref. [2-4]. Although the roll bending process can be performed for a wide range of cylindrical parts, for heavy to extremely thick plate applications, there are several issues that limit its application more widely in metal forming. One of them is the flat areas that are left at the leading and trailing edges of the final shape when the process is completed as shown in Figure 5.1.

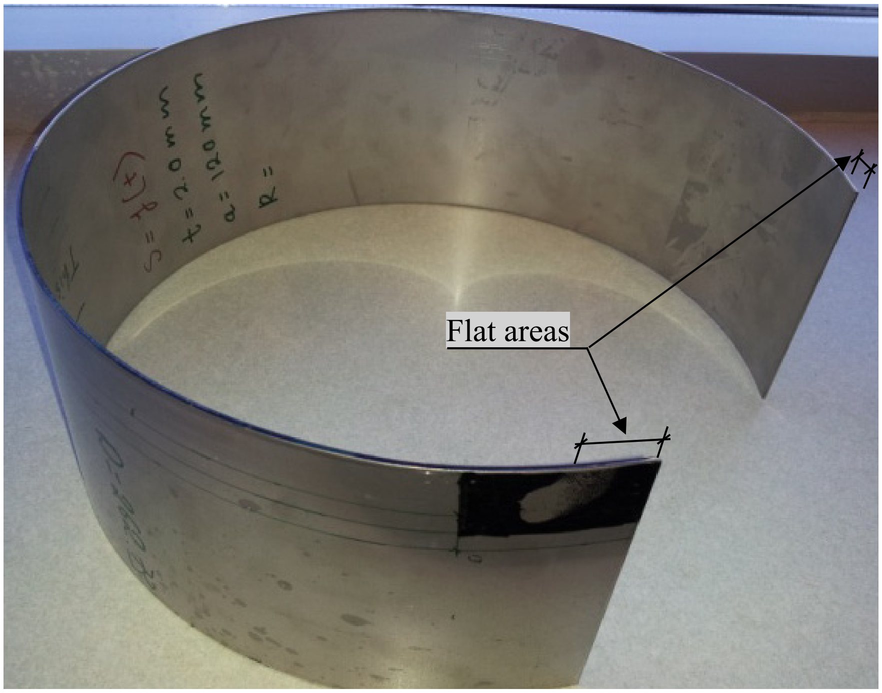

Figure 5.1 Flat areas left by a roll bending process

Forming parts with minimal flat areas on the leading and trailing ends are easier to assemble by welding and obtain a more accurate final shape. However, studies on the mechanisms that produce flat areas are still limited in the literature. Typical studies focus mainly on analyzing the bending mechanism. Hua et al. [5-11] conducted a considerable amount of research studying the four-rolls bending process to understand the bending mechanism. Hu et al. [12] applied an FEM to the study of the mechanism of the roll bending process. Analyses of the pyramidal three-roll bending process and the asymmetrical three-roll bending process can also be found in [13-15]. Zeng et al. [16], Feng et al. [17-19] and Tran et al. [20-24] developed FE models using Ansys/LS-Dyna to simulate the three-roll bending process. However, an analysis of the flat lengths that remain at both ends of the final shape has not been addressed.

The mechanism of the roll bending process inherently produces a certain amount of flat area at the leading and trailing edges of the part. It is observed that this amount of unbent area depends on the machine type. Usually, a three-roll asymmetric model leaves a smaller flat area at the leading and trailing ends of the final shape relative to a pyramid-type model because the workpiece is held more firmly in the former [3]. Zhong et al. [25] analyzed the straight-end problem in a thin-plate, pyramid-type machine through the development of an analytical method. However, the authors did not discuss the flat areas produced by a three-roll asymmetric machine and did not propose a method to reduce these. Therefore, the previous study of Tran [24] is expanded to study in additional detail the effect of the rolls setup on the length of the flat areas in this study.

To reduce or even eliminate the unbent areas, a number of methods can be applied such as a) forming a small amount of extra length at each end and subsequently cutting them off or; b) hand hammering the flat end. However, these techniques are costly or difficult to apply for thick plates made of high-strength steel. Therefore, to obtain a better circularity for the final shape, the most common method used is to pre-bend both ends of the workpiece using the roll bending machine. This is done by inserting the leading end of the workpiece into the machine. A short section of the plate is fed for pre-bending, and, subsequently, the rotation of the rolls is reversed to remove the part. The pre-bending operation is then repeated at the other end of the blank. However, this is a drawback because the plate must be handled twice for pre-bending and requires more intensive labor at the production stage and additional safety measures.

The effect of moving the bottom roll to the left hand side by a distance d_i as shown in Figure 5.2a and adjusting the bottom roll to a "gap" value g_i (see Figure 5.2b) on the flat ends length is presented in this paper. The goal is to propose a new approach to minimize the apparent flat ends and to reduce the forming forces.

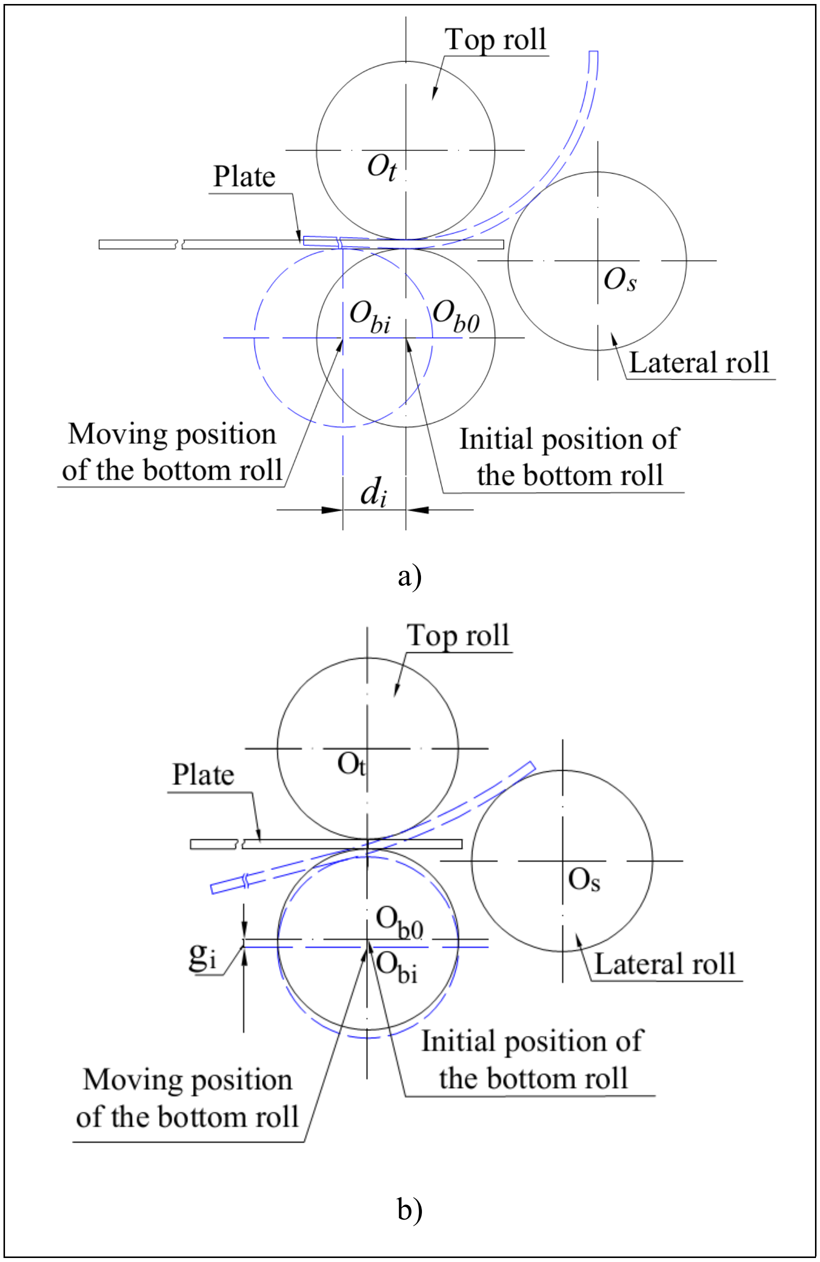
Top roll
Plate
O_t
O_s
O_{bi}
O_{b0}
Lateral roll
Moving position of the bottom roll
Initial position of the bottom roll
d_i
a)
Top roll
Plate
O_t
O_s
O_{b0}
O_{bi}
g_i
Lateral roll
Initial position of the bottom roll
Moving position of the bottom roll
b)

Figure 5.2 Varying the location of the bottom roll a) offset d_i, and b) the "gap" value g_i

The paper is divided in six sections. The content is as follows: Section 2 introduces the asymmetrical roll bending machine setup and flat areas definition. Section 3 details the FE model of the asymmetrical roll bending process. Experimental study to validate the FE model is presented in section 4. Section 5 is the discussion about the results and section 6 summarizes key conclusions of this research.

5.3 Asymmetrical roll bending machine and flat areas definition

In this study, an asymmetrical roll bending machine is used to shape a plate of thickness t as shown in Figure 5.3.

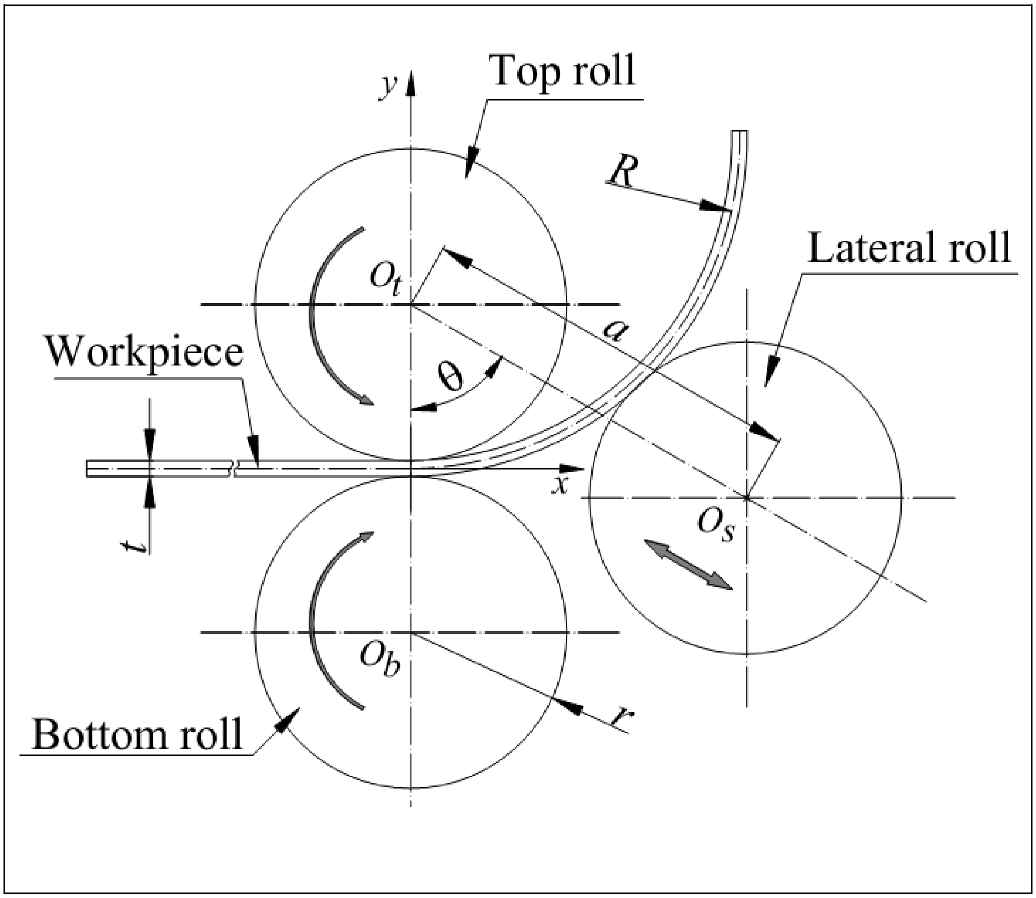

Figure 5.3 Parameter of three-roll asymmetric roll bending machine

The radius R of a formed cylindrical shape depends on the position of the lateral roll [19] and can be expressed by Equation 5. 1.

$$R=\frac{a}{2}\left[\frac{a\sin^2\theta}{2r+t-a\cos\theta}-\cos\theta\right] \tag{5.1}$$

where

a: center location of lateral roll along action line;

r: radius of the rolls;

t: thickness of workpiece; and

θ: operating action line angle of offset cylinder.

The top roll is in a fixed position, while the bottom roll has an adjustable up and down displacement to pinch the workpiece and to allow for the removal of the finished workpiece. The workpiece is fed and “pinched” between the top roll and the bottom roll; the lateral roll location can be adjusted to achieve the desired radius of the final shape. At the end of the forming process, a cylindrical shape with a radius R is obtained if the length of the blank equals the developed length of the cylindrical shape and if the lateral roll is properly positioned. However, the workpiece must remain supported at all time by the rolls as mentioned previously. The process continually produces flat areas along the leading and trailing edges of the workpiece where the plate cannot be completely bent as shown in Figure 5.4.

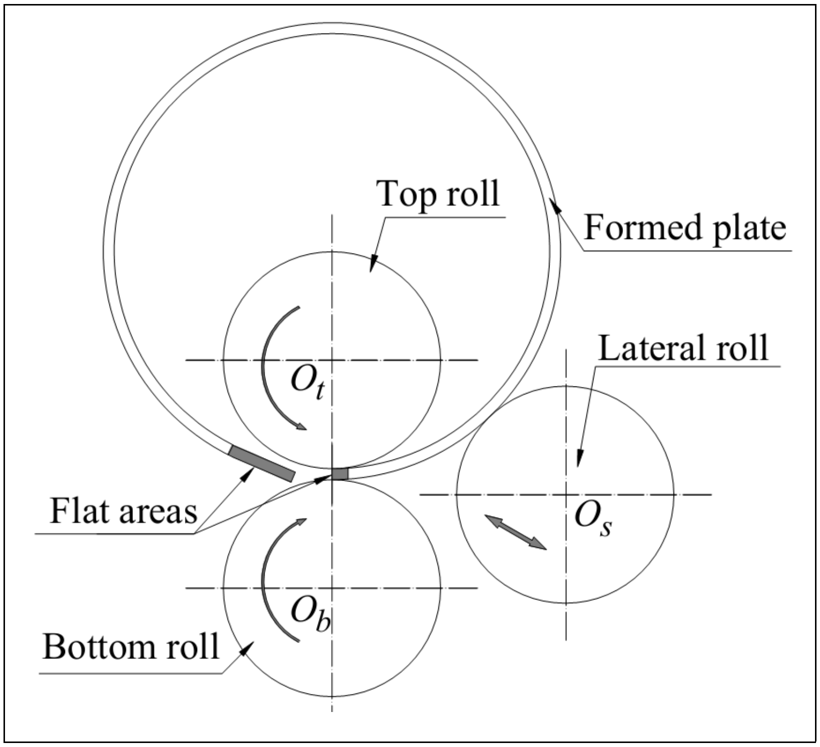
Top roll
Formed plate
Lateral roll
O_t
Flat areas
O_s
O_b
Bottom roll

Figure 5.4 Flat-end definition

5.4 Finite element model of the asymmetrical roll bending process

To study the flat areas produced by the roll bending process, a 3D numerical FE model of an asymmetrical roll bending machine described in the above section was developed in the Ansys/LS-Dyna software package. The FE model consists of four main components: three rigid rolls and one flexible plate, which are illustrated in Figure 5.5. The rolls are considered to be rigid in comparison with the deformable workpiece.

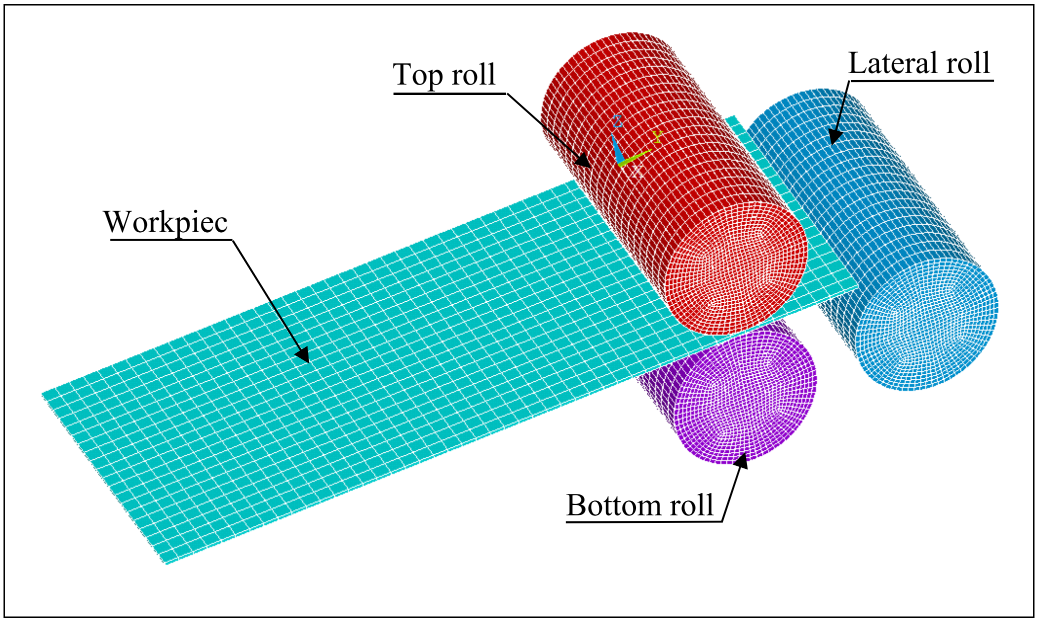

Figure 5.5 FE model of the asymmetrical roll bending process

To describe the nonlinear behavior of the stress-strain curve of the workpiece, a material model obeying the Ludwik-Hollomon equation is used for this nonlinear analysis. Ludwik-Hollomon's equation relates the stress to the amount of plastic strain as a power law

$$\sigma = K\,\varepsilon^{n} \tag{5.2}$$

where

σ: the stress;

K: material constants;

ε: the strain;

n: study hardening exponent.

The constants K and n are approximated by a curve fitting based on the results from a tensile specimen. Figure 5.6 shows the stress-strain curves for the tensile testing model and the approximation model obtained by Ludwik-Hollomon's equation. The rate sensitive power law plasticity (PLAW) model in Ansys/LS-Dyna is applied to determine the stress-strain behavior of the workpiece.

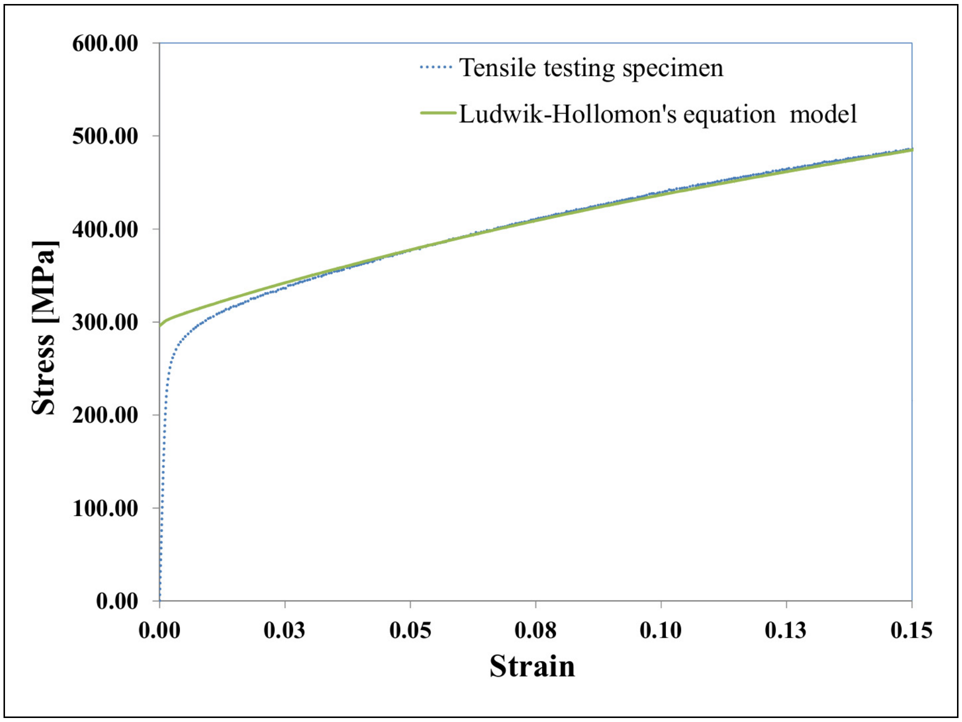

Figure 5.6 Stress-strain curve of plate material

The interaction between the rigid and flexible components is characterized through contact surfaces. In this roll bending model, the surface of the roll is smaller than the surface of the blank. Although in the explicit analysis, Ansys/LS-Dyna supports a large number of contact options to define the interaction between the surfaces. The automatic node-to-surface algorithm was used for the interaction between the rolls and the plate because this type of surface contact is efficient when a smaller surface comes into contact with a larger one. In addition, the static friction coefficient μs between the plate and the rolls is directly measured via experiments.

For the boundary conditions, the top and bottom rolls are driven in rotation and fixed in translation. The lateral roll is constrained in translation and experiences no self-rotation to press the forming plate against the top roll.

5.5 Experimental study to validate the FE model

To validate the FE model developed in Ansys/LS-Dyna, experiments are conducted using the same parameters on an asymmetric roll bending machine. This instrumented roll bending machine has three rolls with diameters of 100.0 mm, roll length of 1500.0 mm and an operating action line angle of the lateral roll (i.e., θ) of 60^0 is shown in Figure 5.7.

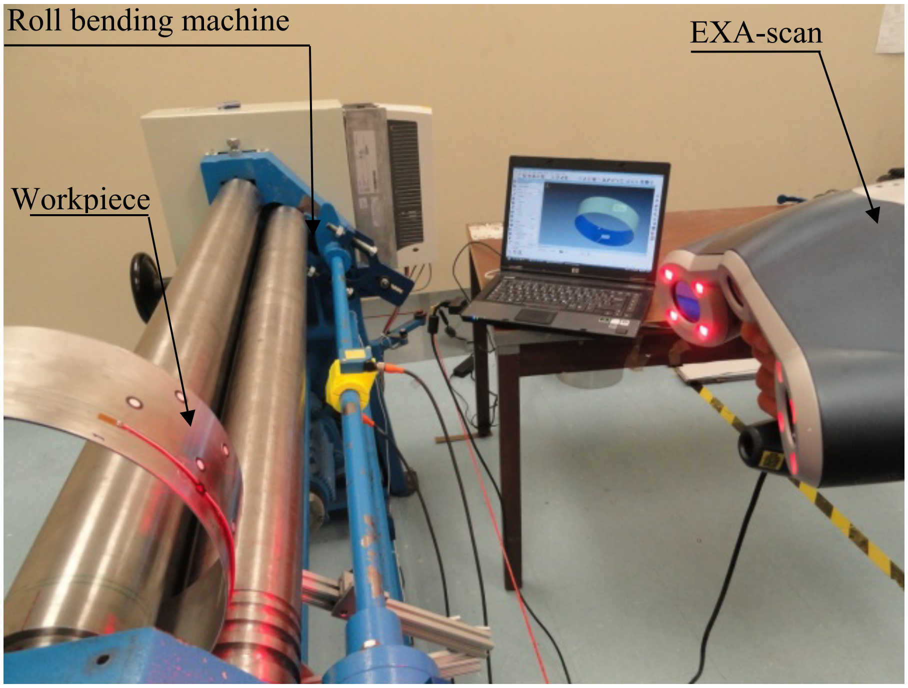

Figure 5.7 Instrumented roll bending machine

The final shape radius from the experiments obtained by the roll bending machine is measured by an EXAscan laser scanner. This device is a hand-held laser system that allows for quick and accurate geometry data acquisition for verifying the characteristics of a formed plate.

Figure 5.8 shows the flat ends at the leading and trailing edges of the cylinder shape in Ansys/LS-Dyna when the roll bending process is completed.

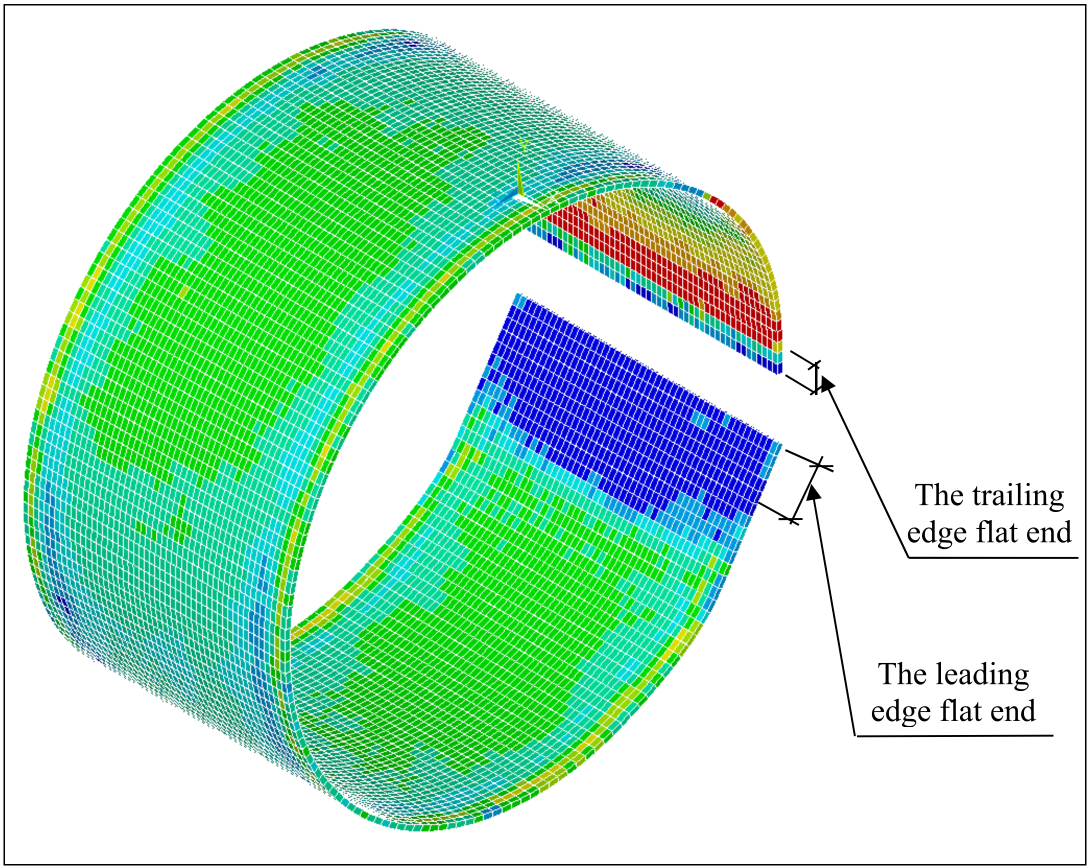
The trailing edge flat end
The leading edge flat end

Figure 5.8 Final shape obtained by the FEM

To compute the flat end lengths of the formed plate from the FE simulations in Ansys/LS-Dyna, a numerical procedure is applied as summarized in Figure 5.9.

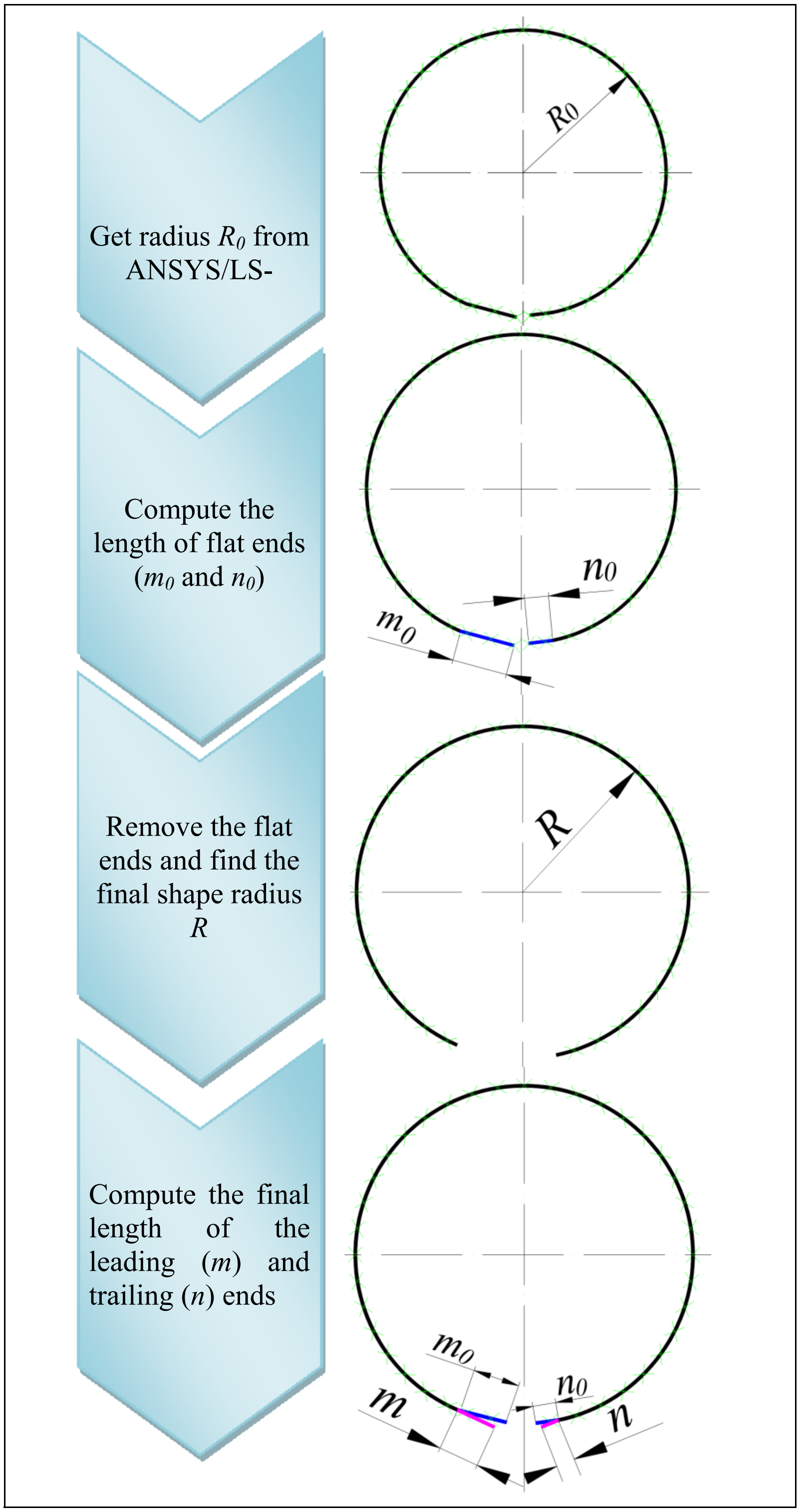
Get radius R_0 from ANSYS/LS-
R_0
Compute the length of flat ends (m_0 and n_0)
m_0
n_0
Remove the flat ends and find the final shape radius R
R
Compute the final length of the leading (m) and trailing (n) ends
m_0
n_0
m
n

Figure 5.9 Flat end and radius computational procedure

Because the nodes of the formed plate are distributed along a cylindrical geometry, the coordinates of the center of the cylinder xC, yC and its radius R_0 are determined using the least squares method

$$\min F(x_c, y_c, R), \text{ with } F=\Sigma (R - R_i)^2 \tag{5.3}$$

Where

$$R_i = [(x_i-x_C)^2 + (y_i-y_C)^2]^{1/2} \tag{5.4}$$

With xi= xi (0) + uxi and yi= yi (0) + uyi.

With grad(F) = 0, three nonlinear equations are simultaneously solved for xc, yc and R_0. Only the initial coordinates xi (0), yi (0) and the displacements uxi and uyi of the nodes located at the mid-width of the plate are imported into Matlab® for numerical processing. A Newton-Raphson scheme is subsequently applied to determine the circle's parameters.

We assume that the nodes at the mid-width and at the trailing or leading edges of the formed plate in Figure 5.8 are distributed along geometry as shown in Figure 5.10.

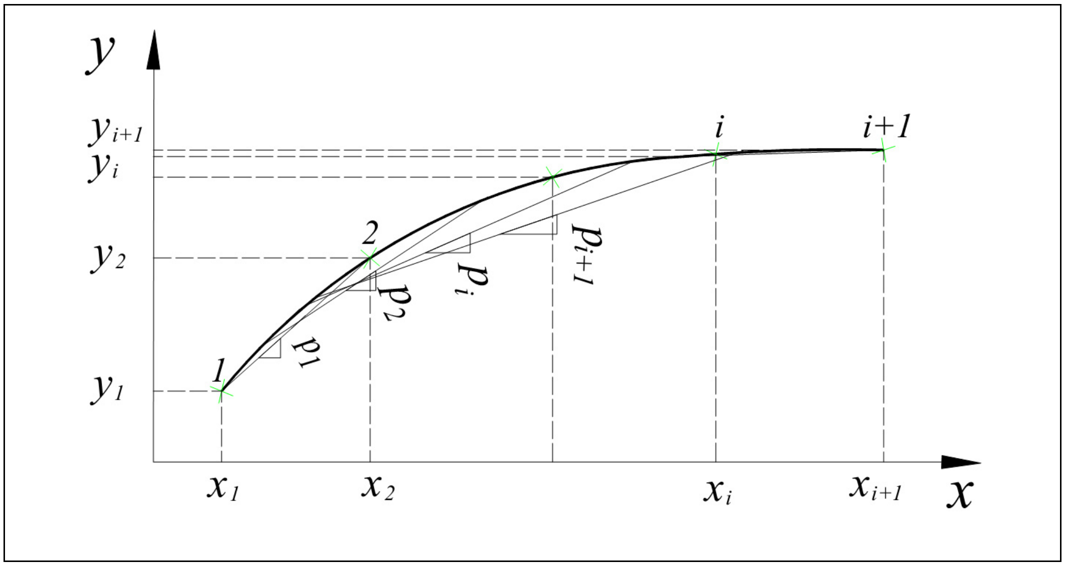

Figure 5.10 Flat end length computational procedure

To determine which nodes at the leading or trailing ends belong to a straight line, based on a number of flatness criteria, a least-squares method was applied to compute the constants p_i and b of the best straight line $y = p_i x + b$ passing through nodes [1 2 3 … i+1].

With Δ = 0.2 t/R [25], the criterion for flatness, a node i+1 is considered to belong to the flat end if and only if the new slope p_i+1 satisfies Equation 5.5:

$$\left| p_{i+1} - p_i \right| \leq \Delta \tag{5.5}$$

The procedure is terminated when adding a new subsequent node does not satisfy Equation 4. The final shape radius R is then recomputed following Equation 5.3 with the remaining nodes, i.e., by removing the flat-end nodes from the initial node list.

It is costly to run a large number of experiments to study how the flat areas are related to the setup. Therefore, the idea is to compare the final shape radius R obtained by both the FE model and the experiment under the same forming conditions. The FE model is used to study the parameters affecting the extent of the flat areas. Figure 5.11 shows comparisons of the final shape radius R for various plate thicknesses, i.e., t = 1.0 mm, 1.5 mm, 2.0 mm or 2.5 mm for four different locations of the lateral roll, i.e., a = 110.0 mm, 115.0 mm, 120.0 mm or 125.0 mm. The final shape radii R obtained by the FE simulations (solid lines in Figure 5.11) are slightly smaller than those obtained through experiments (dotted lines in Figure 5.11). However, a deviation is observed with a highest difference of less than 8.0 %, showing that the developed FE model is capable of accurately predicting the geometry of the formed plate.

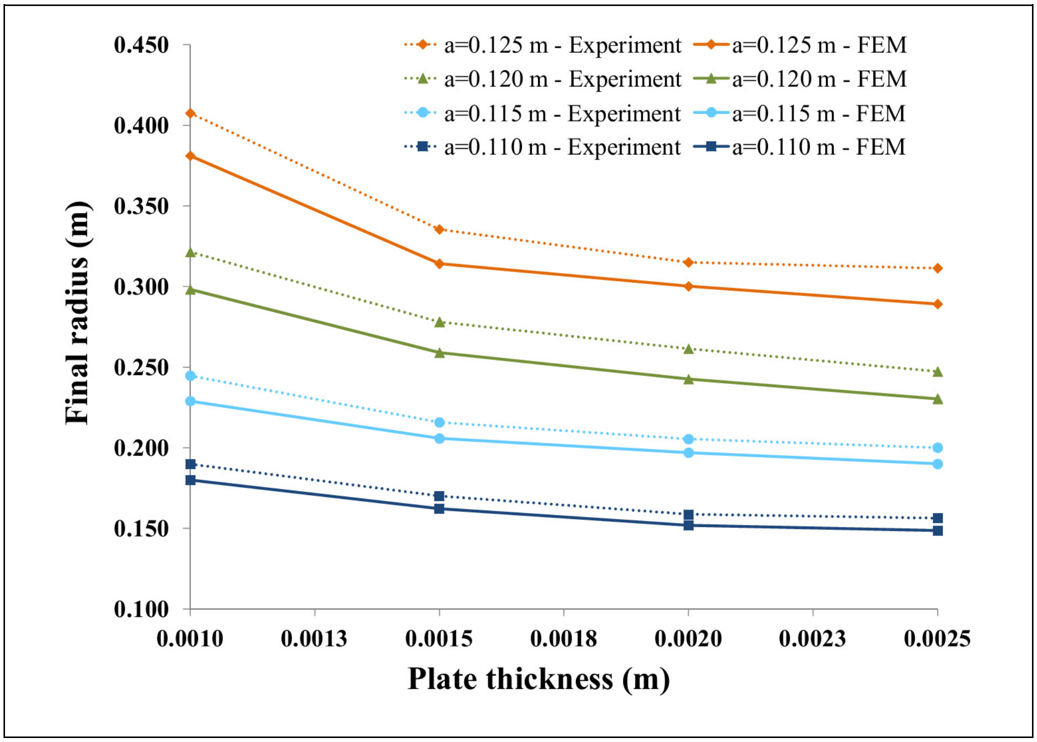

Figure 5.11 Final radius versus plate thickness and location of the lateral roll

5.6 Results and discussion

The flat end length for any given final shape obtained by the roll bending process depends on the machine type, workpiece thickness, final radius, roll positions and even the operators' skills. In this study, correcting the position of the bottom roll of the roll bending machine is considered as a method to reduce the forming forces and flat ends on the leading and trailing edges of the final shape. Correcting the positions of the bottom roll involves moving this roll in the horizontal plane and lowering it vertically. Although it is not possible to eliminate the flat areas inherent to the process, the challenge for future roll bending machine designs is to minimize these areas.

5.6.1 Moving the bottom roll in the horizontal plane

To study the flat area's dependence on the bottom roll positions, the FE simulations were performed using plates 2.0 mm thick, 100.0 mm wide and having a center to center distance "a" (Figure 5.3) from the top roll to the lateral roll of 115.0 mm. While keeping the same input parameters, i.e., the roll radii, material properties, mesh, etc., the position of the bottom roll was moved to the left hand side for various distances d_i. Figure 5.12 shows the values of the forming force's dependence on di, which is expressed as a function of r, ranging from 10.0 % to 70.0 % of the bottom roll radius.

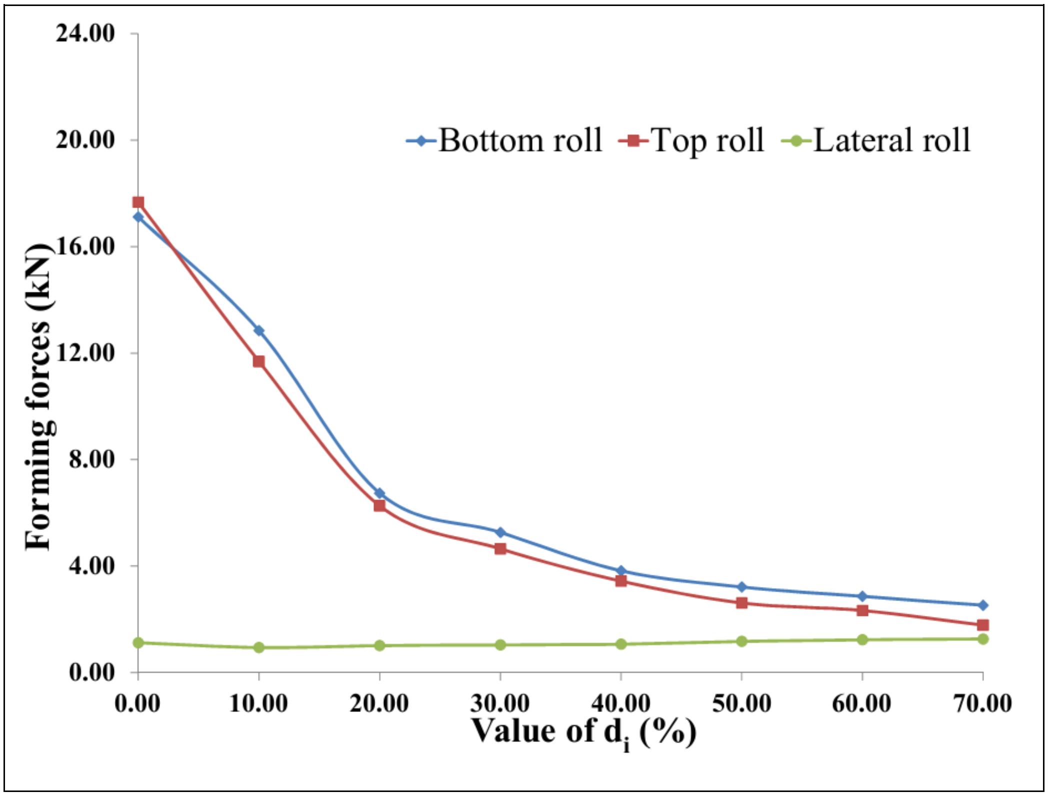

Figure 5.12 Forming force on the rolls versus the values of d_i

The forming forces, for both the top and bottom rolls, quickly decrease when the bottom roll is moved away to the left hand side by a distance di of 20 % of r. The forces then slowly decrease when the bottom roll is moved to a distance d_i that is larger than 20 % of r. Meanwhile, the forming force on the lateral roll (q_1) remains unchanged for every distance d_i.

Figure 5.13 show the instantaneous free body diagram of the system's roll bending process, including the contact forces q_i and their respective angles θ_i. The equilibrium of the moments at point P_2 leads to the Equation 5.7:

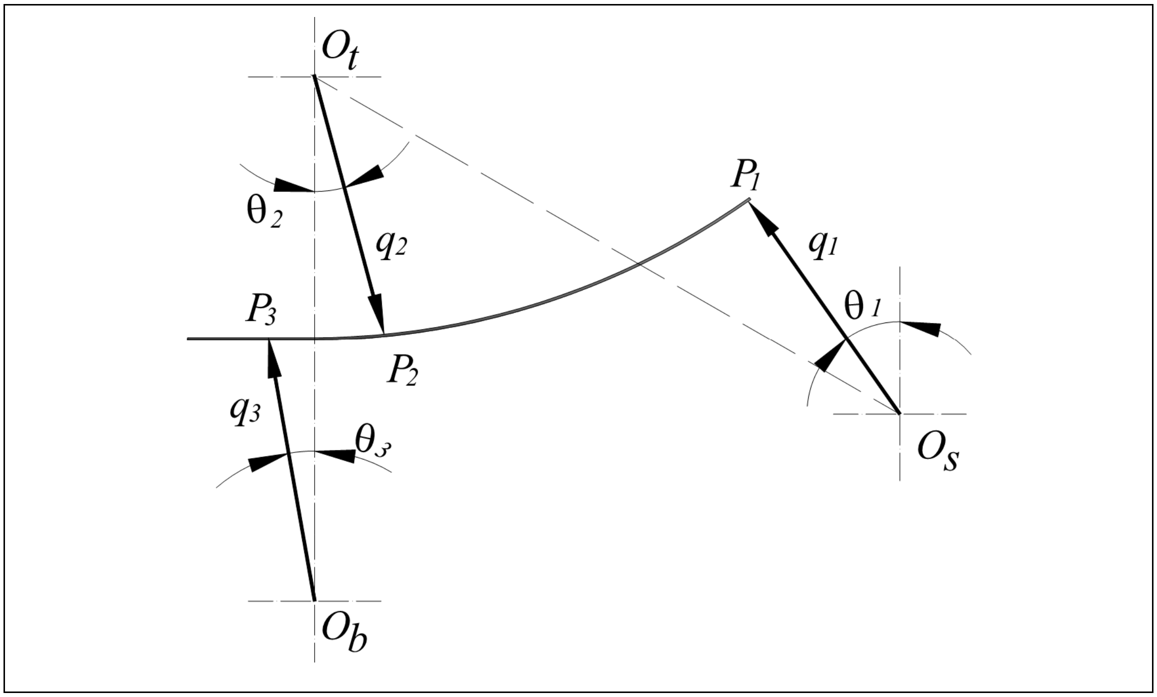

Figure 5.13 Free body diagram of the roll bending process

$$\sum M_{(P_2)} = 0 \tag{5.6}$$

Leading to:

$$q_3 s_3 = q_1 s_1 \tag{5.7}$$

Where s_1 and s_3 are the arc lengths of P_1P_2 and P_2P_3, respectively.

The contact angle between the rolls and the plate varies when the bottom roll is moved to the left hand side. However, the value of s_1 remains quasi constant. This may explain why the forming forces of the lateral roll do not change in Figure 5.12.

The flat ends for various positions d_i of the bottom roll are shown in Figure 5.14. Knowing that the larger flat end is usually left at the leading end of the final shape [3], only the flat end length at this edge is studied in this research.

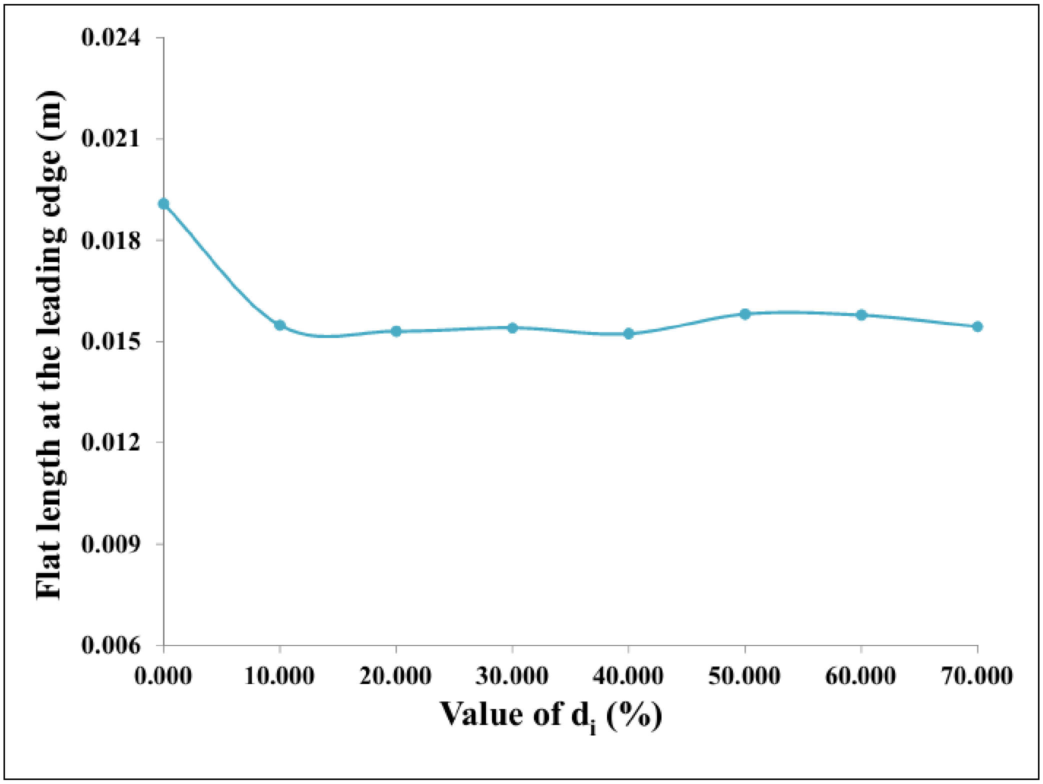

Figure 5.14 Flat-end length at the leading-end versus the value of d_i

The value of the flat end length of the final shape was determined to be monotonically decreasing when the bottom roll is moved to the left hand side by a distance d_i of 10 % of r. This is because at this position, the bottom roll is not only used to "pinch" the plate but, it is also used to support the plate at the contact line "*c*" (Figure 5.15). The plate is therefore more efficiently bent with the lateral roll.

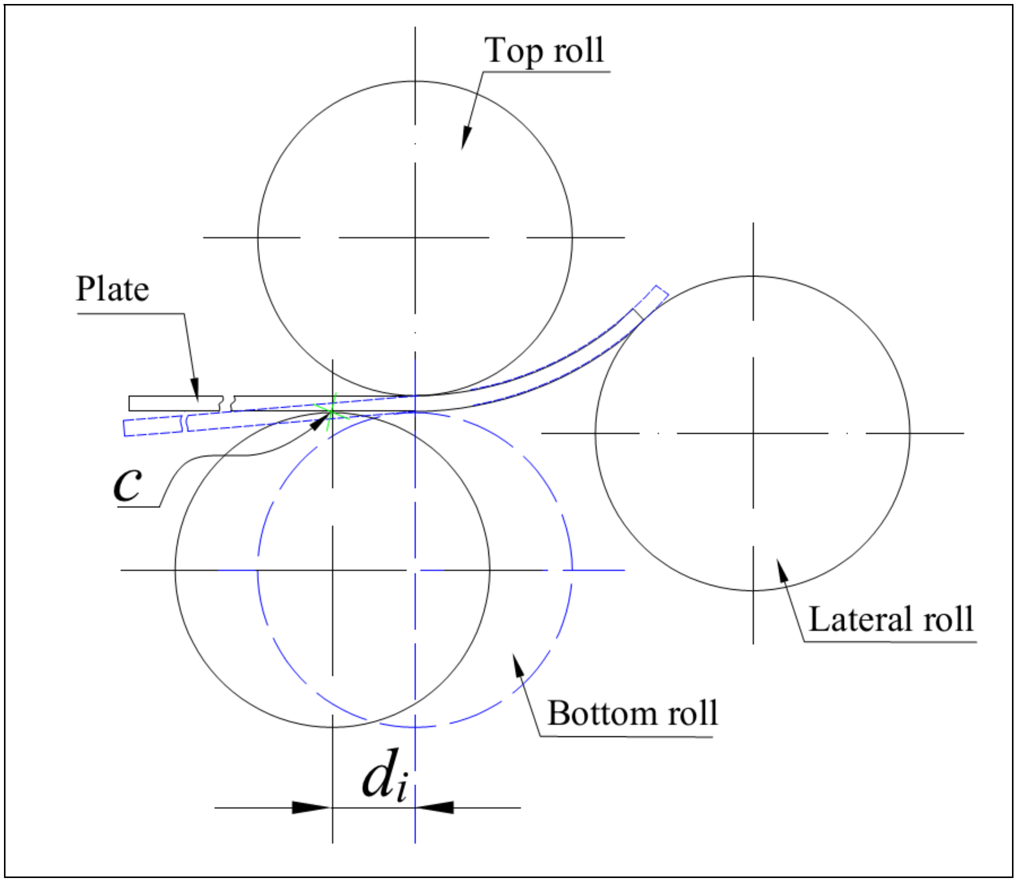

Figure 5.15 Plate configuration when the bottom moves horizontally

5.6.2 Moving the bottom roll in the vertical plane

The bottom roll of the three-roll asymmetric model was adjusted (up or down) in the vertical plane to compensate for the various plate thicknesses and to provide the pressure needed for "pinching". Therefore, choosing the matching "gap" between the top and the bottom roll is very important when using the roll bending process. For example, if the bottom roll pressure is too tight, the final shape obtained may be a bell-mouthed shape. To avoid this defect, the bottom roll should leave a gap that is equal to or greater than the plate thickness.

To study the "gap" effect on the flat ends and the forming forces, a series of FE simulations were performed for various values of the "gap" g_i. These "gap" values range from 10.0 % to 30.0 % of the plate thickness. The center locations of the top and bottom rolls were placed on the same vertical axis. For this FE simulation, the forming parameters and the material conditions held constant were the 2.0 mm plate thickness, 100.0 mm plate width and 115.0 mm center-to-center distance "a" from the top roll to the lateral roll. The forming forces versus the "gaps" g_i are shown in Figure 5.16.

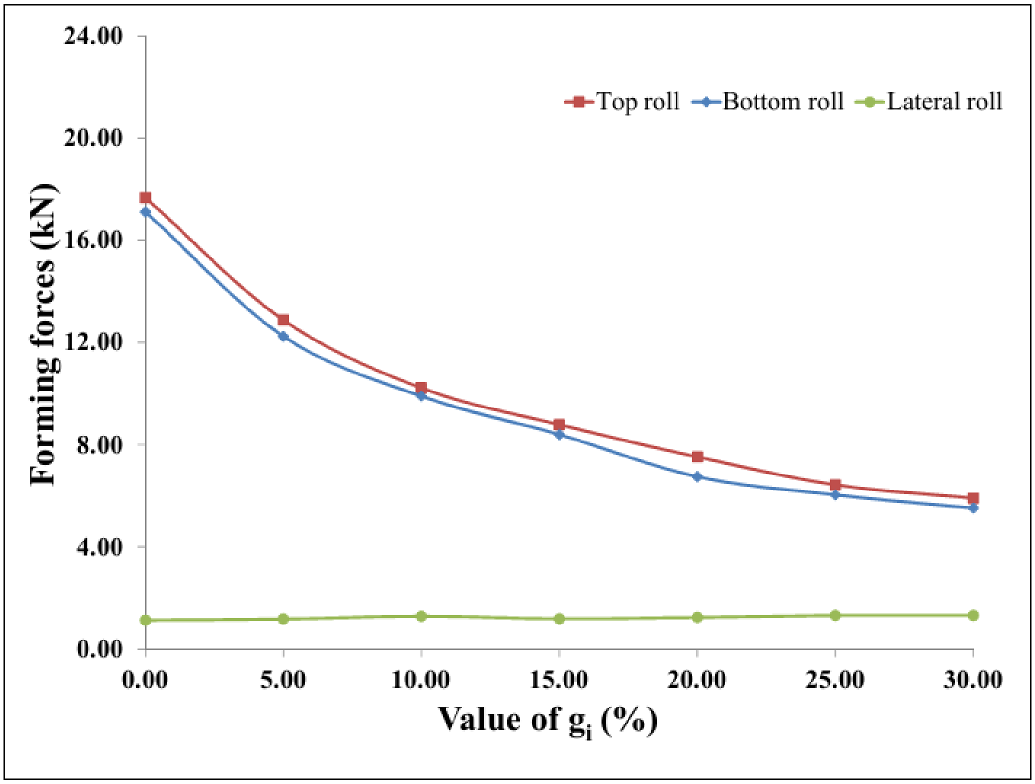

Figure 5.16 Forming force of the rolls versus the value of g_i

The top and bottom forces tend to decrease when the value of g_i increase. A rapid decreasing tendency is observed when the "gap" is set to 5.0 % of the plate thickness. The forming forces then slowly decrease when the "gap" value continually increases, up to 30 % of the plate thickness. The forming force of the lateral roll remains nearly constant for all the values of g_i.

Figure 5.17 shows the flat-end length variation's dependence on the "gap" value g_i. The flat end length monotonically increases when g_i is less than 15 % of the plate thickness. Over this last value, the flat end length is nearly unaffected when the "gap" continues to open.

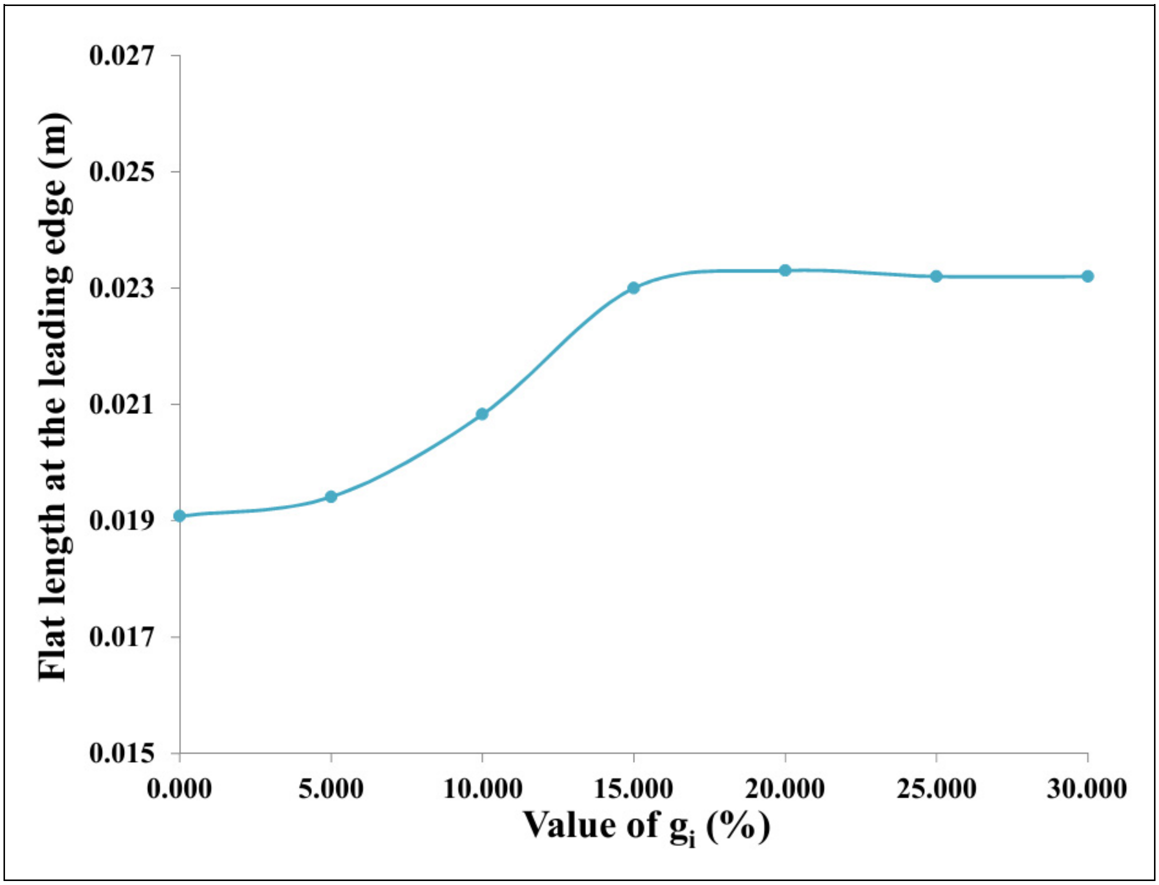

Figure 5.17 Flat end versus the value of g_i.

This interesting phenomenon can be explained with the help of Figure 5.18. The plate is held less firmly when the "gap" in-between the top and bottom rolls is larger than the plate thickness. For these cases, the plate tilts with an angle ε (dotted lines in Figure 5.18), leading to a less bent plate.

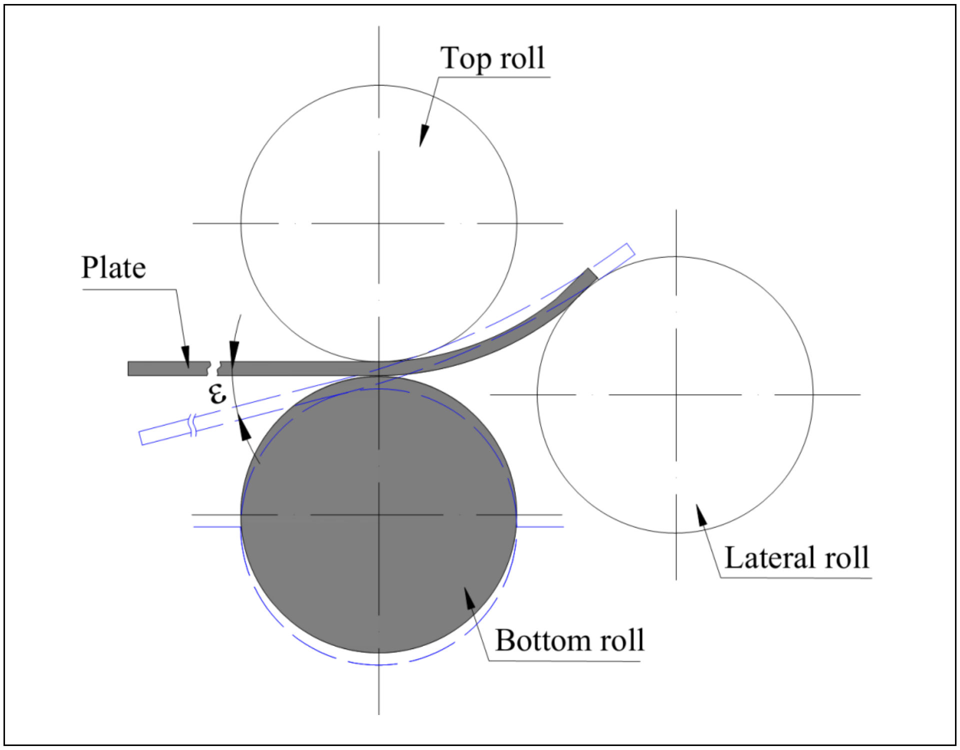

Figure 5.18 Varying plate contact lines with rolls when moving the bottom roll downward

Because the plate cannot be bent sharply, a larger amount of the blank at the leading edge remains flat.

5.7 Conclusions

A dynamic FE model was developed in the Ansys/LS-Dyna environment and was validated satisfactorily through experiments. In this study, we show how the flat-end lengths and forming forces are affected by the bottom roll setup. It is seen that by moving the bottom roll to the left hand side, the flat areas can be minimized, and the forming forces will be reduced on the top and bottom rolls. However, by adjusting the bottom roll with a “gap” value greater than the plate thickness in the vertical plane, the forming forces on the top and bottom roll are also reduced, but the flat area increases slightly. Therefore, in conclusion, maintaining the bottom roll at a gap close to the plate thickness and moving it laterally will produce the best results: lower forming forces and shorter flat-end lengths.

5.8 Acknowledgement

The authors express their thanks to the Natural Sciences and Engineering Research Council (NSERC) of Canada for its financial support during this research.

5.9 References

1. Available online at: http://www.thefabricator.com/article/bending/roll- bending -a-wind-tower-with-a-three-roll-bender.
2. Degarmo E. P. & al.,Materials and processes in manufacturing, John Wiley & Sons, (2008) 417.
3. Semiatin S.L., ASM Handbook: Metalworking: Sheet Forming, (2006) Volume 14B, Pages 386-393.
4. Lascoe O.D., Handbook of fabrication processes. ASM International, (1989) Pages 48-52.
5. Hua M., Baines K. & Cole I.M., Bending mechanisms, experimental techniques and preliminary tests for the continuous four-roll plate bending process, Journal of Material Processing Technology, 2nd Asia Pacific Conference on Materials Processing, (1995) Volume 48, Issues 1-4, Pages 159-172.
6. Hua M., Baines K. & Cole I.M., Continuous four-roll plate bending: a production process for the manufacture of single seamed tubes of large and medium diameters, International Journal of Machine Tools and Manufacture, (1999) Volume 39, Issues 6, Pages 905-935.
7. Hua M. & al., A formulation for determining the single-pass mechanics of the continuous four-roll thin plate bending process, Journal of Materials Processing Technology, Proceedings of the International Conference on Mechanics of Solids and Materials Engineering, (1997) Volume 67, Issues 1-3, Pages 189-194.

8. Hua M. & Lin Y.H., Effect of strain hardening on the continuous four-roll plate edge bending process, Journal of Materials Processing Technology, (1999) Volume 89-90, Pages 12-18.
9. Hua M., Sansome D.H., Baines K., Mathematical modeling of the internal bending moment at the top roll contact in multi-pass four-roll thin-plate bending, Journal of Materials Processing Technology, (1995) Volume 52, Issues 2-4, Pages 425-459.
10. Hua M. & al., Continuous four-roll plate bending process: its bending mechanism and influential parameters, Journal of Materials Processing Technology, (1994) Volume 45, Issues 1-4, Pages 181-186.
11. Hua M., Lin Y. H., Large deflection analysis of elastoplastic plate in steady continuous four-roll bending process, International Journal of Mechanical Sciences, (1999) Volume 41, Issues 12, Pages 1461-1483.
12. Hu W., Wang Z.R., Theoretical analysis & experimental study to support the development of a more valuable roll bending process, International Journal of Machine Tools and Manufacture, (2001) Volume 41, Issues 5, Pages 731-747.
13. Yang M. & Shima S., Simulation of pyramid type three-roll bending process, International Journal of Mechanical Sciences, (1988) Volume 30, Issues 12, Pages 877-886.
14. Bassett M. B., Johnson W., The bending of plate using a three roll pyramid type plate bending machine, The Journal of Strain Analysis for Engineering Design, (1966) Volume 1, Issues 5, Pages 398-414.
15. Hansen N. E., Jannerup O., Modelling of elastic-plastic bending of beams using a roller bending machine, Journal of Engineering for Industry, Transactions of the ASME, (1979) Volume 48101, Issues 3, Pages 304-310.
16. Zeng J., Liu Z., Champliaud H., FEM dynamic simulation and analysis of the roll bending process for forming a conical tube, Journal of Materials Processing Technology, (2008) Volume 198, Issues 1-3, Pages 330-343.
17. Feng Z., Champliaud H., Dao T. M., Numerical study of non-kinematical conical bending with cylindrical rolls, Simulation Modelling Practice and Theory, (2009) Volume 17, Issues 10, Pages 1710-1722.

18. Feng Z., Champliaud H., Three-stage process for improving roll bending quality, Simulation Modelling Practice and Theory, (2011) Volume 19, Issues 2, Pages 887-898.

19. Feng Z., Champliaud H., Modeling and simulation of asymmetrical three-roll bending process, Modelling Practice and Theory, (2011) Volume 19, Issues 9, Pages 1913-1917.

20. Tran H.Q., Champliaud Henri, Feng Zhengkun, Thien-My Dao, FE simulation of heat assisted roll bending process for manufacturing large and thick high strength steel axisymmetric parts. Modelling, Identification, and Simulation, CIB (2011), Track 755-041

21. Tran H.Q., Champliaud Henri, Feng Zhengkun, Thien-My Dao, Analytical modeling and FE simulation for analyzing applied forces during roll bending process, International Design Engineering Technical Conferences & Computers and Information in Engineering Conference, DETC (2012)-71518, pp. 207-215.

22. Tran H.Q., Champliaud Henri, Feng Zhengkun, Thien-My Dao, Dynamic analysis of a workpiece deformation in the roll bending process by FEM simulation, 24th European Modeling and Simulation Symposium, EMSS (2012), Pages 477-482.

23. Tran H.Q. & al. Heat assisted roll bending process dynamic simulation. International Journal of Modelling and Simulation, (2013) Volume 3, Issues 1.

24. Tran H.Q., Champliaud Henri, Feng Zhengkun, Thien-My Dao, Dynamic FE analysis for reducing the flat areas of formed shapes obtained by roll bending process, ASME 2013 International Mechanical Engineering Congress & Exposition IMECE (2013)-63302.

25. Zhong Y.C., Ying W.L, Analysis on the straight-end problem in thin-plate three-roll bending, Applied Mechanics and Materials, (2011) Volume 80-81, Pages 585-590.

CONCLUSION

In this study, theoretical models, FE simulations and experiment verifications have been carried out to study the forming process of a three-roll asymmetric roll bending machine. Key contributions and conclusions on four major aspects of this study are pointed out in this section. Furthermore, for future areas of investigation on roll bending process that still remain open for further research and development are referred in the following recommendation section.

1. Finite element simulation

In this study, 3D-dynamic finite element model was built for simulating forming process of asymmetric roll bending process. This model allowed the authors to identify the primary processing parameters of the roll bending process and to investigate the influence of these process factors on the precision of the final shape. The influence of several forming parameters, such as plate thickness, final shape radius, width of final shape, and reaction forces were studied in detail. Besides that, a three-dimensional thermo-mechanical FE simulation of hot roll bending process has been developed in Ansys/LS-Dyna software. The finite element modelling of the formed geometry is sequential with first a thermal simulation followed by a structural one. The relationships between the heating plate temperature and the output parameters of roll bending process such as applied forces and final shape quality have been studied by performing FE simulations and analytical computations. These results yield to a better understanding of the mechanism of the process and provide an opportunity for the design of an efficient heating system to control the heat energy to be input in the plate during the roll bending process.

2. Experiments verification

A three-roll asymmetric model machine was used to validate the FE simulations. A series of experiments were conducted to investigate the bending force variations and factors that may affect the accuracy of the final shape. The input parameters of a roll bending machine (rotational speed of the rolls, supplied power, friction coefficient between the plate and rolls …) and plate properties were carefully checked with suitable equipment. In addition, to verify the same output quantities of forming forces, different measuring devices such as indicators, load-cells and laser sensors were used to ensure qualitative experimental results. The final shape radii obtained by roll bending machine were evaluated by an accurate data acquisition-EXAscan laser scanner. Besides that, strain gauges were also stuck on the plate to investigate the strain variation, during and after the process, left in the formed plate

3. Theory approach

In this thesis, the analytical model is established based on equilibrium of forces approach to compare FE simulation results. The theory approach can applied to study the variation of the forming forces of the roll bending process depending on the various forming parameters. Besides that, to verify the geometry of the final shapes of the forming plate obtained from FE simulations in Ansys/LS-Dyna, a numerical check based on a Newton-Raphson scheme is applied to determine the geometry parameters. In addition, to compute the flat-end lengths of the formed plate from the FE simulations in Ansys/LS-Dyna, a numerical procedure is also developed and performed in this thesis.

4. Reducing flat end areas

As mentioned, a roll bending process that minimizes the flat areas on the leading and trailing ends of formed plates will produce more accurate and easier to assemble final shapes. In this study, a new and simple approach that reduces these flat areas is proposed. This approach includes moving the bottom roll slightly along the feeding direction and adjusting the bottom roll location. It is seen that by moving the bottom roll to the left hand side, the flat areas can be minimized, and the forming forces will be reduced for the top and bottom rolls. However, by adjusting the bottom roll with a “gap” value greater than the plate thickness in the vertical plane, the forming forces on the top and bottom roll are also reduced, but the flat area increases slightly. Therefore, in conclusion, maintaining the bottom roll at a gap close to the plate thickness and moving it laterally will produce the best results: lower forming forces and shorter flat-end lengths.

RECOMMENDATIONS

The research trends of asymmetrical roll bending process can be enhanced in the future as listed below:

1. Multi-pass roll bending process

To the author's knowledge, up to now, there is no published study about multi-pass roll bending process, although multi-pass forming is an interesting strategy for reducing the bending force and improving the accuracy of the final shape. Forming plate with multi-pass roll bending machines slows production and increases cost. However, this is a real opportunity and a new avenue in the manufacturing domain for finding interesting alternatives to forming large and high strength steel parts that cannot be achieved in one pass forming. Therefore, multi-pass roll bending process should be further investigated by 3-D dynamic finite element as well as experiments to explore the advantages of multi-pass roll bending process for forming thick and high strength steel.

2. Heat assisted roll bending machine experiment

In this research, a 3-D thermo-mechanical FE simulation of hot assisted roll bending process has been developed in the Ansys/LS-Dyna environment to study the relationships between temperature, applied forces and plate thickness. The FE results are then compared with the analytical results. In addition, some experiments of heating a plate with an induction heating system were also conducted as shown in Appendix I. The experiment results are preliminary, but very promising i.e. the plate forming temperature can be reached very quickly. However, the current roll bending machine does not allow performing the heat assisted roll bending as described in the FE simulations. Therefore, the integration of the induction unit into the roll bending machine for heat assisted forming process is a recommendation for future work.

3. Multi-pass optimization

Manufacturing time and cost for a multi-pass roll bending process relates to the number of passes involved. Reducing the number of steps could enhance the current research work. For this reason, optimization is strategic to determine the minimum number of passes within the machine capacity and the final shape quality.

APPENDIX I: EXPERIMENTS OF HEATING PLATE BY INDUCTION

The heat energy that the induction system generated in the plate depends on the current and the frequency of the equipment as well as the plate material properties. Therefore, the aim of this test is to determine the relationship between the induction machine parameters and the heat temperature generated on the plate surface. All experiments were conducted using high permeability (600-1100) - AISI 430 stainless steel plate having dimensions as shown in Figure I.1.

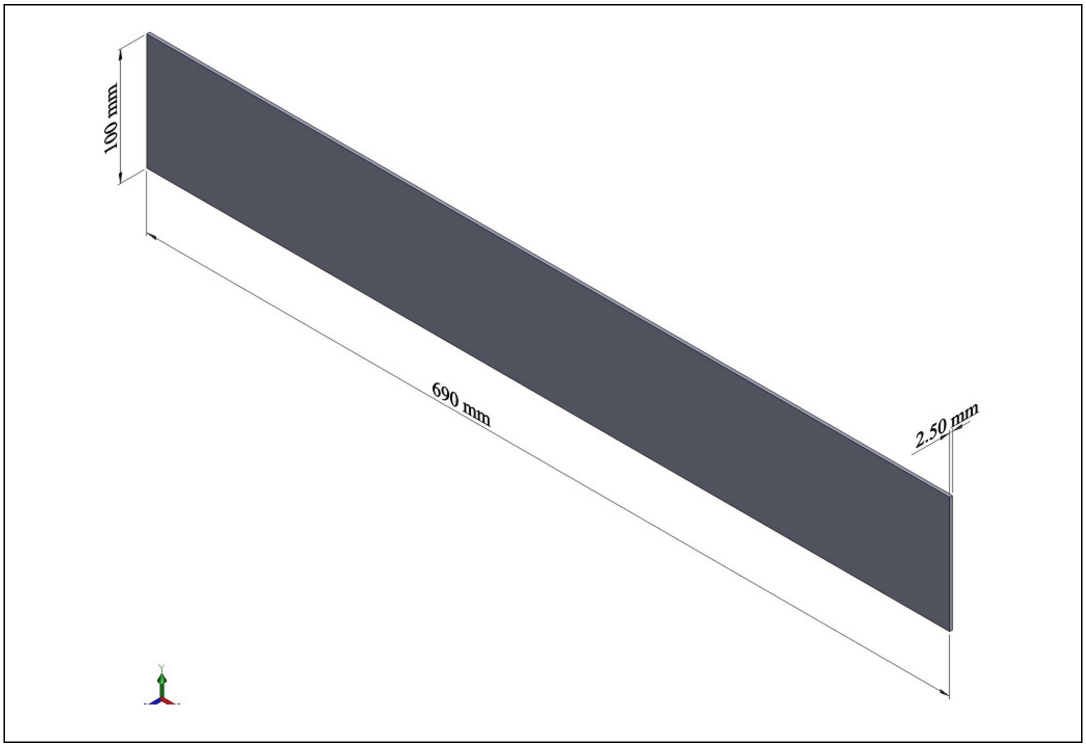

Figure I.1 Specimen dimensions

As shown in Figure I.2, the specimen was located inside the coil of the induction system. According to Faraday's Law as mentioned above, the plate will be induced in the object when alternating voltage is applied. As a result of the Joule effect, eddy currents will produce heat.

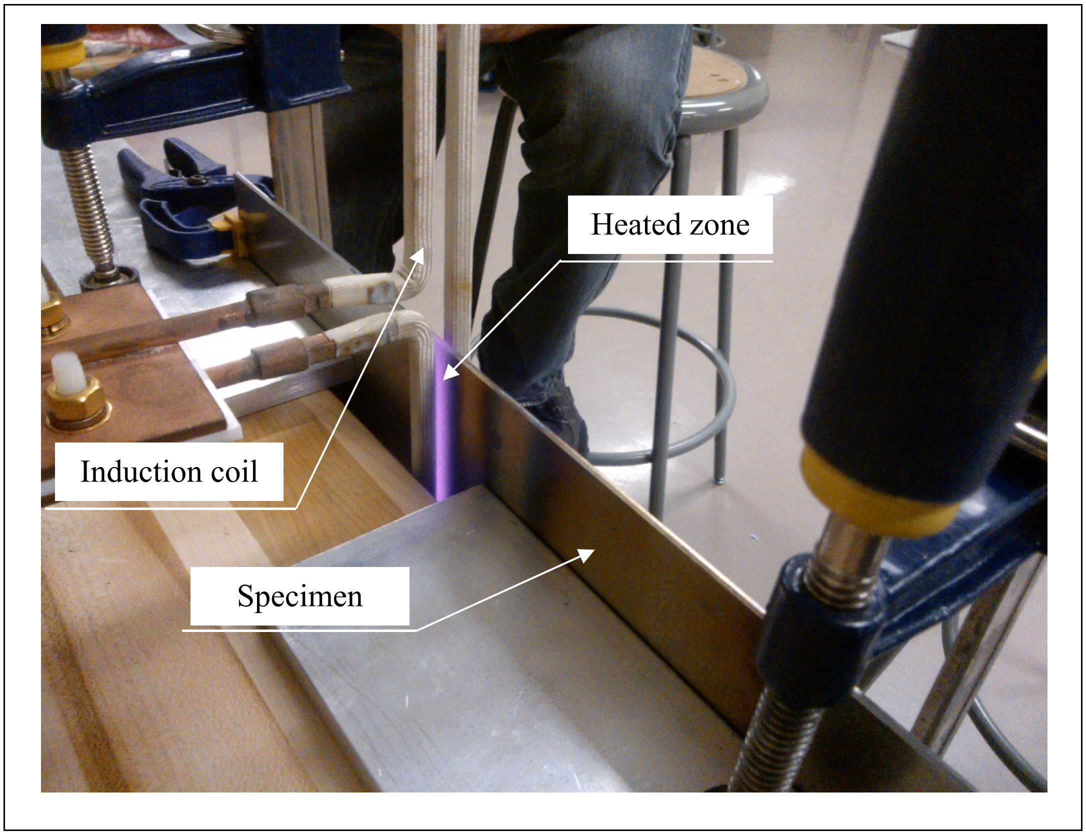

Figure I.2 Heating plate experiment setup

Two cases of experiment were performed to check the relationship between induction machine parameters and heat generated into the surface of steel: stationary and moving heat source

1. Stationary case

This test is intended to examine the effects of current on temperature induced on the surface of the plate. The experiments were performed for two levels of induction currents with other parameters remaining unchanged. The plate was placed into the coil as shown in Figure I.3. The results showed that, with 100 amperes (A), it takes 90 seconds to heat the plate up to 190^{o}C on the outer surface.

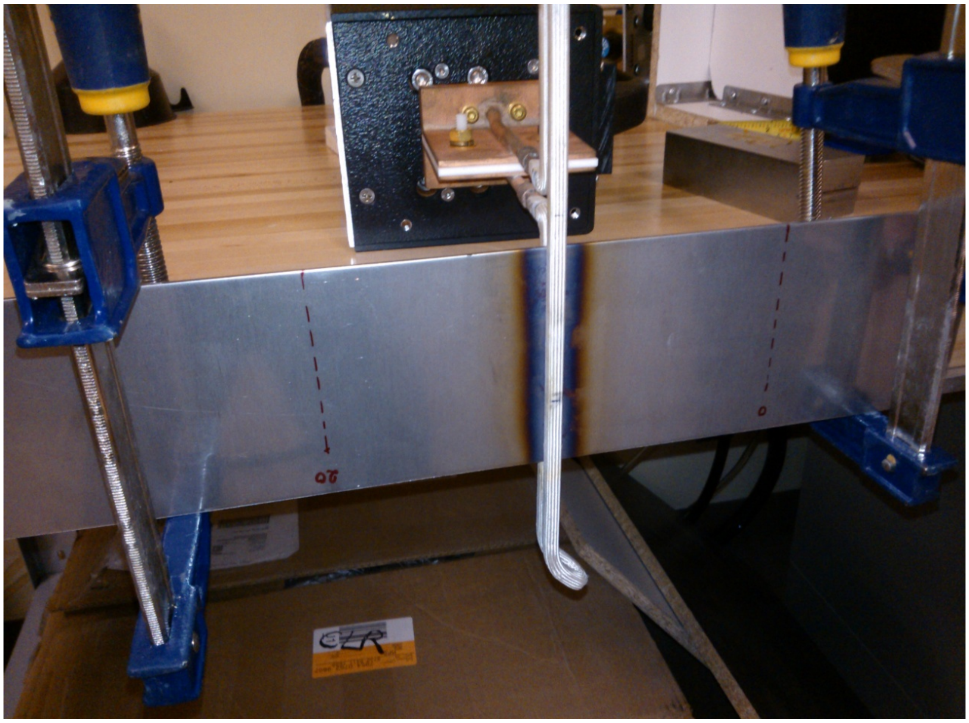

Figure I.3 Heating plate experiment: stationary case

However, with the same heating time (90 seconds), when the current of the induction machine was increased to 200 A, the temperature gain at the surface of the plate increased to 260^{o}C.

2. Moving heat source case

It was interesting to perform the experiment of heat conduction with a moving heat source because heat assisted roll bending process is a dynamic process, with the plate flowing in between forming rolls. In this experiment, as shown in Figure I.4, the plate moved from point A to point B inbetween the induction coil at a constant speed of 1.25 mm/s. The coil current of the induction system was set to 100 A.

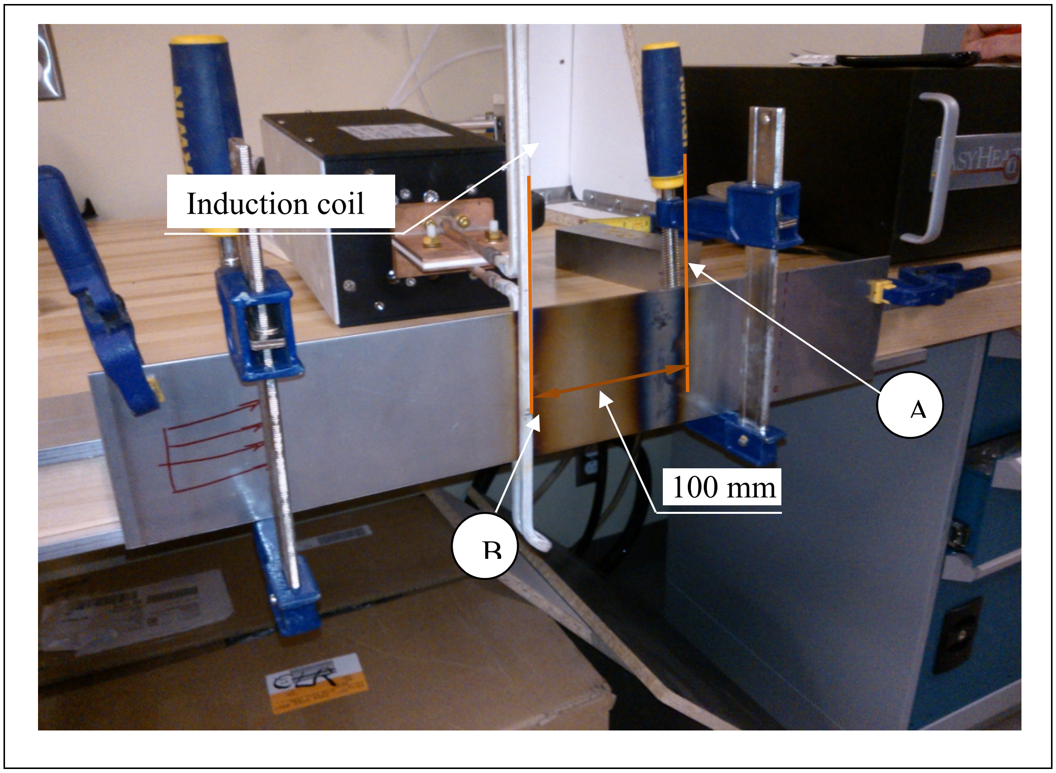

Figure I.4 Heating plate experiment: moving heat source case

It has been observed that the temperature gain of the 2.5 mm AISI - 430 stainless steel plate at point B was 140^{o}C.

LIST OF BIBLIOGRAPHICAL REFERENCES

Allen, Chris. 1985. "Plate bending rolls, Sheepford Boiler Works." Online. <http://www.geograph.org.uk/photo/1042075>. Retrieved 20/04/2014.

Alstom. 2014. "Francis hydro turbine at a manufacturing facility." Online. <http://www.alstom.com/power/renewables/hydro/hydro-turbines/>. Retrieved 20/04/2014.

Cai, Z. Y. and Lan Y.W. 2011. «Analysis on the straight-end problem in thin-plate three-roll bending». Applied Mechanics and Materials, Vol.80-81, p.585-590.

Chudasama, M. K. and Raval H. K. 2012. «Analytical model for prediction of force during 3-roller multipass conical bending and its experimental verification». International Journal of Mechanical Engineering and Robotics Research, Vol.1, No.3, p.91-105.

Chudasama, M. K. and Raval H. K. 2013. «An approximate bending force prediction for 3-roller conical bending process». International Journal of Material Forming, Vol.6, No.2, p.303-314.

Chudasama, M. and Raval H. 2014. «Development of analytical model for dynamic bending force during single pass 3-roller cone frustum bending technique». Universal Journal of Mechanical Engineering, Vol.2, No.4, p.148-154.

Faccin. 2014. "General catalogue." Online. <http://www.platerolls.com/CATALOGO/index.html>. Retrieved 20/10/2014.

Feng, Z. and Champliaud H. 2011. «Modeling and simulation of asymmetrical three-roll bending process». Simulation Modelling Practice and Theory, Vol.19, No.9, p.1913–1917.

Feng, Z. and Champliaud H. 2011. «Three-stage process for improving roll bending quality». Simulation Modelling Practice and Theory, Vol.19, No.2, p.887–898.

Feng, Z. and Champliaud H. 2012. «Investigation of non-kinematic conical roll bending process with conical rolls». Simulation Modelling Practice and Theory, Vol.27, p.65–75.

Feng, Z., Champliaud H. and Dao T. M. 2009. «Numerical study of non-kinematical conical bending with cylindrical rolls». Simulation Modelling Practice and Theory, Vol.17, No.10, p.1710–1722.

Fu, Z., Tian X., Chen W., Hu B. and Yao X. 2013. «Analytical modeling and numerical simulation for three-roll bending forming of sheet metal». The International Journal of Advanced Manufacturing Technology, Vol.69, No.5-8, p.1639-1647.

Gajjar, H. V., Gandhi A. H., Jafri T. A. and Raval H. K. 2007. «Bendability analysis for bending of C-Mn steel plates on heavy duty 3-roller bending machine ». World Academy of Science, Engineering and Technology, Vol.1, No.8, p.86-91.

Gandhi, A. H., Shaikh A. A. and Raval H. K. 2009. «Formulation of springback and machine setting parameters for multi-pass three-roller cone frustum bending with change of flexural modulus». International Journal of Material Forming, Vol.2, No.1, p.45-57.

Gandhi, A.H. and Raval H.K. 2008. «Analytical and empirical modeling of top roller position for three-roller cylindrical bending of plates and its experimental verification». Journal of Materials Processing Technology, Vol.197, No.1-3, p. 268–278.

Haeusler. 2010. "Brochure-Plate Bending Machine VRM." Online. <http://www.haeusler.com/en/products/plate-bending.html>. Retrieved 20/10/2010.

Hansen, N. E. and Jannerup O. 1979. «Modelling of elastic-plastic bending of beams using a roller bending machine». Journal of Manufacturing Science and Engineering Vol.103, No.03, p.304-310.

Hardt, D. E., Roberts M. A. and Stelson K. A. 1982. «Closed-loop shape control of a roll-bending process». Journal of Dynamic Systems, Measurement, and Control, Vol.104, No.04, p.317-322.

Hu, W. and Wang Z.R. 2001. «Theoretical analysis and experimental study to support the development of a more valuable roll-bending process». International Journal of Machine Tools and Manufacture, Vol.41, No.5, p.731-747.

Hua, M., Baines K. and Cole I.M. 1999. «Continuous four-roll plate bending: a production process for the manufacture of single seamed tubes of large and medium diameters». International Journal of Machine Tools and Manufacture, Vol.39, No.6, p.905–935.

Hua, M., Cole I.M., Baines K. and Rao K.P. 1997. «A formulation for determining the single-pass mechanics of the continuous four-roll thin plate bending process». Journal of Materials Processing Technology, Vol.67, No.1-3, p.189–194.

Hua, M. and Lin Y.H. 1999. «Effect of strain hardening on the continuous four-roll plate edge bending process». Journal of Materials Processing Technology, Vol.89-90, p.12-18.

Hua, M. and Lin Y.H. 1999. «Large deflection analysis of elastoplastic plate in steady continuous four-roll bending process». International Journal of Mechanical Sciences, Vol.41, No.12, p.1461-1483.

Hua, M., Sansome D.H. and Baines K. 1995. «Mathematical modeling of the internal bending moment at the top roll contact in multi-pass four-roll thin-plate bending». Journal of Materials Processing Technology, Vol.52, No.2-4, p.425–459.

Hua, M., Sansome D.H., Rao K.P. and Baines K. 1994. «Continuous four-roll plate bending process: Its bending mechanism and influential parameters». Journal of Materials Processing Technology, Vol.45, No.1-4, p.181–186.

Iseltek Co., Ltd. 2010. Online. <http://www.isel.jp/english/ben/ben.htm>. Retrieved 20/10/2010.

Jenkins, Rhys. 1936. Links in the history of engineering and technology from tudor times: The collected papers of Rhys Jenkins. Comprising articles in the professional and technical press mainly prior to 1920 and a catalogue of other published work, Books for Libraries Press, 246 p.

Juneja, B. L. 2013. Fundamentals of metal forming processes, New Age International Pvt Ltd Publishers, 406 p.

Ktari, A., Antar Z., Haddar N. and Elleuch K. 2012. «Modeling and computation of the three-roller bending process of steel sheets». Journal of Mechanical Science and Technology, Vol.26, No.1, p.123-128.

Larsson, Linus. 2005. «Warm sheet metal forming with localized in-tool induction heating». Master thesis, Lund University, 76 p.

Lin, Y. H. and Hua M. 1999. «Mechanical analysis of edge bending mode for four-roll plate bending process». Computational Mechanics, Vol.24, No.5, p.396-407.

Lin, Y.H. and Hua M. 2000. «Influence of strain hardening on continuous plate roll-bending process». International Journal of Non-Linear Mechanics, Vol.35, No.5, p.883–896.

Liu, F., Shi Y. and Lei X. 2009. «Numerical investigation of the temperature field of a metal plate during high-frequency induction heat forming». Proceedings of the Institution of Mechanical Engineers Part C Journal of Mechanical Engineering Science, Vol.223, p.979–986.

Logan, Daryl. 2006. A first course in the finite element method, Thomson engineering, 808 p.

Marshall, Sonja. 2010. "Comparing 4-rolls and 3-rolls – Advantages & Disadvantages." Online. <http://cmarshallfab.com/comparing-4-rolls-vs-3-rolls-advantages-and-disadvantages/>. Retrieved 20/04/2014.

Mukherjee, Syamal. 2013. Metal fabrication technology, PHI Learning Private Limited, 505 p.

Patented-Us807352a. 1905. "Stripper for bending rolls." Online. <http://www.google.com/patents/US807352>. Retrieved 20/04/2014.

Ramamurti, V., Rao V. R. S. and Sriram N. S. 1992. «Design aspects and parametric study of 3-roll heavy-duty plate-bending machines». Journal of Materials Processing Technology, Vol.32, No.3, p.585–598.

Roundo. 2012. "Brochure smt- 4 roll plate bender." Online. <http://www.roundo.com/products/platebending/4-roll/pas/#panel4>. Retrieved 20/10/2014.

Schleifstein. 2014. "Brochure smt-Roll bending machines." Online. <http://www.schleifstein.de/index.php?id=3&L=2>. Retrieved 20/10/2014.

Schuler, Gmbh. 1998. *Metal forming handbook*, Springer Berlin Heidelberg, 568 p.

Seddeik, M.M. and Kennedy J.B. 1987. «Deformations in hollow structural section (HSS) members subjected to cold-bending». International Journal of Mechanical Sciences, Vol. 29, No.03, p.195-212.

Semiatin, S.L. 2006. ASM Handbook: metalworking sheet forming, Volume 14B, ASM international, 924 p.

Seravesi, Paolo. 2006. "Roll bending a wind tower with a three-roll bender." Online. <http://www.thefabricator.com/article/bending/roll-bending-a-wind-tower-with-a-three-roll-bender>. Retrieved 20/10/2010.

Shin, J. G., Lee J. H., Kim Y. I. and Yim H. 2001. «Mechanics-based determination of the center roller displacement in three-roll bending for smoothly curved rectangular plates». KSME International Journal, Vol.15, No.12, p.1655-1663.

Tangirala, Sailesh K. 2006. «Experimental and numerical investigation of plasma-jet forming». Master thesis, University of Kentucky, 104 p.

Todd, Robert, Allen Dell and Alting Leo. 1994. Manufacturing processes reference guide, Published by Industrial Press Inc., 512 p.

Yang, G., Mori K. and Osakada K. 1994. «Determination of forming path in three-roll bending using FEM simulation and fuzzy reasoning». Journal of Materials Processing Technology, Vol.45, No.1-4, p.161-166.

Yang, M. and Shima S. 1988. «Simulation of pyramid type three-roll bending process». International Journal of Mechanical Sciences, Vol. 30, No.12, p.877-886.

Yang, M., Shima S. and Watanabe T. 1990. «Model-based control for three-roll bending process of channel bar». Journal of Manufacturing Science and Engineering Vol.112, No.04, p.346-351.

Yoshihiko, T., Morinobu I. and Hiroyuki S. 2011. «"IHIMU- a" A fully automated steel plate bending system for shipbuilding». IHI ENGINEERING REVIEW, Vol.44, No.01, p.6-11.

Yu, G., Anderson R.J., Maekawa T. and Patrikalakis N.M. 2001. «Efficien simulation of shell forming by line heating». International Journal of Mechanical Sciences, Vol.43, p.2349-2370.

Yu, G., Masubuchi K., Maekawa T. and Patrikalakis N. M. 2001. «FEM Simulation of laser forming of metal plates». Journal of Manufacturing Science and Engineering, Vol.123, No.13, p.405–410.

Zeng, J., Liu Z. and Champliaud H. 2008. «FEM dynamic simulation and analysis of the roll-bending process for forming a conical tube». Journal of Materials Processing Technology, Vol.198, No.1-3, p.330–343.

Zeng, Jun. 2007. "Finite element modeling and simulation of roll bending process for forming a thick conical hollow shape." Online. <http://espace.etsmtl.ca/608/1/ZENG_Jun.pdf>. Retrieved 20/10/2010.

LIST OF PUBLICATIONS

International journals

H. Q. Tran, Champliaud Henri, Feng Zhengkun, Jamel Salem and Thien-My Dao (2013). Heat assisted roll bending process dynamic simulation. International Journal of Modelling and Simulation, Volume 3, Issues 1, pp. 54 – 62.

H. Q. Tran, Champliaud Henri, Feng Zhengkun and Thien-My Dao (2014). FE study for reducing forming forces and flat end areas of cylindrical shapes obtained by roll bending process. Journal of Mechanics Engineering and Automation, Volume 4, Issues 6, pp. 467 – 475.

H. Q. Tran, Champliaud Henri, Feng Zhengkun and Thien-My Dao (2014). Analysis of the asymmetrical roll bending process through dynamic FE simulations and experimental study. Accepted for publication in International journal of Advanced manufacturing technology, Volume 75, Issues 5, pp. 1233 – 1244

International conferences

H. Q. Tran, Champliaud Henri, Feng Zhengkun and Thien-My Dao (2011). FE simulation of heat assisted roll bending process for manufacturing large and thick high strength steel axisymmetric parts. Modelling, Identification, and Simulation, Track 755-041.

H. Q. Tran, Champliaud Henri, Feng Zhengkun and Thien-My Dao (2012). Analytical modeling and FE simulation for analyzing applied forces during roll bending process. ASME-DETC-2012-71518, pp. 207-215.

H. Q. Tran, Champliaud Henri, Feng Zhengkun and Thien-My Dao (2012). Dynamic analysis of a workpiece deformation in the roll bending process by FEM simulation. 24th European Modeling and Simulation Symposium, EMSS, Pages 477-482.

H. Q. Tran, Champliaud Henri, Feng Zhengkun and Thien-My Dao (2013). Dynamic FE analysis for reducing the flat areas of formed shapes obtained by roll bending process. ASME-2013 International Mechanical Engineering Congress & Exposition IMECE (2013)-63302.